



National Library  
of Canada

Bibliothèque nationale  
du Canada

Canadian Theses Service

Service des thèses canadiennes

Ottawa, Canada  
K1A 0N4

## NOTICE

The quality of this microform is heavily dependent upon the quality of the original thesis submitted for microfilming. Every effort has been made to ensure the highest quality of reproduction possible.

If pages are missing, contact the university which granted the degree.

Some pages may have indistinct print especially if the original pages were typed with a poor typewriter ribbon or if the university sent us an inferior photocopy.

Previously copyrighted materials (journal articles, published tests, etc.) are not filmed.

Reproduction in full or in part of this microform is governed by the Canadian Copyright Act, R.S.C. 1970, c. C-30.

## AVIS

La qualité de cette microforme dépend grandement de la qualité de la thèse soumise au microfilmage. Nous avons tout fait pour assurer une qualité supérieure de reproduction.

S'il manque des pages, veuillez communiquer avec l'université qui a conféré le grade.

La qualité d'impression de certaines pages peut laisser à désirer, surtout si les pages originales ont été dactylographiées à l'aide d'un ruban usé ou si l'université nous a fait parvenir une photocopie de qualité inférieure.

Les documents qui font déjà l'objet d'un droit d'auteur (articles de revue, tests publiés, etc.) ne sont pas microfilmés.

La reproduction, même partielle, de cette microforme est soumise à la Loi canadienne sur le droit d'auteur, SRC 1970, c. C-30.

The University of Alberta

# Application of Acoustic Intensity Technique to the Sound Transmission of Panels

by

Vincent Y.C. Lau

A thesis  
submitted to the Faculty of Graduate Studies and Research  
in partial fulfilment of the requirements for the degree of

M.Sc.

Department of Mechanical Engineering

Edmonton, Alberta

Fall, 1988

Permission has been granted to the National Library of Canada to microfilm this thesis and to lend or sell copies of the film.

The author (copyright owner) has reserved other publication rights, and neither the thesis nor extensive extracts from it may be printed or otherwise reproduced without his/her written permission.

L'autorisation a été accordée à la Bibliothèque nationale du Canada de microfilmer cette thèse et de prêter ou de vendre des exemplaires du film.

L'auteur (titulaire du droit d'auteur) se réserve les autres droits de publication; ni la thèse ni de longs extraits de celle-ci ne doivent être imprimés ou autrement reproduits sans son autorisation écrite.

ISBN 0-315-45696-5

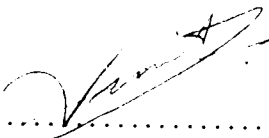
The University of Alberta

Release Form

Name of Author: Vincent Y.C. Lau  
Title of Thesis: Application of Acoustic Intensity Technique to  
the Sound Transmission of Panels  
Degree: M.Sc.  
Year this degree granted: Fall 1988

Permission is hereby granted to The University of Alberta Library to reproduce single copies of this thesis and to lend or sell such copies for private, scholarly, or scientific research purposes only.

The author reserves other publication rights, and neither the thesis nor extensive tracts from it may be printed or otherwise reproduced without the author's written consent.

  
.....  
(Student's signature)

Vincent Y.C. Lau

16603-95 Ave.

Edmonton, Alberta

T5P 0B1

Date : September 22, 1988

The University of Alberta  
Faculty of Graduate Studies and Research

The undersigned certify that they have read, and recommend to the Faculty of Graduate Studies and Research for acceptance, a thesis entitled

**Application of Acoustic Intensity Technique to the Sound Transmission of  
Panels**

submitted by

**Vincent Y.C. Lau**

in partial fulfilment of the requirements for the degree of

M.Sc..

*Gary Faulkner*  
.....  
(Supervisor)

*J. H. Arnold*  
.....  
*A. Cross*  
.....

Date : *7<sup>th</sup> Oct 88*

To my mom,  
S. Y. Leung

## **ABSTRACT**

The sound intensity technique, with the transmitted intensity measured directly, was evaluated as an alternative to the conventional dual-room technique to measure sound transmission loss of wall panels. The results compare favourably with the conventional method. In addition to the point by point measurement procedure, a sweeping technique was tested. It is shown to provide equivalent results in a shorter test time with a higher precision for the ASTM proposed reference panel. In both the conventional and intensity technique, the reliability in low frequencies is limited by the diffusivity of the sound field in the reverberation room(s). The potential of the intensity technology to improve low frequency reliability in sound transmission testing has been investigated. It is proposed that the incident sound intensity can be measured directly without the presence of the wall or indirectly away from the wall surface where the reflected intensity is negligible. (ie. in an anechoic environment) Preliminary testing, in which both incident and transmitted intensity were directly measured on a smaller specimen in an anechoic chamber, is also provided.

## ACKNOWLEDGMENTS

I gratefully acknowledge the contributions of my colleagues at the Mechanical Engineering Acoustics and Noise Unit. Professor A. Craggs of the University of Alberta and Dr. A. C. C. Warnock of NRC contributed with their helpful discussions. Dr. Warnock also provided his test results for comparison. Most importantly, I would like to thank sincerely my supervisor, Professor Gary Faulkner, for his guidance and patience towards my growth both professionally as well as personally. Funding for this work was provided by Professor Faulkner through the NSERC grant A 7514.



# TABLE OF CONTENTS

Chapter		Page
1.	INTRODUCTION .....	1
	1.1 Sound Intensity Technique .....	1
	1.2 Sound Transmission Loss Test - Conventional and Intensity Method .....	2
	1.3 Scope of the Investigation .....	6
2	CONVENTIONAL SOUND TRANSMISSION LOSS TEST (CTL) .....	8
	2.1 Microphone Boom Qualification .....	8
	2.2 Test Room Qualification for the Measurement of Broadband Sound .....	20
	2.3 Coherent and Incoherent Noise Source .....	22
3	SOUND INTENSITY TECHNIQUE (ITL) .....	28
	3.1 Fast Fourier Transform and Digital Filtering .....	28
	3.1.1 Fast Fourier Transform .....	28
	3.1.2 Digital Filtering .....	39
	3.2 System Overview .....	44
	3.3 Error Analysis .....	46
	3.3.1 Finite Difference Approximation .....	46
	3.3.2 Phase Mismatch Error .....	48
	3.3.3 Interference Effects of Microphones .....	59
	3.3.4 Phase Mismatch of Recorders .....	60
	3.3.5 Random Error .....	61
	3.3.6 Near Field Limitations .....	62
	3.3.7 Reverse Intensity .....	63
	3.3.8 Sound Intensity in the Presence of Flow .....	65
	3.4 Calibration .....	66

4	SOUND TRANSMISSION LOSS USING SOUND INTENSITY (ITL) .....	76
	4.1 Point by Point Technique Test Procedure .....	76
	4.2 Sweeping Technique Test Procedure .....	79
5	PROPOSED OUTDOOR ITL TEST TO IMPROVE LOW FREQUENCY RELIABILITY .....	82
	5.1 Concept Development .....	82
	5.2 Preliminary Test .....	89
6	RESULTS AND DISCUSSIONS .....	94
	6.1 Comparison between CTL Results .....	94
	6.2 Comparison between CTL and ITL Results .....	99
	6.3 Comparison between Sweeping ITL to Point by Point ITL Results .....	116
	6.4 Preliminary Direct and Semi-direct ITL Results .....	120
7	CONCLUSIONS AND RECOMMENDATIONS .....	128
	REFERENCES .....	131

## **Chapter 1 INTRODUCTION**

### **1.1 SOUND INTENSITY TECHNIQUE**

Sound intensity is a relatively new measurement technique in acoustics. The first commercial intensity analyser was introduced by Bruel and Kjaer (B & K) in 1981. Sound intensity is essentially a two microphone technique that provides the magnitude as well as the direction of the net flow of acoustic energy. While sound pressure level (SPL) is a scalar quantity, sound intensity is a vector. Since most common acoustics measurements, such as sound absorption, sound power and sound transmission loss (TL), are based on energy flow concepts, it would seem advantageous to measure the energy flow vector directly. Conventionally, these measurements are made by measuring SPL in acoustically idealized environments, such as the anechoic chamber or reverberation chambers. With sound intensity or generally the two microphone technique, these specialized facilities are no longer necessary.<sup>1,2,3,4,5,6,7</sup> This means that the high cost of building these chambers may be eliminated in the future. In addition, sound intensity is superior to SPL in noise source localization<sup>8,9,10</sup> because it provides the direction of the cause whereas SPL can only indicate the effects of the sound source at that measurement point in space.

Sound intensity, which has the units of Watt/m<sup>2</sup>, is defined as the time average of the product of pressure and particle velocity of the medium, ie.

$$I = \overline{p(t) \cdot u(t)}$$

From Newton's Second Law, particle velocity  $u$  can be obtained

by the pressure gradient,

$$u_r = - (1/\rho) \int \partial p / \partial r dt \quad (1.1.1)$$

The pressure gradient can be approximated by measuring the pressures at two closely spaced points and dividing the difference by the microphone separation. It can be shown that, assuming free propagating plane waves, the time averaged particle velocity  $u$  can be obtained by a finite difference approach yielding

$$u = - (1/\rho \Delta r) \int (p_B - p_A) dt \quad (1.1.2)$$

where  $\rho$  = density of air

$\Delta r$  = microphone separation

$p_A, p_B$  = pressures obtained from the two microphones

and pressure  $p$  can be approximated from the average of the two measurements at the two microphones,

$$p = (p_A + p_B) / 2 \quad (1.1.3)$$

Therefore, the sound intensity probe, consisting of two phase-matched microphones, provides enough information to obtain sound intensity by measuring two SPL's. It will be shown that the accuracy of the intensity measurement is strongly related to the measurement of the phase difference of the sound field between the microphone positions. Therefore, the use of phase-matched microphones will reduce the error of the measured field phase and consequently the error in the true sound intensity.

## 1.2 SOUND TRANSMISSION LOSS TEST - CONVENTIONAL AND

## INTENSITY METHOD

The characterization of the acoustic isolation of wall panels is to provide a measure of how well a panel insulates one room from sounds in another. The sound transmission loss (TL) is defined as

$$TL = 10 \log (1/\tau) \quad (1.2.1)$$

where  $\tau = I_t / I_i$  (1.2.2)

is the ratio of transmitted acoustic power  $I_t$  and the incident acoustic power  $I_i$ . In the conventional TL test the intensities are not measured directly but are inferred from an energy balance concept, which requires only an average SPL to be measured. The actual test is performed in a pair of reverberation rooms in which the test wall is essentially the only acoustic path between the two rooms.

The test is performed in a dual reverberation room facility according to the ASTM E-90 standard. The wall specimen is set on a test opening adjoining two adjacent reverberation rooms while the SPL of the reverberant field in each room is measured. In order to obtain the incident intensity,  $I_i$ , it is necessary to assume a perfectly diffuse sound field in the source room. One can write the one sided intensity  $I_i$  as  $\langle p \rangle_1^2 / 4 \rho_0 c_0$  where  $\rho_0$  is the density of air and  $c_0$  is the speed of sound in air. Therefore, the rate of energy transmitted to the receiving room through the wall panel is  $\tau S \langle p \rangle_1^2 / 4 \rho_0 c_0$  where  $S$  is the wall surface area. The rate of energy loss in the receiving room is  $(d/dt) \int_{V_2} E_2 dV$  where  $E_2$  is the energy density in the receiving room with volume  $V_2$ . In steady state, these two rates

must equal, ie

$$\tau S \langle p \rangle_1^2 / 4 \rho_0 c_0 = (d/dt) \int_{V_2} E_2 dV$$

Assuming an exponential decay of energy with a time constant  $b$  and, also that the sound field is totally diffuse in the receiving room, the total energy can be written as  $V_2 \langle p \rangle_2^2 / 4 \rho_0 c_0^2$ . One can then write

$$\tau S \langle p \rangle_1^2 / 4 \rho_0 c_0 = b V_2 \langle p \rangle_2^2 / 4 \rho_0 c_0^2$$

Substituting  $A = 4bV_2/c_0$  where  $A$  is the room absorption by the walls and the air and taking logarithms, one obtains the equation

$$TL = L_1 - L_2 + 10 \log(S/A)$$

where  $L_1 =$  reverberant SPL in source room, dB

$L_2 =$  reverberant SPL in receiver room, dB

$A =$  absorption in receiver room, metric sabine

The room absorption is actually obtained indirectly by measuring the sound decay rate in the receiving room.

With the sound intensity technology, it would seem logical to measure both the incident and transmitted intensity to determine sound transmission loss as suggested by (1.2.1) and (1.2.2). In practice, however, it is difficult to measure the incident sound intensity. On the receiver side of the wall surface, there are incident as well as reflected waves. It is the net energy flow in the orientation of the sound intensity probe which is being measured. Assuming steady state, this net flow of energy is equal to the transmitted energy since the wall does not store up energy. Therefore, one would

be misled to believe that the wall is acoustically transparent if the incident intensity is measured directly on the receiver side of the wall.

The new TL test using sound intensity<sup>5,6,7</sup> suggests that the transmitted intensity can be measured directly with an intensity analyser whereas the incident intensity is still measured by measuring the SPL in the source room as described earlier. There are two main advantages in this approach. First, a more detailed transmission pattern can be obtained and studied. Second, the receiving room only needs to be a nonreverberant space instead of a costly reverberation room.

It is now clear that the conventional method (CTL) assumes a perfectly diffuse field in both rooms whereas the intensity method requires that in only the source room. Practically, however, the sound field cannot be diffuse at all frequencies. At low frequencies, the wavelengths become comparable to the room dimensions requiring larger rooms. As the room size increases, diffusivity for low frequency sound increases. Unfortunately, air absorption increases dramatically for the high frequency sound reducing its diffusivity. As a result, the size of the reverberation rooms is optimized for cost and an overall frequency diffusivity. With the help of moving vane diffusers, the reverberation chambers at the Mechanical Engineering Acoustics and Noise Unit (MEANU) are reverberant down to as low as 100 Hz with acceptable limitations, which is typical for most facilities. Because of this limitation, the TL values obtained by either method at frequencies below this are not reliable.

### 1.3 SCOPE OF THE INVESTIGATION

Numerous noise problems exist at low frequencies as low frequency noise can easily be transmitted through obstacles because of the relatively long wavelength. The ultimate goal of this research work is to find a method, probably with the help of sound intensity, to improve the reliability of the TL test at low frequencies (down to possibly 50 Hz). Before that could be achieved, a few other obstacles have to be overcome.

A "home made" sound intensity system based on the FFT technique has been assembled and calibrated at discrete frequencies. The system was recalibrated at frequencies below the limiting anechoic frequency of the anechoic chamber, where the original calibration was made. Also, the constant bandwidth FFT measurements were converted to third octave based values in order to comply with the data from other researchers, who commonly use a digital filtering system.

Work has been done in comparing the conventional method and the intensity method in TL testing.<sup>5,6,7</sup> The same was done on the ASTM wall at MEANU to obtain insights in applying the intensity method on TL testing. In addition, by comparing results with other researchers, confidence will be gained on the instrumentation overall. In the intensity approach, it has been reported that equally good results can be obtained by sweeping the microphone probe over the wall surface instead by stationary point by point measurement. This was also investigated.

An idea was developed to improve the TL test at low



frequency applying the sound intensity technique. A preliminary test was carried out to provide supportive as well as critical information before full scale test equipment is built. Future work can be carried out with the help of the findings and recommendations resulting from this investigation.

Chapter 2 provides the background information on the wall specimen and the conventional transmission loss test (CTL). Details of the microphone boom qualification, test room qualification and the effects of an incoherent noise source compared to the coherent one are also provided.

The next chapter covers the principles of the two types of dual channel analysers capable of obtaining sound intensity, the Fast Fourier Transform (FFT) and Digital Filtering. The errors and limitations due to instrumentation, statistics and special measurement situations are discussed. Finally, a system overview of the FFT system at MEANU and the calibration procedure and results are presented.

Chapter 4 discusses the test procedure for the point by point and sweeping technique for the TL test using sound intensity. (ITL) This is followed by chapter 5, which describes the development of the concept of measuring incident sound intensity directly in an anechoic situation to improve the ITL test at low frequencies. The preliminary test set up is also provided.

Chapter 6 contains test results and discussions, while the final chapter lists the conclusions and recommendations of this work.

## Chapter 2 Conventional TL test

As mentioned above the conventional test for sound transmission is done in a reverberation suite. In this case a simple single panel wall was used as it is the one suggested by ASTM to be used for round robin tests in various facilities throughout North America. It consists of three 24 gauge galvanized steel panels riveted onto three 1"x1" steel angles, screwed onto a wood frame (see fig. 2.1). Testing in this investigation was done on this proposed ASTM reference steel panel, which will be referred to as the ASTM wall.

### 2.1 Microphone Boom Qualification

The conventional test was carried out according to the ASTM E-90 standard(1985) entitled "Standard Method of Laboratory Measurement of Airbourne Sound Transmission Loss of Building Partitions". While the conventional test relies on multiple stationary microphone positions to establish the reverberant sound field, a rotating microphone boom is used at MEANU to obtain the spacial and time average. In this situation, it is recommended in the standard that data may be obtained from stationary positions taken along the microphone traverse path at points approximately half a wavelength apart at the lowest test frequency. These are then compared with those of a complete survey described in the standard. However, since the rotating boom approach actually samples over the traverse continuously, it is more reasonable to compare results obtained from the continuous sweep to the complete survey. As a result, several complete sweeps of 10 boom cycles each were carried

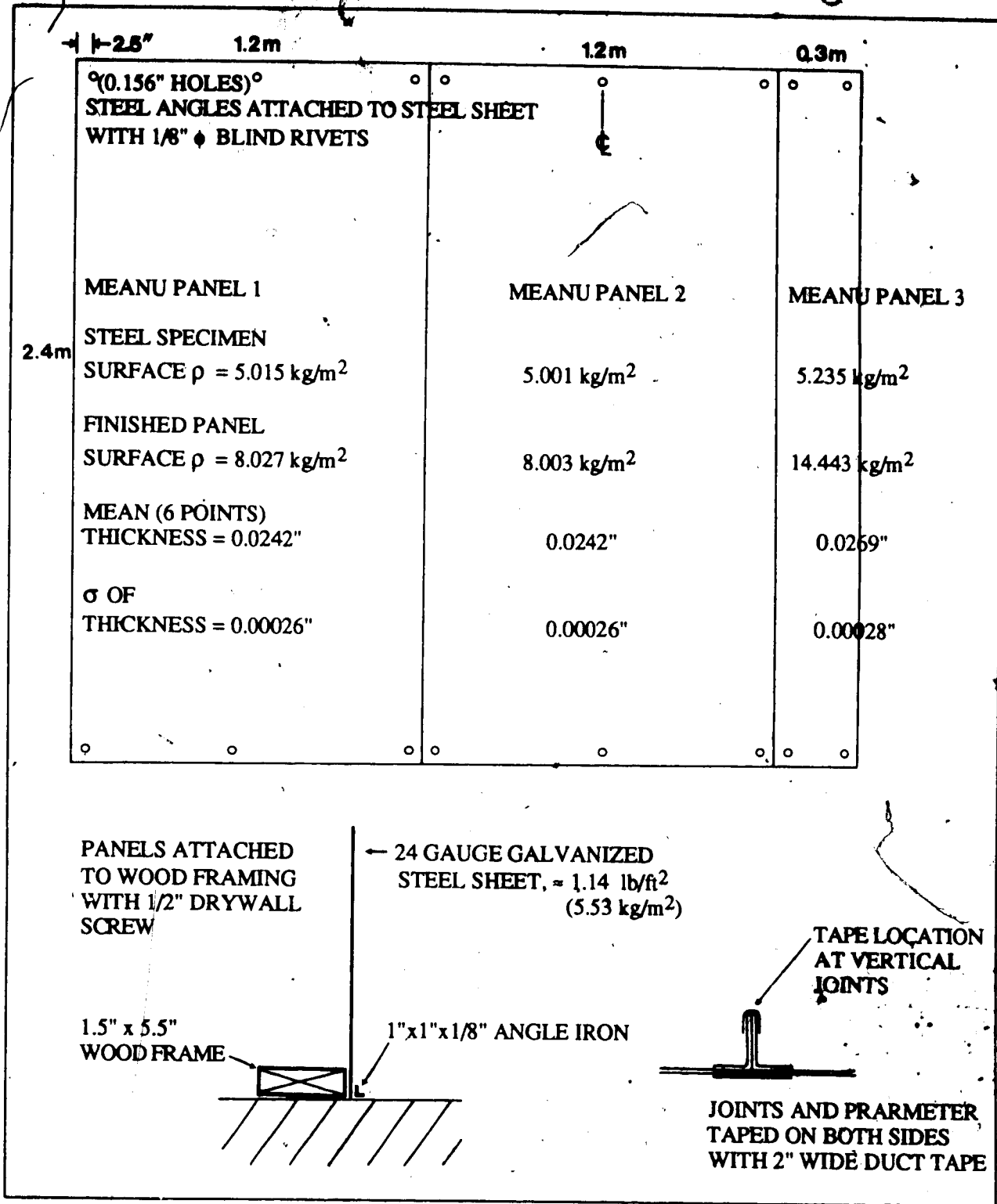


**FIG. 2.1 ASTM REFERENCE SPECIMEN CONSTRUCTION SPECIFICATIONS WITH MEANU SPECIMEN DATA**

out and compared to several complete surveys of the same time duration.

For the complete survey, eleven and six points were used in the large and small room respectively. A distance between microphone positions of 1.6m was chosen based on a test frequency limit of about 100 Hz. The layout of the microphone is shown in fig. 2.2. Four sets of complete surveys and four complete boom sweeps were carried out for the large room. On the other hand, six sets of testing were done in the small room since the number of stationary positions was less. For these qualification tests, the wall panel was a plug wall instead of the ASTM wall. The plug wall is commonly inserted when the chambers are used for sound power or sound absorption tests. It is not clearly stated in the standard whether the boom must be qualified specifically for each wall panel tested. However, it is reasonable to assume that the ability of the rotating boom to survey the SPL of the reverberant field does not depend on the wall panel unless it is acoustically very transparent such that the direct field from the panel extends far into the region of the boom traverse. It will be shown that the critical distance between the wall panel to the first microphone position in the receiving room is mainly determined by the amount of air absorption, rather than the transmissibility of the wall panel. Therefore, the results from the plug wall can be generally applied for TL tests using other wall panels.

According to the standard, the region of the reverberant field can be calculated for the wall panel tested by these formulas:

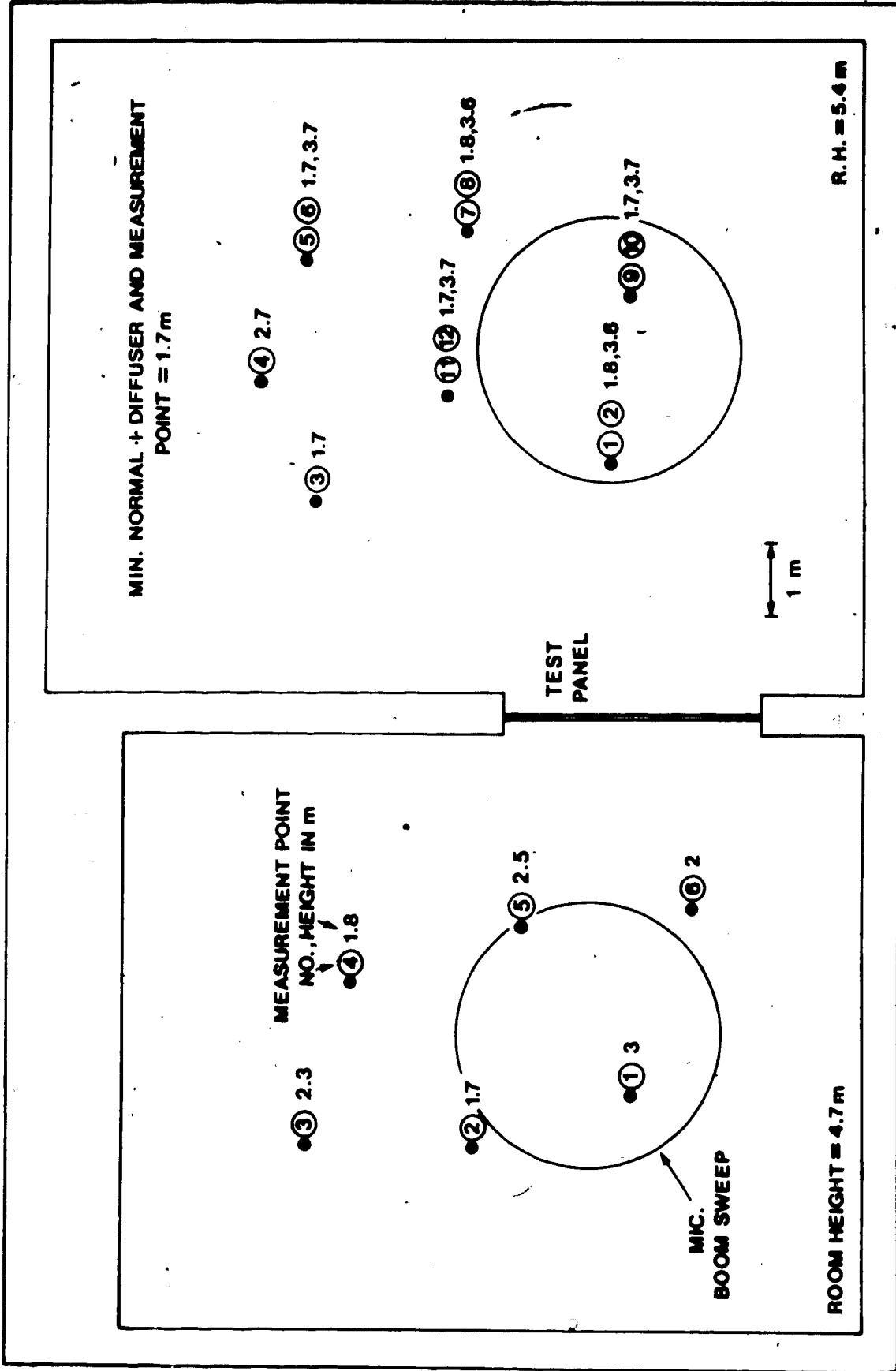


FIG. 2.2 LAYOUT OF MICROPHONE POSITIONS FOR BOOM QUALIFICATION TESTS

$$A = 0.921 V d / c \quad (2.1.1)$$

$$d_{\min} = 0.63 A^{1/2} \quad (2.1.2)$$

where  $A$  = room absorption, metric sabines

$c$  = speed of sound in medium, m/s

$V$  = volume of room,  $m^3$

$d$  = rate of decay of SPL, dB/s

$d_{\min}$  = minimum distance from the sound source to the test partition in the source room,

or minimum distance from the sound source to the nearest measurement point in the source room,

or minimum distance from the wall panel to the nearest measurement point in the receiving room

The rate of decay can be calculated from the 60 dB reverberation times (RT), which are listed in table 2.1. The absorption in metric sabines at 6.3 kHz are 21.6  $m^2$  and 28.3  $m^2$  for the small and large room while the wall could contribute a maximum of its own area of 6.6  $m^2$  as if it was an open area. Therefore,  $d_{\min}$  is mainly determined by air absorption. Following (2.1.2), simple calculations show that the minimum distance is 2.93m and 3.35m for a limiting qualification frequency of 6300 Hz. As shown from Fig. 2.2, the minimum distance criterion is satisfied when the rooms are used as the source room. As suggested by the standard, the  $L_{eq}$  mean is used to determine space-average levels and the arithmetic standard deviation of the SPL values is used to determine the precision of the measurement. Therefore, for each data set of a complete surveys, the

**TABLE 2.1 60 dB REVERBERATION TIMES FOR BOOM QUALIFICATION TESTS**

SMALL ROOM WITH PLUG WALL		LARGE ROOM WITH PLUG WALL
VOLUME:	227 m <sup>3</sup>	313 m <sup>3</sup>
TEMPERATURE:	14.4 C	15.4 C
REL. HUMIDITY:	71.0%	71.5%
BAR. PRESSURE:	705 mm Hg	697.5 mm Hg
BAR. TEMP.:	17.5 C	18.6 C
FREQ.(Hz)	REVERBERATION TIME(s)	REVERBERATION TIME(s)
100	3.71	4.48
125	4.45	5.43
160	4.71	5.67
200	5.38	6.19
250	5.59	6.28
315	5.90	6.52
400	5.83	6.22
500	5.61	6.15
630	5.35	5.91
800	5.19	5.64
1000	4.95	5.44
1250	4.69	5.09
1600	4.41	4.83
2000	4.14	4.62
2500	3.71	4.15
3150	3.24	3.60
4000	2.63	2.90
5000	2.14	2.31
6300	1.70 → 21.6 m <sup>2</sup> metric sabine	1.78 → 28.3 m <sup>2</sup> m.s.

$L_{eq}$  means and arithmetic standard deviations are calculated from all the microphone positions. It would be adequate to compare the  $L_{eq}$  and standard deviation values of one complete survey to one complete boom test (10 sweeps). Since there were four sets of complete survey for the large room, the arithmetic means of the  $L_{eq}$  and standard deviations from the four sets of complete survey data were calculated, and compared with the first order arithmetic means and standard deviations of the four sets of boom results. A similar calculation was carried out for the six sets of complete surveys and boom data for the small room. The results over the frequency bands of 100 to 6300 Hz for each room used as the source room are shown in fig. 2.3 and 2.4.

As shown in fig. 2.2, some measurement points in the complete survey did not satisfy the minimum distance requirement when either room was used as the receiving room. They were too close to the panel surface, which was the case for points 1 and 2 for the large room and points 5 and 6 for the small. Furthermore, points 11 and 12 in the large room were removed to satisfy more absorptive conditions, as observed from other CTL tests, as shown in table 2.2. The same test results were analysed with these points eliminated assuming the field diffusivity is the same whether the sound comes from the wall transmission or the speakers. These results represent a complete survey of the sound field for the rooms being used as the receiving room. Similarly, they are compared to the rotating boom results in fig. 2.5 and 2.6.



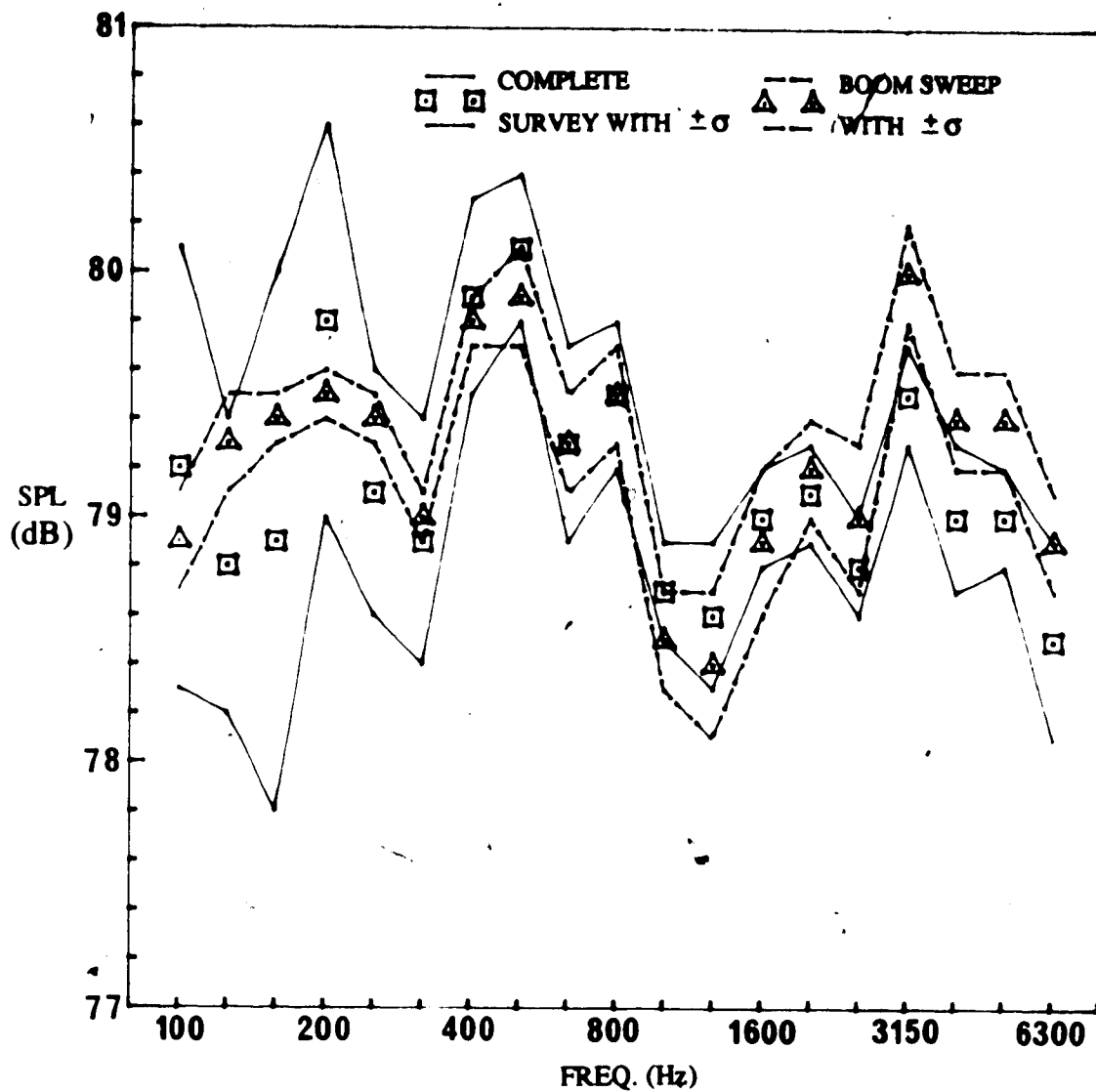


**FIG. 2.3 BOOM QUALIFICATION FOR THE LARGE CHAMBER AS THE SOURCE ROOM**

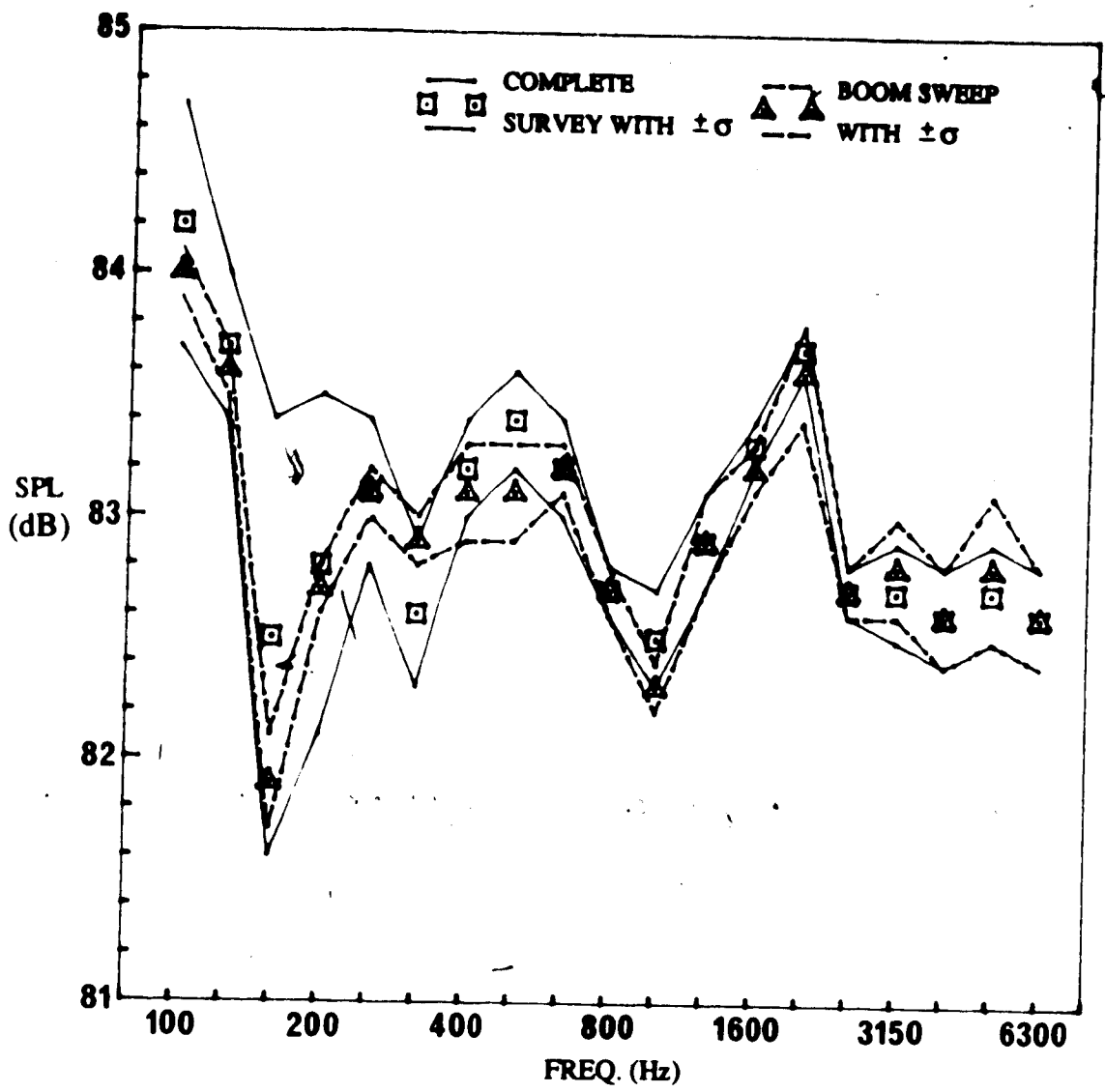


**FIG. 2.4 BOOM QUALIFICATION FOR THE SMALL CHAMBER AS THE SOURCE ROOM**

**TABLE 2.2 MINIMUM DISTANCES FOR OTHER ENCOUNTERED TEST CONDITIONS**

DATE	REVERSED CTL APPROACH <sup>1</sup> (RT MEASURED IN SMALL ROOM)		FORWARD CTL APPROACH <sup>2</sup> (RT MEASURED IN LARGE ROOM)	
	2-11-87	29-3-88	2-11-87	29-3-88
TEMPERATURE	10.1 °C	4.4 °C	11.2 °C	4.5 °C
RELATIVE HUMIDITY	53.7 %	48.0 %	52.3 %	49.2 %
ATMOSPHERIC PRESSURE	42.63 kPa	93.25 kPa	92.81 kPa	93.27 kPa
RT at 6.3 kHz	1.35 s	1.07 s	1.38 s	1.10 s
METRIC SABINE	27.9 m <sup>2</sup>	35.5 m <sup>2</sup>	37.1 m <sup>2</sup>	47.2 m <sup>2</sup>
d <sub>min</sub> *	3.3 m	3.8 m	3.8 m	4.3 m

\* based on equation (2.1.2) <sup>1</sup> large room as source room <sup>2</sup> small room as source room

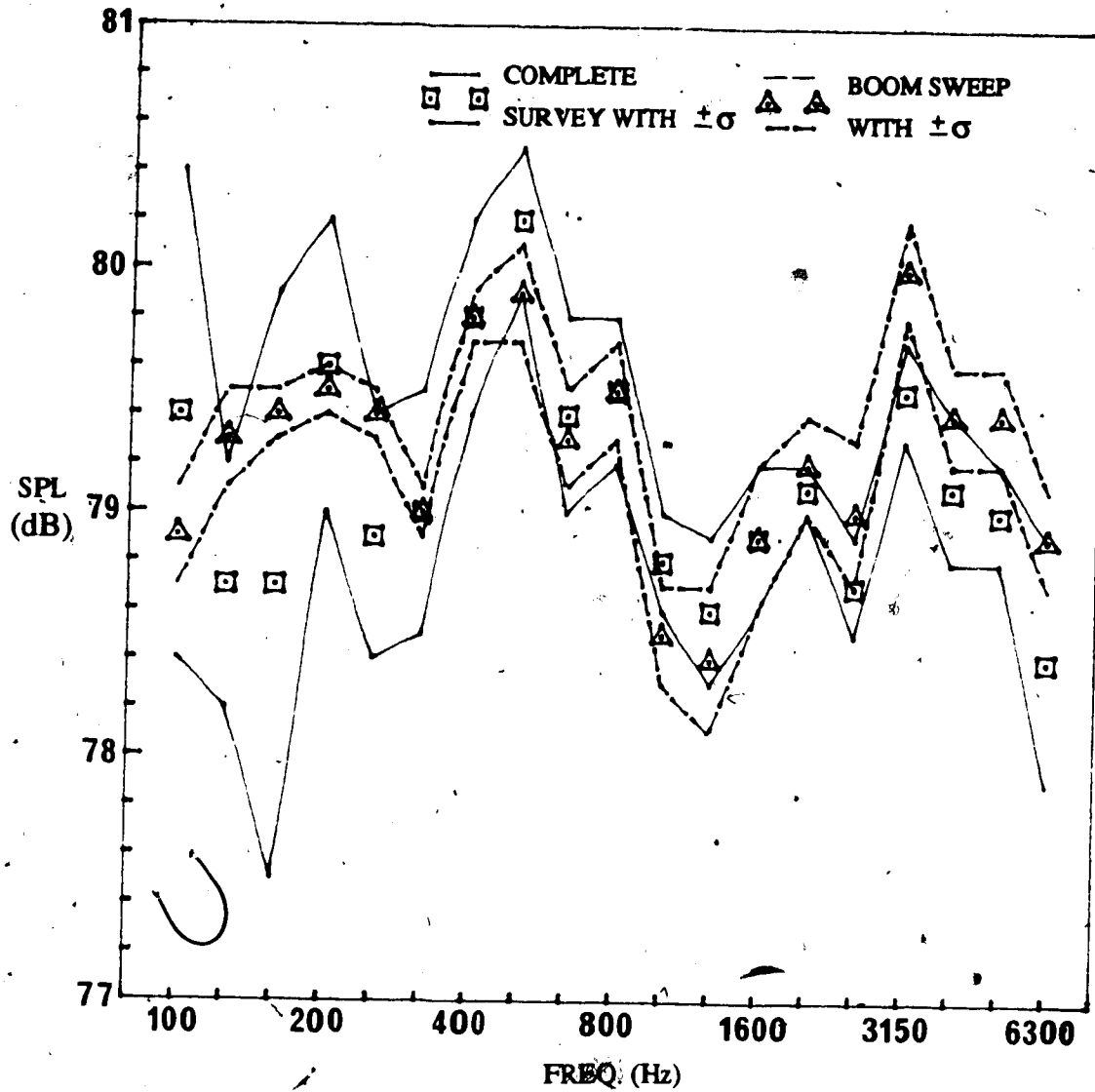


**FIG. 2.5 BOOM QUALIFICATION FOR THE LARGE CHAMBER AS THE RECEIVER ROOM**

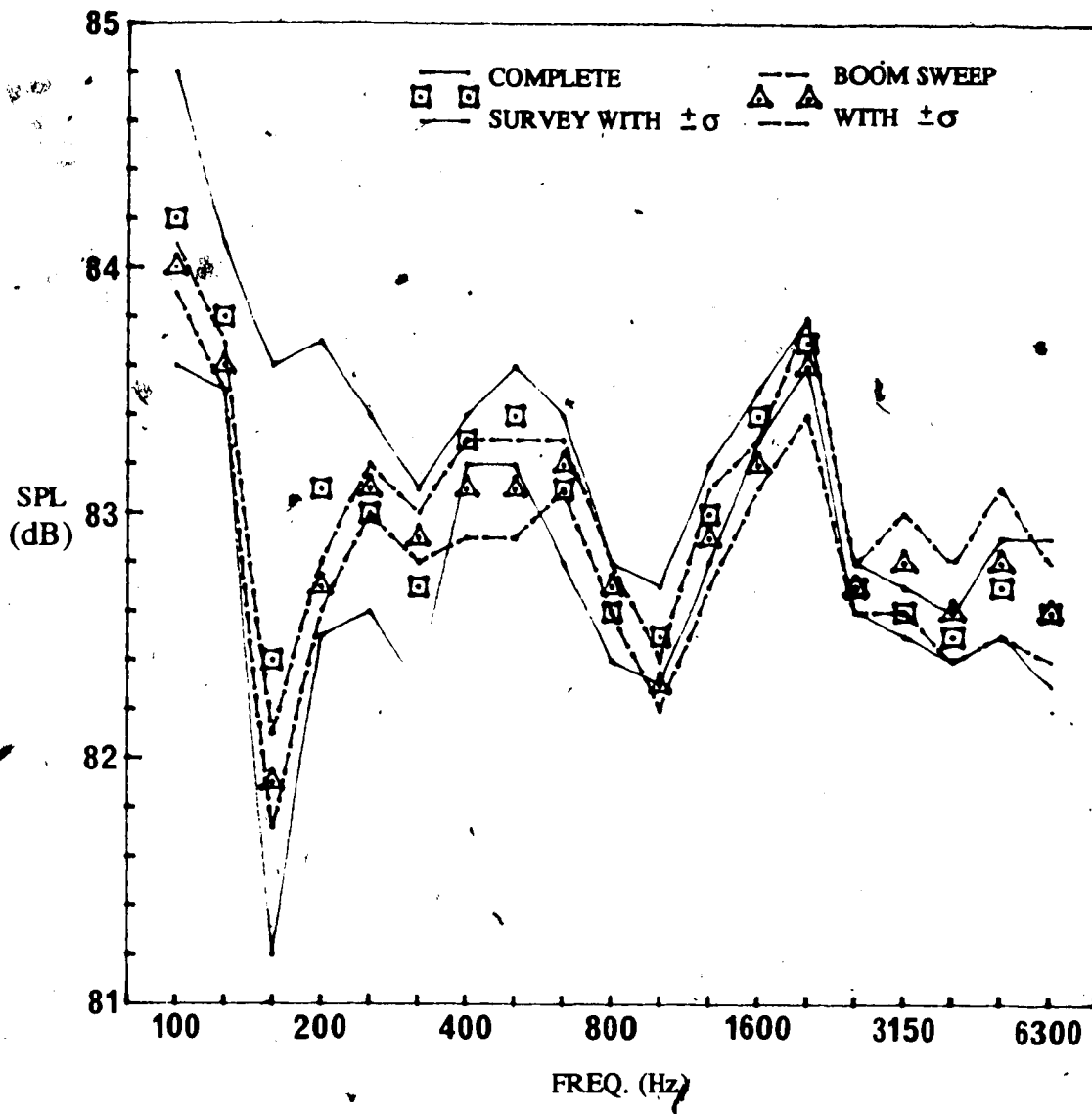


**FIG. 2.6 BOOM QUALIFICATION FOR THE SMALL CHAMBER AS THE RECEIVER ROOM**

As shown from these figures, the standard deviations of the boom sweep are much less since each complete sweep only produces one SPL for each frequency band, whereas a complete survey contains many SPL measurements depending on the number of measurement points. In general, the agreement between the two methods is better for the smaller test room. As shown from fig. 2.3, when the larger room is used as the source room, the means differ between 0 and 0.5 dB. However, the standard deviation band of the boom sweep still falls within the one from the complete survey, with acceptable limitations from the 2 kHz band and up. This could be contributed by a small change in air temperature or relative humidity during the test, since air absorption is very sensitive to these environmental factors at high frequencies. A change in air absorption would in turn affect the sound field being surveyed. As shown in fig. 2.4, when the smaller room is used as the source room, the means usually differ by only 0.1 dB. Again, the standard deviation band of the boom falls essentially within the other. Similar conclusions can be drawn from fig. 2.5 and 2.6, when the test rooms are used as receiver rooms. These results indicate that the rotating boom can adequately survey the reverberant field in any of the test rooms, whether used as the source or receiver room, with an acceptable difference of 0.5 dB compared to the point by point complete survey.

## 2.2 Test Room Qualification for The Measurement of

### Broadband Sound

The earlier sections deals with how well the rotating boom surveys the reverberant field in the test room. It is also necessary to determine the diffusivity of the reverberant field as generated by the room shape and moving diffusers. A test room qualification procedure is clearly outlined in the American National Standard ANSI 1.31-1980. (Revised 1986) entitled "Precision Methods for the Determination of Sound Power Levels of Broad-band Noise Sources in Reverberation Rooms". The test provides more information about the uncertainties in the space and time average procedure but more importantly a measure of the uncertainties in the coupling between the noise source and the sound field.

The instrumentation and microphone traverse were the same as the CTL test with the addition of a reference sound source (Bruel and Kjaer 4204). The plug wall was placed in the test opening. Again, the results can be generally applied to situations when a different wall is placed because of the relatively small significance of the wall compared to air absorption. Eleven measurements of SPL by the rotating boom with the same duration of a CTL test were made, each with the reference sound source placed on the floor no closer than 1.5 m from a wall and not closer to any microphone traverse position than 1.8 m for the small room and 2.1 m for the large, as calculated from the equation

$$d = 0.16 ( V / T )^{1/2} \quad (2.2.1)$$

where  $V$  = volume of the test room,  $m^3$

$T$  = 60 dB reverberation time, s

The distance between any two source locations was 1.1 m, which was greater than 0.85 m, the quarter wavelength of the lowest qualifying frequency of 100 Hz. The arithmetic means and standard deviations of all source locations for each frequency band and the specified limits are listed in table 2.3a and 2.3b. Since no standard deviations exceed the specified limits, it was concluded that the sound field was sufficiently diffuse in each room down to 100 Hz with acceptable uncertainties.

### 2.3 Coherent and Incoherent Noise Source

It should be mentioned that the boom qualification test was done with the two speaker channels driven simultaneously by a coherent noise source. This is not recommended by the ASTM standard. A new sound system with an incoherent noise generator was later installed to improve the facility at MEANU. CTL tests were repeated with the two speaker channels driven simultaneously by the incoherent noise source and the results are compared with the results obtained earlier with the coherent sound system, as shown in fig. 2.7 and 2.8 for the forward and reverse approach.

The results of the frequency bands within the limiting qualified frequencies of 100 to 6300 Hz were compared only. Fig. 2.7 shows that the CTL results differ by an average of 0.5 dB and the difference exceeds 0.5 dB in 4 of the 19 frequency bands for the forward approach, when the source room is the smaller one. In comparison, fig. 2.8 shows that the CTL results differ by an average of 0.3 dB, and more than 0.5 dB only in 2 frequency bands for the reverse



**TABLE 2.3a LARGE ROOM QUALIFICATION WITH REFERENCE SOURCE**

FREQUENCY (Hz)	ARITHMETIC MEAN (dB)	ARITHMETIC STANDARD DEVIATION $\sigma$ (dB)	SPECIFIED LIMITS ON $\sigma$ (dB)
100	74.7	1.0	1.5
125	76.1	0.3	1.5
160	76.7	0.4	1.5
200	76.6	0.2	1.0
250	78.1	0.2	1.0
315	78.2	0.1	1.0
400	77.5	0.1	1.0
500	77.6	0.1	1.0
630	78.4	0.1	1.0
800	80.3	0.1	0.5
1000	81.8	0.1	0.5
1250	82.6	0.1	0.5
1600	82.4	0.1	0.5
2000	82.1	0.1	0.5
2500	80.5	0.1	0.5
3150	78.6	0.1	1.0
4000	77.5	0.1	1.0
5000	76.1	0.1	1.0
6300	74.1	0.2	1.0
8000	72.2	0.3	1.0
10000	69.8	0.3	1.0

**TABLE 2.3b SMALL ROOM QUALIFICATION WITH REFERENCE SOURCE**

FREQUENCY (Hz)	ARITHMETIC MEAN (dB)	ARITHMETIC STANDARD DEVIATION $\sigma$ (dB)	SPECIFIED LIMITS $Q_N \sigma$ (dB)
100	73.5	0.9	1.5
125	75.1	0.5	1.5
160	76.2	0.2	1.5
200	76.8	0.3	1.0
250	78.3	0.3	1.0
315	78.6	0.1	1.0
400	78.1	0.1	1.0
500	78.0	0.1	1.0
630	78.9	0.2	1.0
800	81.0	0.2	0.5
1000	82.5	0.2	0.5
1250	83.4	0.2	0.5
1600	83.1	0.1	0.5
2000	82.8	0.2	0.5
2500	81.1	0.2	0.5
3150	79.3	0.2	1.0
4000	78.3	0.2	1.0
5000	77.0	0.2	1.0
6300	75.2	0.2	1.0
8000	73.0	0.2	1.0
10000	70.3	0.4	1.0

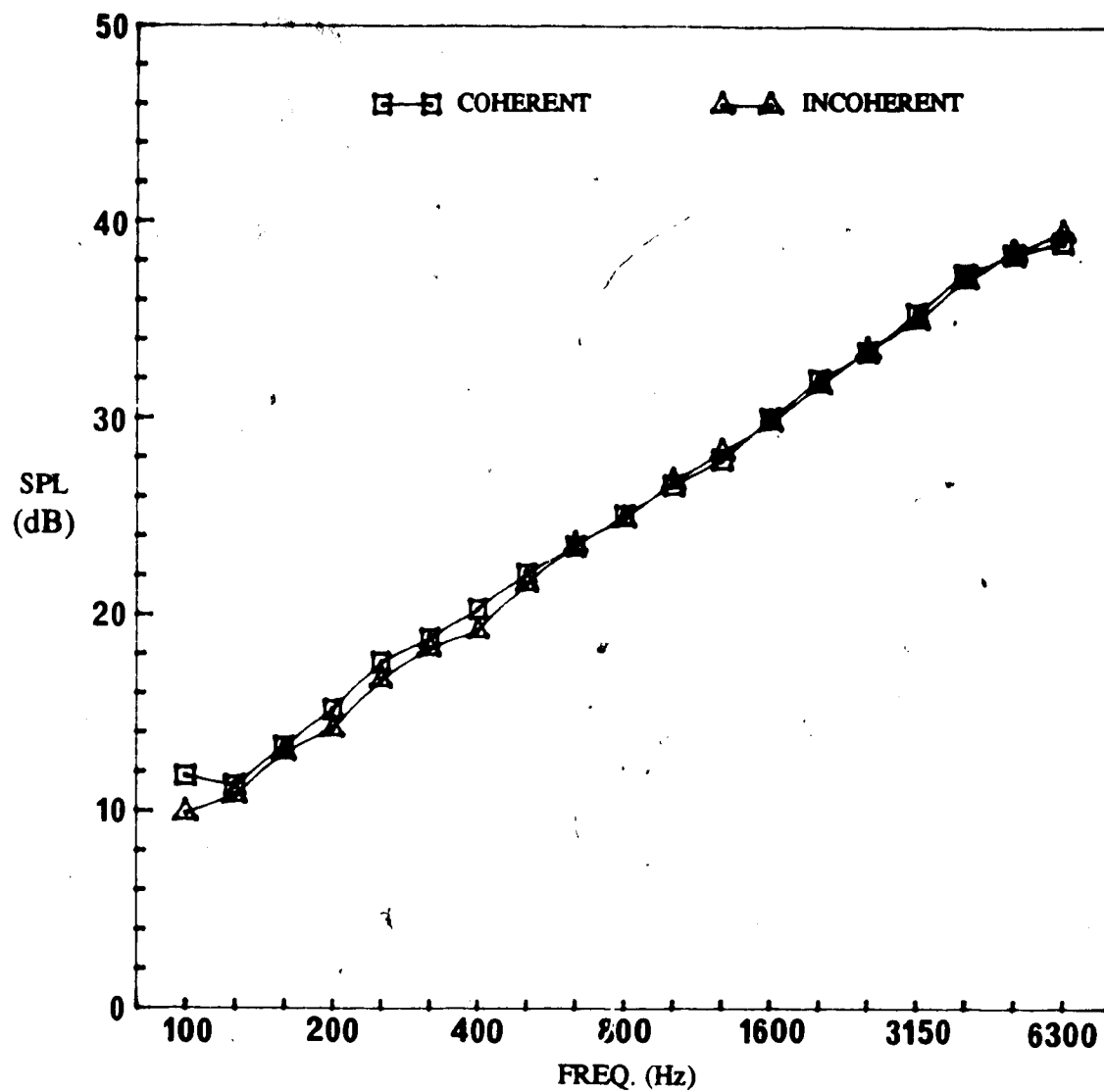


**FIG. 2.7 FORWARD CTL TESTS OF USING COHERENT AND INCOHERENT NOISE SOURCE**

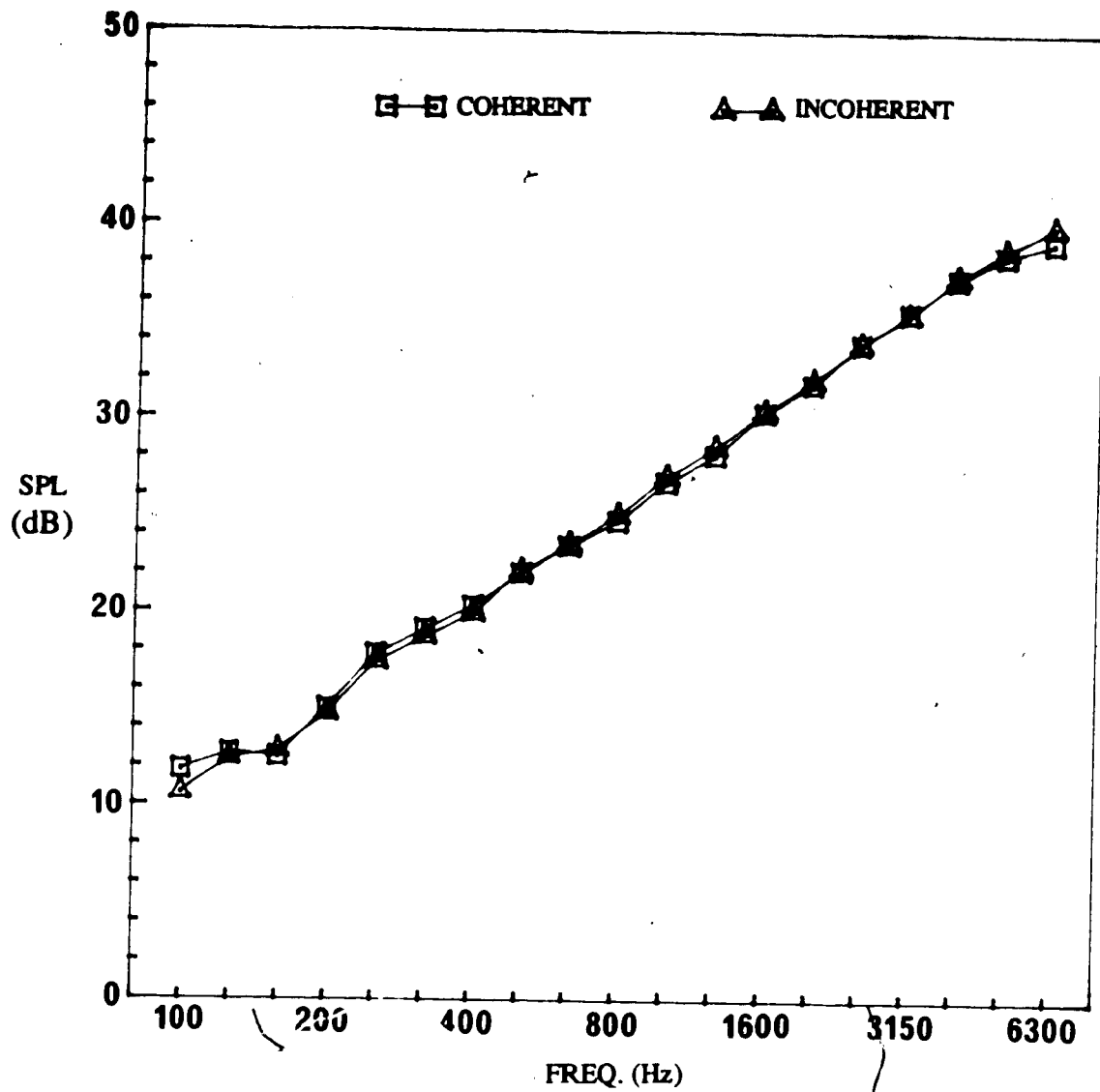


**FIG. 2.8 REVERSE CTL TESTS OF USING COHERENT AND INCOHERENT NOISE SOURCE**

approach, when the source room is the larger one. These results generally indicate the errors due to the use of a coherent noise source. Also, the comparison shows that the coherent noise source has a larger effect in a smaller space, which is the case for the forward approach.

## Chapter 3 Sound Intensity Techniques

In order to use the sound intensity analyser system with confidence in any particular application, the fundamental nature of the hardware and its limitations towards the application have to be understood.

There are basically two types of dual channel analysers for frequency analysis, namely Fast Fourier Transform (FFT) and Digital Filtering. Each system is based on fundamentally different principles, which are favourable for certain applications. As the system is used to obtain sound intensity, this application would impose certain requirements on the hardware. Since no hardware is perfect, the errors and limitations of a sound intensity analyser system have to be investigated.

With this background information, a system overview and the calibration procedure and results will also be presented in this chapter.

### 3.1 Fast Fourier Transform & Digital Filtering

The following discussion in section 3.1.1 and 3.1.2 is essentially based on "An Introduction to Random Vibration and FFT Analysis"<sup>11</sup> by D. E. Newland and "Application of B & K Equipment to Frequency Analysis"<sup>12</sup> by R. B. Randall.

#### 3.1.1 FFT

For stationary signals, one can write

$$I(r) = \overline{p(r,t) \cdot u(r,t)} \quad (3.1.1)$$

where the bar indicates suitably long averaging time. The cross correlation function  $R_{pu}$  of  $p(r,t)$  and  $u(r,t)$  is expressed as

$$R_{pu}(r,\tau) = \overline{p(r,t) \cdot u(r,t + \tau)} \quad (3.1.2)$$

where  $\tau$  is the time difference. For  $\tau = 0$ , sound intensity can be written as

$$I(r) = R_{pu}(r,0) \quad (3.1.3)$$

Using the spectral density function  $S_{pu}(r,\omega)$ , which is the Fourier Transform of  $R_{pu}(r,\tau)$ , ie.

$$S_{pu}(r,\omega) = 1/2\pi \int_{-\infty}^{\infty} R_{pu}(r,\tau) e^{-i\omega\tau} d\tau \quad (3.1.4)$$

with its inverse

$$R_{pu}(r,\tau) = \int_{-\infty}^{\infty} S_{pu}(r,\omega) e^{i\omega\tau} d\omega \quad (3.1.5)$$

it can be shown that  $\text{Re}\{S_{pu}(r,\omega)\}$  is even and  $\text{Im}\{S_{pu}(r,\omega)\}$  is odd, when  $R_{pu}(r,\tau)$  is a real function, and that (3.1.3) can be written as

$$I(r,\omega) = -2 \text{Im}(S_{AB}) / \omega \rho \Delta r = - \text{Im}(G_{AB}) / \omega \rho \Delta r \quad (3.1.6)$$

where  $G_{AB}$  is the one sided spectra, obtained by folding the two sided spectra  $S_{AB}$  to the positive frequency domain.

A FFT analyser is used to calculate the cross spectrum. The nature and accuracy of sound intensity is then a direct result of the algorithm of the FFT transform. When the cross correlation function of two identical signals is obtained instead of two different ones, it is

called the auto correlation function described by

$$R_x(\tau) = x(t) x(t + \tau)$$

The Fourier Transform of an auto correlation function is called the auto spectrum function

$$S_x(\omega) = 1/2\pi \int_{-\infty}^{\infty} R_x(\tau) e^{-i\omega\tau} d\tau \quad (3.1.7)$$

Since the statistical nature of the auto spectrum is very close but simpler than the cross spectrum, it is used here to illustrate some fundamental properties they both share.

A measurement record is only available for the period from  $t=0$  to  $t=T$ . The auto correlation function can only be determined for  $|\tau| < T$ . Therefore,  $S_x(\omega)$  can only be approximated by truncating the integral in (3.1.7) such that

$$S_x(\omega) = 1/2\pi \int_{-T}^T R_x(\tau) e^{-i\omega\tau} d\tau \quad (3.1.8)$$

This is a fundamental difficulty in accurately obtaining  $S_x(\omega)$  since it is impossible to have an infinite record. It can be shown that an infinite record of a single sinusoidal function will be transformed to a delta function in the positive and negative frequency of the function. However, a finite record will smear out the sharp spectral line of the delta function over a band of frequencies of width  $\Delta\omega = 2\pi/T$  with small fluctuations in the neighborhood frequencies (fig. 3.1). One way of reducing these fluctuations is to smooth the spectrum such that the smoothed spectrum is



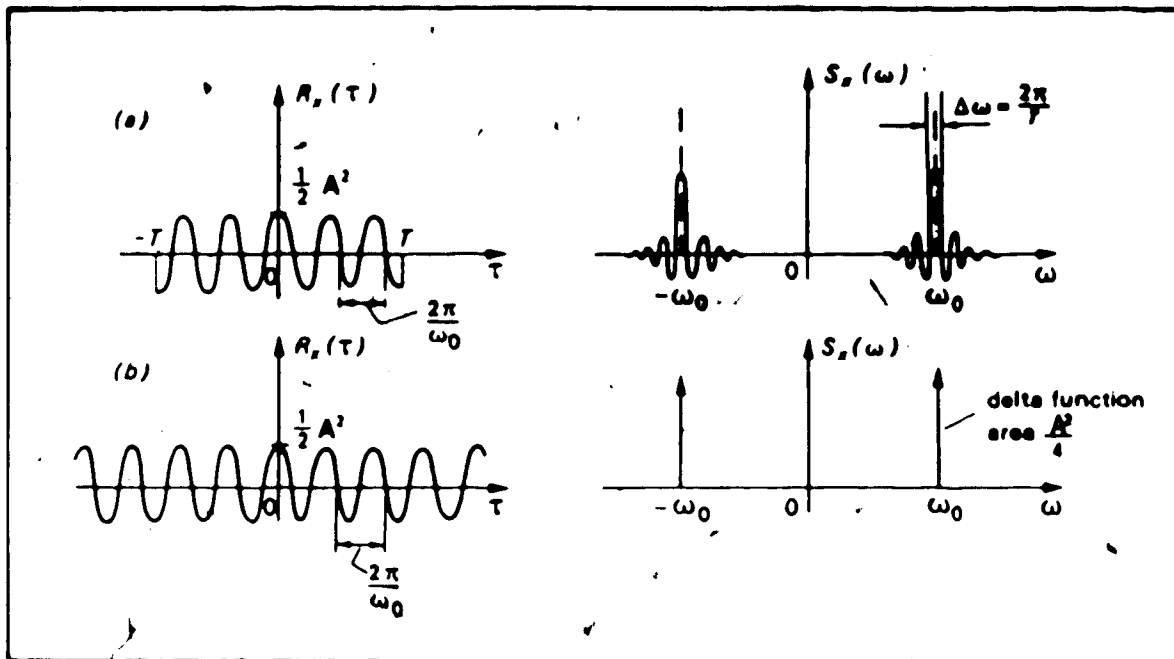


**FIG. 3.1 FOURIER TRANSFORM OF A FINITE LENGTH OF A COSINE WAVE COMPARED WITH THE TRANSFORM OF AN INFINITE LENGTH (ADAPTED FROM NEWLAND<sup>11</sup>)**

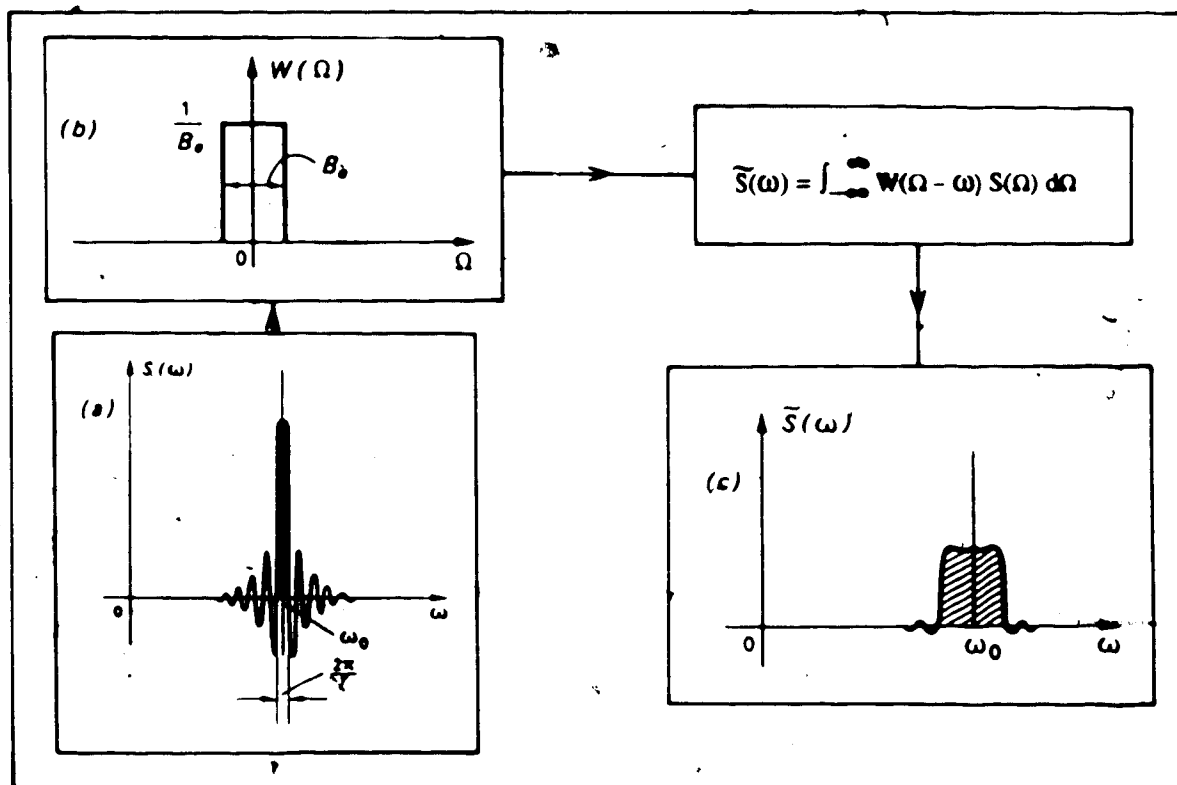


**FIG. 3.2 SMOOTHING WITH A RECTANGULAR SPECTRAL WINDOW (ADAPTED FROM NEWLAND<sup>11</sup>)**

$$\bar{S}(\omega) = \int_{-\infty}^{\infty} W(\Omega - \omega) S(\Omega) d\Omega$$

in which  $\Omega$  = dummy variable and the weight function  $W(\Omega)$ , or commonly called the spectral window function, satisfies

$$\int_{-\infty}^{\infty} W(\Omega) d\Omega = 1 \quad (3.1.9)$$

The effective bandwidth of a spectral window is defined by

$$B_e = 1 / \int_{-\infty}^{\infty} W^2(\Omega) d\Omega$$

A rectangular spectral window is shown and the smoothed spectrum is shown in fig. 3.2. The fluctuation will be less for a  $W(\Omega)$  with a larger effective bandwidth. The shaded area in fig. 3.2.a & 3.2.c is the same but a less rippled spectrum is obtained. However, the frequency resolution is also decreased. Therefore, it is clear that the accuracy of the auto spectrum depends on two factors, the record length and the effective bandwidth of the spectral window. A higher value of either will decrease the amount of ripples. It can be shown<sup>13</sup> that the relative variance of the spectrum  $\sigma/m$  is described by

$$\sigma/m = 1 / \sqrt{B_e T} \quad (3.1.10)$$

where  $\sigma$  = standard deviation of auto spectrum

$m$  = mean value of auto spectrum

$B_e$  = effective bandwidth of the spectral window, rad/s

$T$  = record length, s

For a discretized signal input obtained from a digital analyser, the record length is  $N\Delta$ , in which  $\Delta$  = sampling interval and  $N$  is the total

number of data points. The Discrete Fourier Transform (DFT) is used to calculate Fourier Transform in a digital manner. In digital analysis, a discrete time series  $x_r$ ,  $r=0,1,2,3,\dots,(N-1)$ , is generated from a continuous source of signal. Following (3.1.8), a discrete Fourier Transform  $X_k$  is

$$X_k = 1/N \sum_{r=0}^{N-1} x_r e^{-i(2\pi kr/N)}, \quad k=0,1,2,3,\dots,(N-1) \quad (3.1.11)$$

and the auto correlation function  $R_x(r)$  is

$$R_x(r) = 1/N \sum_{s=0}^{N-1} x_s x_{s+r}, \quad r=0,1,2,3,\dots,(N-1) \quad (3.1.12)$$

From (3.1.11) & (3.1.12), it can be shown that  $S_x(\omega)$  can be written in the discrete form as

$$S_x(\omega) = 1/N \sum_{r=0}^{N-1} \left\{ 1/N \sum_{s=0}^{N-1} x_s x_{s+r} \right\} e^{-i(2\pi kr/N)} \quad (3.1.13)$$

such that

$$S_x(\omega) = X_k X_k^* \quad (\text{a product of the conjugate pair}) \quad (3.1.14)$$

In other words, the correlation function is not calculated first to obtain the spectral density function  $S_x(\omega)$ . It is replaced by the calculation of the DFT of the series  $\{x_r\}$ .

The definition of DFT (3.1.12) suggests that the sequence of  $\{x_r\}$  is periodic such that  $x_{s+r} = x_s$ . Because of this implied periodicity,  $R_x$  differs from the true correlation function it is meant to represent, as illustrated in fig. 3.3 for the case of  $N=10$ ,  $r=4$ .

$$R_x(4) = 1/10 \{ x_0x_4 + x_1x_5 + x_2x_6 + x_3x_7 + x_4x_8 + x_5x_9 \} \\ + 1/10 \{ x_6x_0 + x_7x_1 + x_8x_2 + x_9x_3 \} \quad (3.1.15)$$

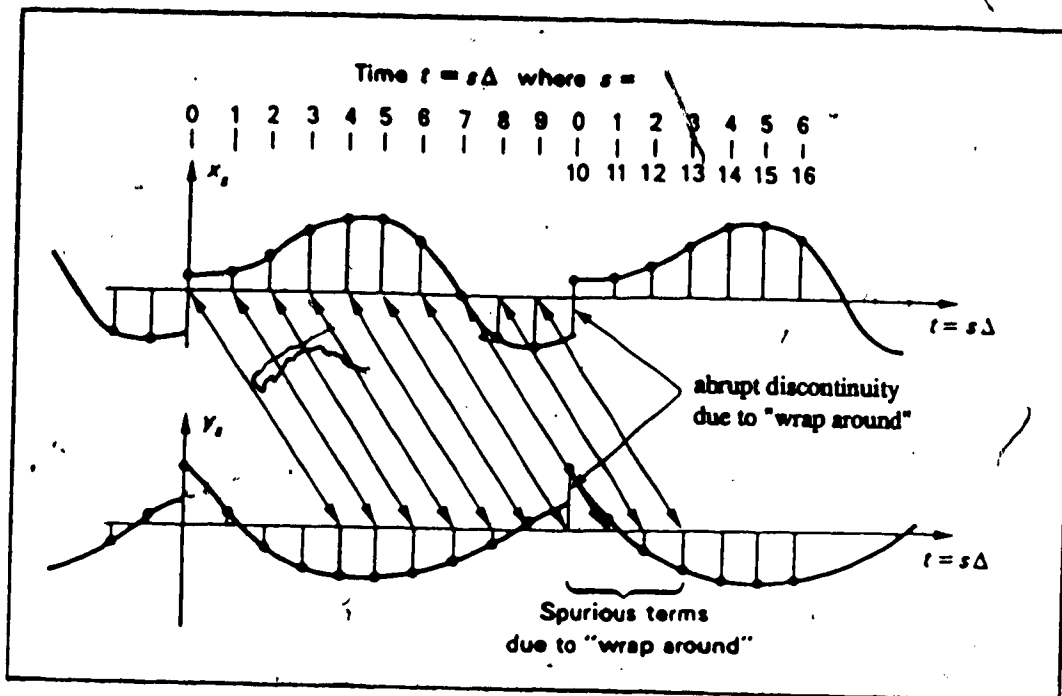


**FIG. 3.3 EFFECT OF "WRAP AROUND" ON THE CALCULATION OF CORRELATION FUNCTIONS (ADAPTED FROM NEWLAND<sup>11</sup>)**

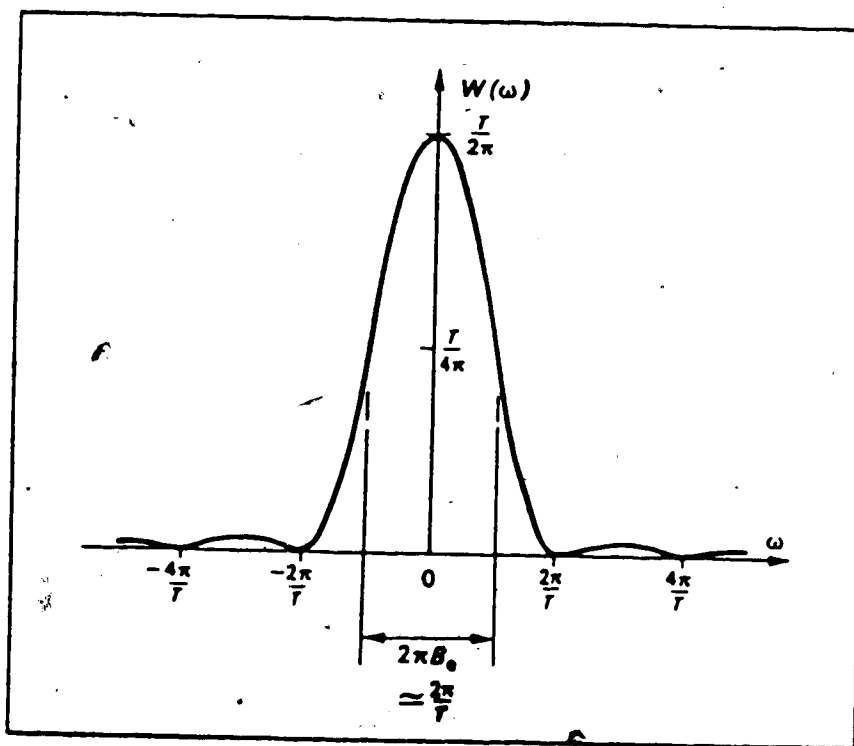


**FIG. 3.4 BASIC LAG AND SPECTRAL WINDOWS FOR SPECTRAL ANALYSIS BY DFT (ADAPTED FROM NEWLAND<sup>11</sup>)**

The first term in (3.1.15) is an estimate for  $R(\tau = 4\Delta)$  but the second term in (3.1.15) has nothing to do with  $R_x(\tau = 4\Delta)$  at all. Instead, it is an estimate for  $R(\tau = -6\Delta)$ . Furthermore, both terms are biased estimates for  $R_x(\tau)$  since the denominator would obviously have to be 6 (not 10) in the first case and 4 (not 10) in the second. Therefore, it is apparent that there is some subtle approximation in using (3.1.11) and (3.1.14) to calculate the spectral density function. Actually, an estimated spectrum  $S(\omega)$  is obtained effectively to be a smoothed version of the true and the effective spectral window of the DFT which can be approximated by

$$W(\omega) = T/2\pi [ \sin(\omega T/2) / (\omega T/2) ]^2 \quad (3.1.16)$$

with its shape shown in fig. 3.4. This is not quite the ideal rectangular window described earlier.

The effective bandwidth  $B_e$  has been calculated for many window approximations, including (3.1.16). It turns out that

$$B_e = 1/T \text{ Hz}$$

is a satisfactory approximation for most practical calculations. Recalling that

$$\sigma/m = 1/\sqrt{B_e T}$$

one obtains  $\sigma/m = 1$ . This means that the accuracy is very poor. Intuitively one would expect to increase accuracy by increasing record length  $T$ . But since  $B_e = 1/T$ ,  $B_e T = 1$  regardless of the magnitude of  $T$ . Therefore, increasing  $T$  only improves resolution

(smaller  $B_e$ ) but the accuracy maintains the same.

To improve the accuracy, the only thing to do is to average adjacent estimates of the smoothed spectrum  $\tilde{S}(\omega_k)$ . If  $n+1$  adjacent values are averaged, the further smoothed spectrum  $\hat{S}(\omega_k)$  is described by

$$\hat{S}(\omega_k) = (1/(2n+1)) \sum_{m=-n}^n \tilde{S}(\omega_{k+m})$$

For the case of  $(2n+1)=3$ , the shape of the resulting spectral window is sketched in fig. 3.5. The equivalent bandwidth is now  $(n+1) \cdot 2\pi/T$  instead of  $2\pi/T$ . Therefore,  $B_e$  has been increased while  $T$  is kept the same, and now

$$\sigma/m = \sqrt{1/(2n+1)} \quad (3.1.17)$$

However, the resolution has been decreased. After averaging  $(2n+1)$  adjacent values, not all  $N$  points are independent of each other anymore. Actually, only  $N/(2n+1)$  points should be plotted with the  $n^{\text{th}}$  point from the D.C. ( $\omega=0$ ) point as the first valid point.

It can be easily be shown that, the coefficients  $X$  calculated by DFT are only correct and unique for frequencies up to  $\omega_k = 2\pi k/N\Delta = \pi/\Delta$  as shown in fig 3.6. Second, if there are frequencies above  $\omega_k$  present in the original signal, the spectrum will have a distortion, called aliasing. If  $\omega_0$  is the maximum frequency component present in  $x(t)$ , then aliasing can be avoided by ensuring that the sampling interval  $\Delta$  is small enough that

$$\pi/\Delta \geq \omega_0$$

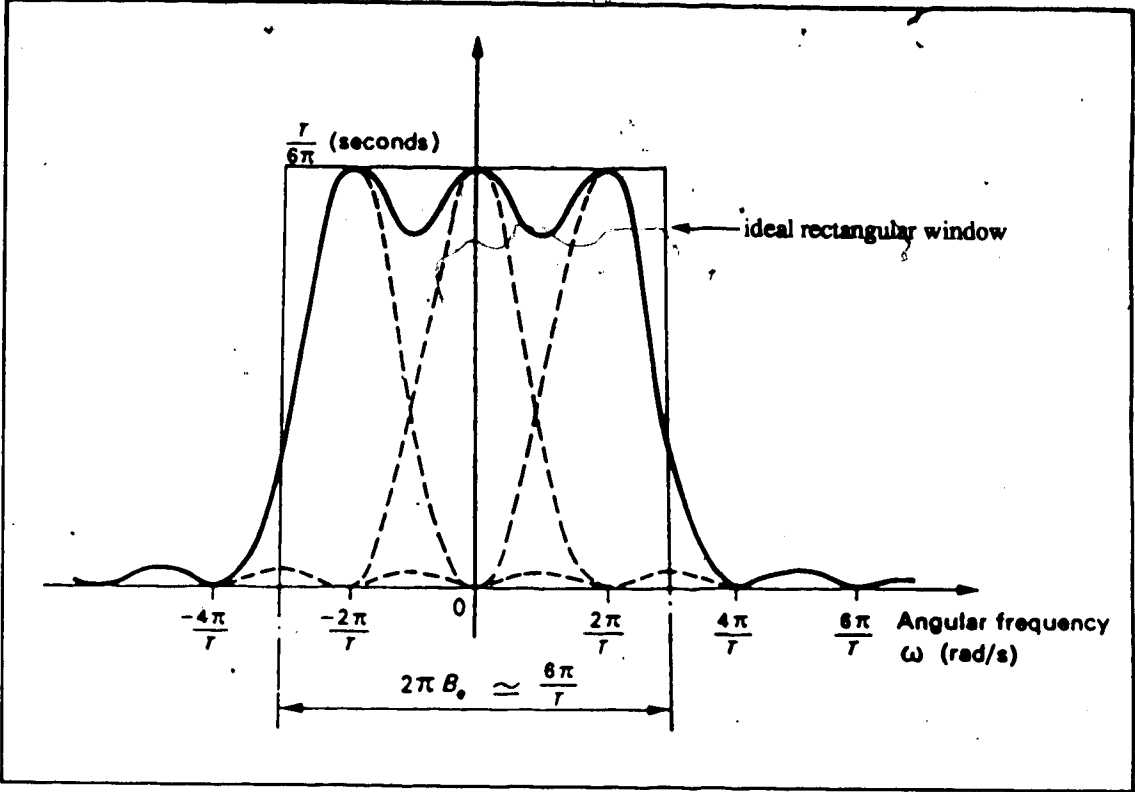


**FIG. 3.5 EQUIVALENT SPECTRAL WINDOW AFTER AVERAGING THREE ADJACENT SPECTRAL ESTIMATES (ADAPTED FROM NEWLAND<sup>11</sup>)**

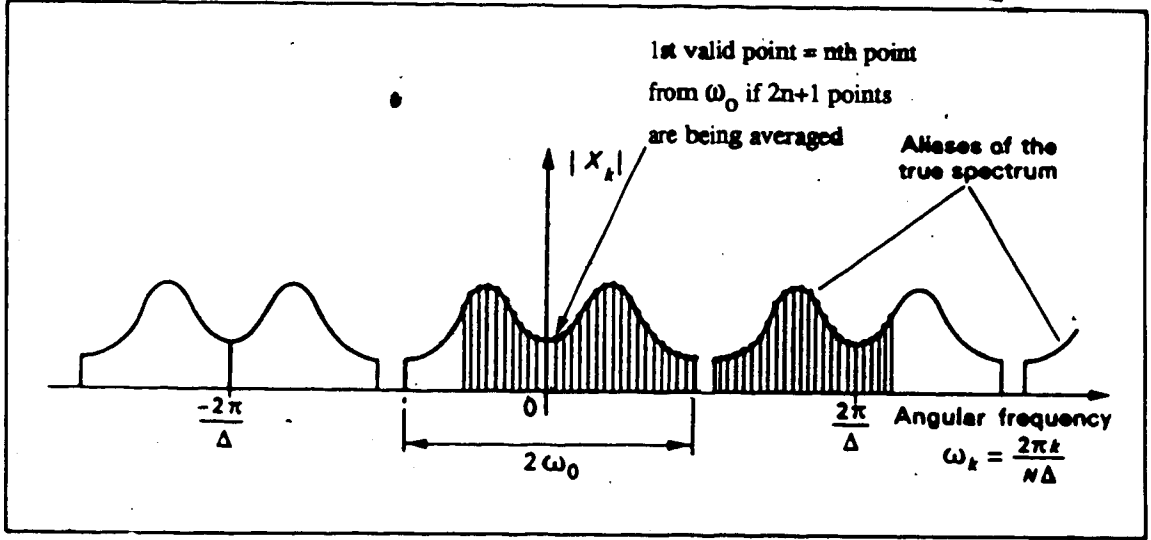


**FIG. 3.6 PERIODICITY OF FOURIER COEFFICIENTS CALCULATED BY THE DFT (ADAPTED FROM NEWLAND<sup>11</sup>)**

ie  $1/2\Delta \geq f_0$  if  $f_0 = \omega_0/2\pi$

The frequency  $1/2\Delta$  Hz is called the Nyquist frequency, which is the maximum frequency that can be detected from data which are sampled at the time spacing  $\Delta$ . In other words, the maximum significant frequency of the signal dictates that data should be sampled at twice the rate. The above result could also be derived from Shannon's sampling theorem, which states generally that the spacing of data should be at least half as small as the required resolution in order to represent the function accurately. The Nicolet dual channel analyser uses a sampling rate of 2.56 times of the most significant frequency.

FFT is an effective means to calculate DFT's. It can be shown that FFT only requires  $1/2 N \log_2 N$  complex multiplications and  $N \log_2 N$  complex additions, compared to  $N^2$  complex multiplications and  $N(N-1)$  complex additions required by calculating  $R_x$  directly by DFT. If  $1/2 \log_2 N$  and  $\log_2 N$  are compared to  $N$  for large values of  $N$ , one can begin to appreciate the savings in data processing time by FFT. However, according to the calculation scheme of FFT, a discrete data series of length  $2^n$  ( $n$  is a positive integer) is usually required. For the Nicolet FFT analyser, the choice of a sampling rate of 2.56 times of the most significant frequency ensures a total of  $2^{10}$  data points are available over the sampling period determined by  $B_e T = 1$ .

It has been shown that FFT produces a spectrum with a



constant bandwidth (or resolution) by analyzing a block of data which arrived over a sampling period. The freedom to choose a short sampling time for faster calculation is limited because of the problem of antialiasing and the  $B_e T$  product relationship. If a high resolution spectrum is required,  $T$  has to be long. This also results in a lower frequency range, which requires filtering of the original signals, but this may unfortunately filter off some of the significant signals as well. On the other hand, resolution can be sacrificed for a shorter sampling period  $T$ .

The limitation of FFT in "real time" analysis is then obvious. On the other hand, it will be shown that Digital Filtering offers a higher potential in that regard but it produces a spectrum on a constant percentage bandwidth basis, which generally does not have as high a resolution as the constant absolute bandwidth offered by FFT.

### 3.1.2 Digital Filtering

As mentioned in the introduction, the particle velocity and the pressure at the midpoint of the microphone positions can be approximated by (1.1.2) and (1.1.3). Following these equations and the definition of sound intensity, it can easily be shown<sup>14</sup> that Digital Filtering processes the pressure data based on the equation

$$I = - (1/2 \rho \Delta r) (p_A + p_B) \int (p_A - p_B) dt$$

to obtain sound intensity.

To achieve "real time" capability, the Digital Filtering analyser

has a network of filtering systems, which time-share very efficiently. The shape of the filters can usually be defined by 2<sup>nd</sup> order differential equations. It can be shown<sup>12</sup> that the application of the z transform to the difference equation equivalent to a 2<sup>nd</sup> order differential equation yields the transfer function of the digital system as follows:

$$H(z) = (A_0 + A_1 Z^{-1} + A_2 Z^{-2}) / (1 - B_1 Z^{-1} - B_2 Z^{-2}) \quad (3.1.18)$$

and the general flow diagram for this 2<sup>nd</sup> order (2 pole) system is shown in fig. 3.7, where  $A_0$ ,  $A_1$ ,  $A_2$  are the zeros and  $B_1$  and  $B_2$  are the poles of the filter. These five coefficients completely define the shape of the filter, such as highpass, lowpass, bandstop or bandpass, with its relative bandwidth. However, the absolute range of frequencies being filtered is defined by the sample frequency, ie. the frequency at which signals are fed to the filter.

The B & K Digital Frequency Analyser Type 2131 is used here to illustrate how the Digital Filtering system works. The block diagram of such filtering system is shown in fig. 3.8. Each 2-pole digital filter has the same configuration as shown in fig. 3.7. This analyser basically does third octave analysis. In fig 3.8, each sample coming from the A/D converter is passed simultaneously through a 1/3 octave bandpass filtering section (bottom right). In fact, each sample is passed through each section 3 times for the following reasons:

- (1) 1/3 octave band pass filtering

The 1/3 octave filter section consists of three 2-pole filter

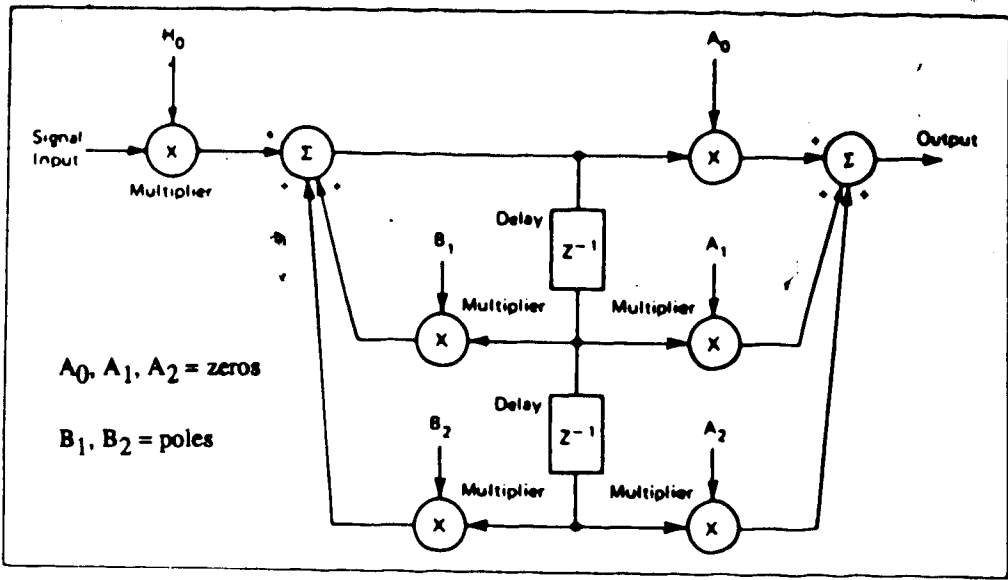


**FIG. 3.7 GENERALIZED BLOCK DIAGRAM OF A 2-POLE RECURSIVE DIGITAL FILTER (ADAPTED FROM RANDALL<sup>12</sup>)**

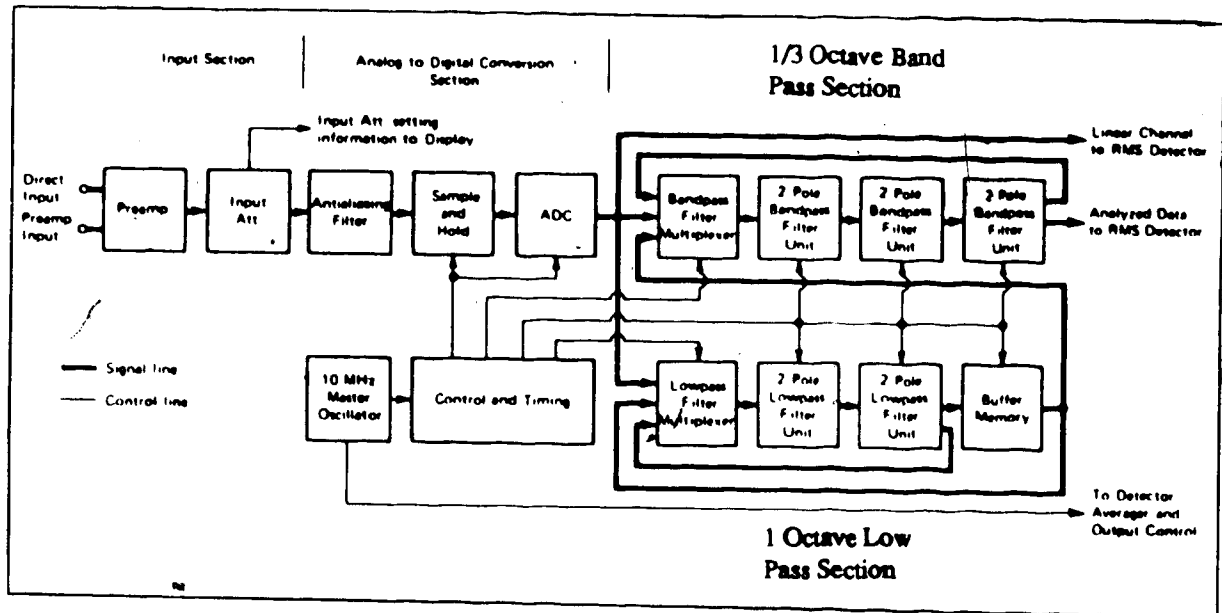


**FIG. 3.8 BLOCK DIAGRAM OF INPUT AND FILTER SECTION OF 2131 (ADAPTED FROM RANDALL<sup>12</sup>)**

units in series and for each pass, specific coefficients are used to give an effectively 6-pole filter of a  $1/3$  octave bandwidth. For each pass, the filter coefficients are changed by the control and timing box so as to obtain successively the three  $1/3$  octave center frequencies in each  $1/3$  octave. These frequencies are 20 kHz, 16 kHz, and 12.5 kHz in the highest octave for a type 2131 analyser. The change of coefficients is necessary because the sample frequency is the same for the three passes. The filter characteristics are illustrated in fig 3.9.

(2) low-pass filtering

The low-pass section consists of two 2-pole filter units in series. Thus, during the three passes used to obtain the three  $1/3$  octave filtered values, it is possible to circulate the data value three times through the effectively 4-pole low-pass filter section, achieving a 12-pole low-pass filtration. In this case, a Butterworth filter is constructed such that the cut-off frequency of the lowpass filter is one octave lower than the previous maximum frequency content. This means that the cut-off frequency decreases by  $1/2$  for each complete 12-pole filtering.

When the data sample has been passed 3 times through each filter section, three  $1/3$  octave spectra of an octave and a set of data of one octave lower are obtained. This new sample will then be fed to the bandpass section for another three passes. As explained earlier, the three  $1/3$  octave passes

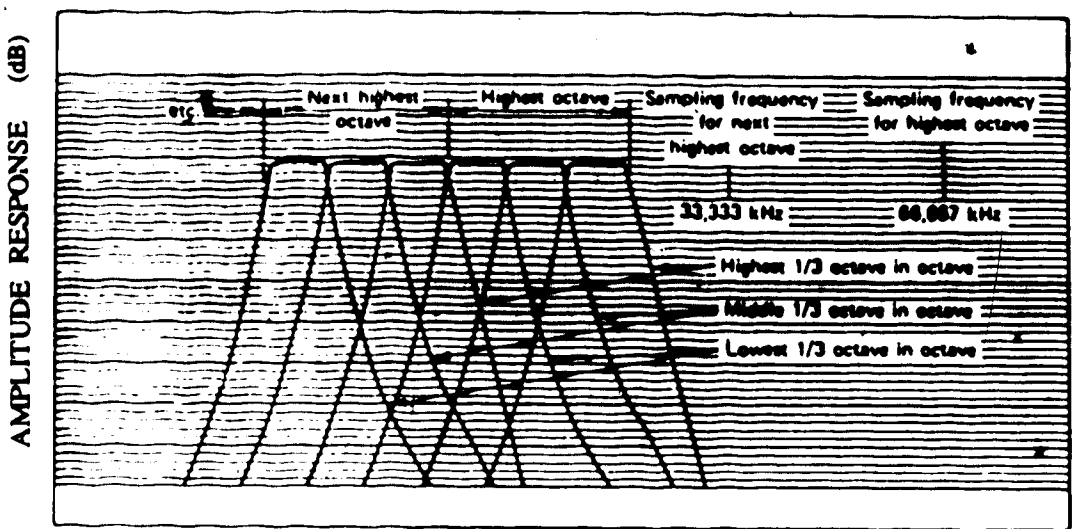


**FIG. 3.9 FILTER CHARACTERISTIC VS. SAMPLING FREQUENCY**  
(ADAPTED FROM RANDALL<sup>12</sup>)

automatically shift to an octave lower since the sample frequency has been decreased by an octave by the low-pass filter section. The same three sets of coefficients will be used for the new three passes.

The ability to time-share efficiently when the frequency scale is based on octaves is the major reason that digital filters are so well adapted to logarithmic frequency scales and constant percentage bandwidth.

It is therefore apparent that because of the nature of the operating system, Digital Filtering continuously decomposes the time domain pressure data into frequency domain results in real time and is particularly suited to detect transient signals. On the other hand, FFT is only appropriate for steady state problems since it analyses data blockwise, obtained in a delayed fashion. Also, Digital Filtering can more readily provide broad band third octave measurements, but FFT is advantageous in narrow band analysis, such as discrete frequency or harmonics monitoring.

### 3.2 System Overview

The process of TL tests is steady state and a FFT system is adequate. Instead of a commercial unit, the sound intensity system used consisted of different modular components to allow for a better understanding of the working process. A schematic of the set up is shown in fig. 3.1. The B & K microphone probe with a pair of 1/2" and 1/4" phase matched microphones sends the signals through the

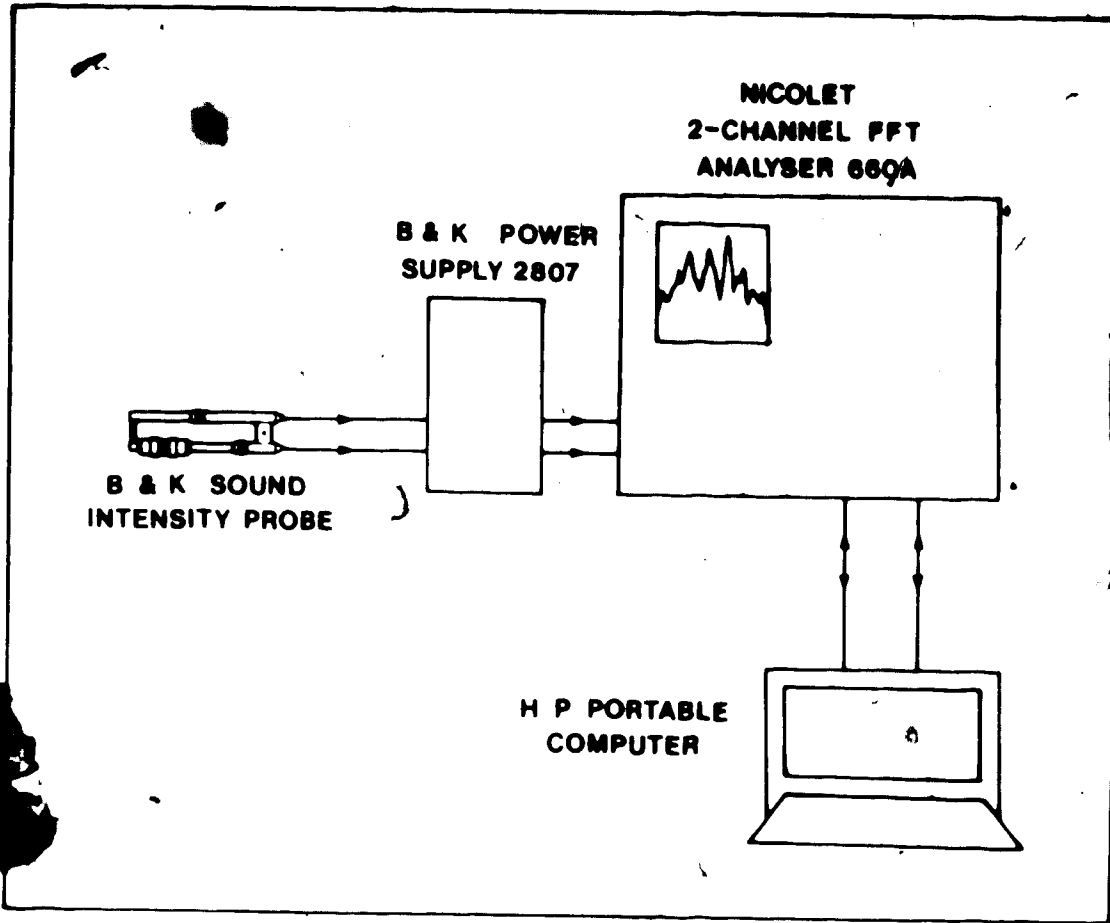


**FIG. 3.10 THE FFT SOUND INTENSITY SYSTEM AT MEANU**

B & K power supply to the Nicolet dual channel analyser. The imaginary part of the cross spectrum is calculated by the analyser and sent to the Hewlett Packard portable computer for calculations of sound intensity. The whole data collection process is essentially controlled by the computer.

### 3.3 Error Analysis

The most common sources of errors and limitations of measuring sound intensity are listed in table 3.1. As indicated in the introduction, sound intensity is defined as the time average of the product of pressure and particle velocity, which can be calculated from (1.1.1) & (1.1.3), as

$$u' = -1/\rho \int (\partial p / \partial r) dt \quad (1.1.1)$$

$$p = (p_A + p_B) / 2 \quad (1.1.3)$$

Therefore, the accuracy of sound intensity depends on how accurate by these two variables are obtained.

#### 3.3.1 Finite Difference Approximation

Ignoring the second and higher order terms, (1.1.1) can be written as  $u = -(1/\rho \Delta r) \int (p_B - p_A) dt$  (1.1.2), which is used in both FFT and Digital Filtering systems. It can be shown<sup>14</sup> that the higher order terms ignored will lead to an error in the estimated intensity measured  $\hat{I}$  as described by

$$\hat{I}/I = \sin(k\Delta r) / k\Delta r \quad (3.3.1)$$



**TABLE 3.1 ERRORS AND LIMITATIONS OF SOUND INTENSITY MEASUREMENT**

<b>ERRORS AND LIMITATIONS</b>		
<b>INSTRUMENTATION</b>	<b>STATISTICAL</b>	<b>SPECIAL SITUATION</b>
(1) FINITE DIFFERENCE APPROXIMATION	RANDOM ERROR (A FUNCTION OF REACTIVITY)	(1) NEGATIVE INTENSITY (VERY CLOSE FIELD)
(2) PHASE MISMATCH BETWEEN TWO CHANNELS a) MICROPHONES, PREAMPS, POWER SUPPLY, FFT b) RECORDER		(2) SPHERICAL WAVE REGION (NEAR FIELD)  (3) MEDIUM WITH FLOW

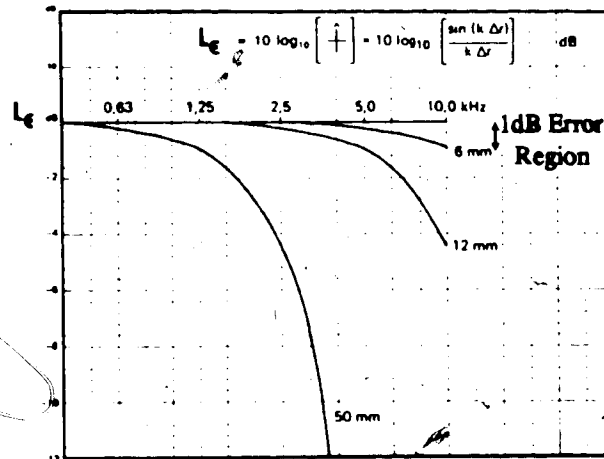


**FIG. 3.11 FINITE DIFFERENCE APPROXIMATION ERROR,  $L_e$  AT HIGH FREQUENCIES IN AN ACTIVE SOUND FIELD FOR VARIOUS SPACERS (ADAPTED FROM GADE<sup>15</sup>)**

where  $I$  = the true intensity

$k$  = the wave number =  $2\pi/\lambda$

$\Delta r$  = microphone spacing

For a plane wave propagating along the axis of the microphone probe, the 1<sup>st</sup> order approximation assumes the free field phase between the microphones is  $\sin(k\Delta r)$  instead of the true value of  $k\Delta r$ , i.e. the measurement technique underestimates by a  $(\sin x / x)$  function. If there exists an angle  $\alpha$  between the probe orientation and the direction of propagation, (3.3.1) becomes

$$\hat{I}_\alpha / I_\alpha = \sin(k\Delta r \cos \alpha) / k\Delta r \cos \alpha \quad (3.3.2)$$

where  $\hat{I}_\alpha$  = estimated intensity in the probe direction

$I_\alpha$  = true intensity in the probe direction

(3.3.1) and (3.3.2) both imply a high frequency limitation. A high frequency implies a shorter wavelength and higher wave number, which means that the ratio in (3.3.1) or (3.3.2) differs further from unity. Fig. 3.11 illustrates this phenomenon in an active sound field for various spacers.

### 3.3.2 Phase Mismatch Error

The finite difference approximation does not introduce any phase shift. Actually, multiplication of two signals in conjunction with time averaging is unaffected by any phase shifts of signals occurring between the measurement points to the computer, providing both signals undergo the same shifting. However, if the phase shifts in the

two channels,  $\phi_1$  and  $\phi_2$ , are different, it can be shown<sup>15</sup> that (3.3.1) becomes

$$\hat{I}/I = \sin(k\Delta r + \phi)/k\Delta r \quad (3.3.3)$$

where  $\phi$  is the relative phase shift (or phase mismatch) and

$$\hat{I}/I \approx (k\Delta r + \phi)/k\Delta r \quad \text{for small measured phases (3.3.4)}$$

In the case of using the FFT analyser used,  $\phi$  has to be obtained indirectly. If the instrument frequency response is taken into consideration, the measured cross spectrum  $\overline{G_{AB}}$  can be expressed by  $G_{AB}(H_A H_B^*)$  where  $G_{AB}$  is the true spectrum and  $H_A$  and  $H_B$  are the transfer function of the two channels. The phase of  $H_A H_B^*$  is the phase mismatch  $\phi$  for (3.3.3) or (3.3.4).

For the more general case where free field conditions cannot be assumed, (3.3.4) becomes

$$\hat{I}/I = (\phi + \phi) / \phi \quad (3.3.5)$$

where  $\phi$  is the normalized phase difference<sup>16</sup>. When the propagating sound field is contaminated by diffuse background noise, the actual phase is smaller than the corresponding free field phase  $k\Delta r$ . Evidently,  $\phi$  is critical under any of these following conditions. First, low frequencies imply a small  $k$  and a small  $\phi$ . Second, a small  $\Delta r$  possibly implies a small  $k\Delta r$  and  $\phi$ . Third, a reactive or diffuse field will lead to a smaller  $\phi$ . Usually, a phase mismatch between the two channels imposes a low frequency limit on the analyser system.

Logically,  $\phi$  and  $\phi$  have to be computed or measured to estimate

the error due to phase mismatch. As shown in section 3.1, intensity can be calculated from the cross spectrum of the two pressure signals by

$$\hat{I} = -\text{Im}(G_{AB}) / \omega \rho \Delta r \quad (3.3.6)$$

It can be shown<sup>15</sup> that (3.1.6) can lead to the intensity index nomogram relation:

$$k\Delta r / \phi = (P_{\text{rms}}^2 / \rho c) / \hat{I}$$

where the left hand side is the ratio of the free field phase to the measured phase and the right hand side is the ratio of the free field intensity to the measured intensity. This relation can also be obtained directly from

$$I = - (P_{\text{rms}}^2 / \rho c) (1/k) (\partial \phi / \partial r) \quad (3.3.7)$$

by replacing  $(\partial \phi / \partial r)$  by  $-\phi / \Delta r$ . Since (3.3.7) can be obtained from (1.1.1), and it also is the origin of (1.1.2), which is used for Digital Filtering, the nomogram can be applied to both FFT and Digital Filtering systems.

The reactivity index  $K$  is defined<sup>17</sup> as

$$K = k\Delta r / \phi \quad (3.3.8)$$

and in the logarithmic form (also called reactivity index)

$$L_K = -10 \log [(P_{\text{rms}}^2 / \rho c) / \hat{I}] = L_I - L_P \quad (3.3.9)$$

Therefore, measuring both sound intensity and SPL in the field and knowing  $k$  and  $\Delta r$  will indicate  $\phi$  as indicated by (3.3.8). From (3.3.8) & (3.3.9), the nomogram relation can be written as

$$\phi = 10^{(L_K/10)} (k\Delta r) \quad (3.3.10)$$

If a phase mismatch exists, (3.3.10) becomes

$$\phi \pm \phi = 10^{(L_K/10)} (k\Delta r) \quad (3.3.11)$$

When the same broadband signal is fed simultaneously to the two measuring channels, a sound field with 0° phase  $\phi$ , between the two measurement positions is simulated. Therefore, (3.3.11) becomes

$$\phi = 10^{(L_{K,0}/10)} (k\Delta r) \quad (3.3.12)$$

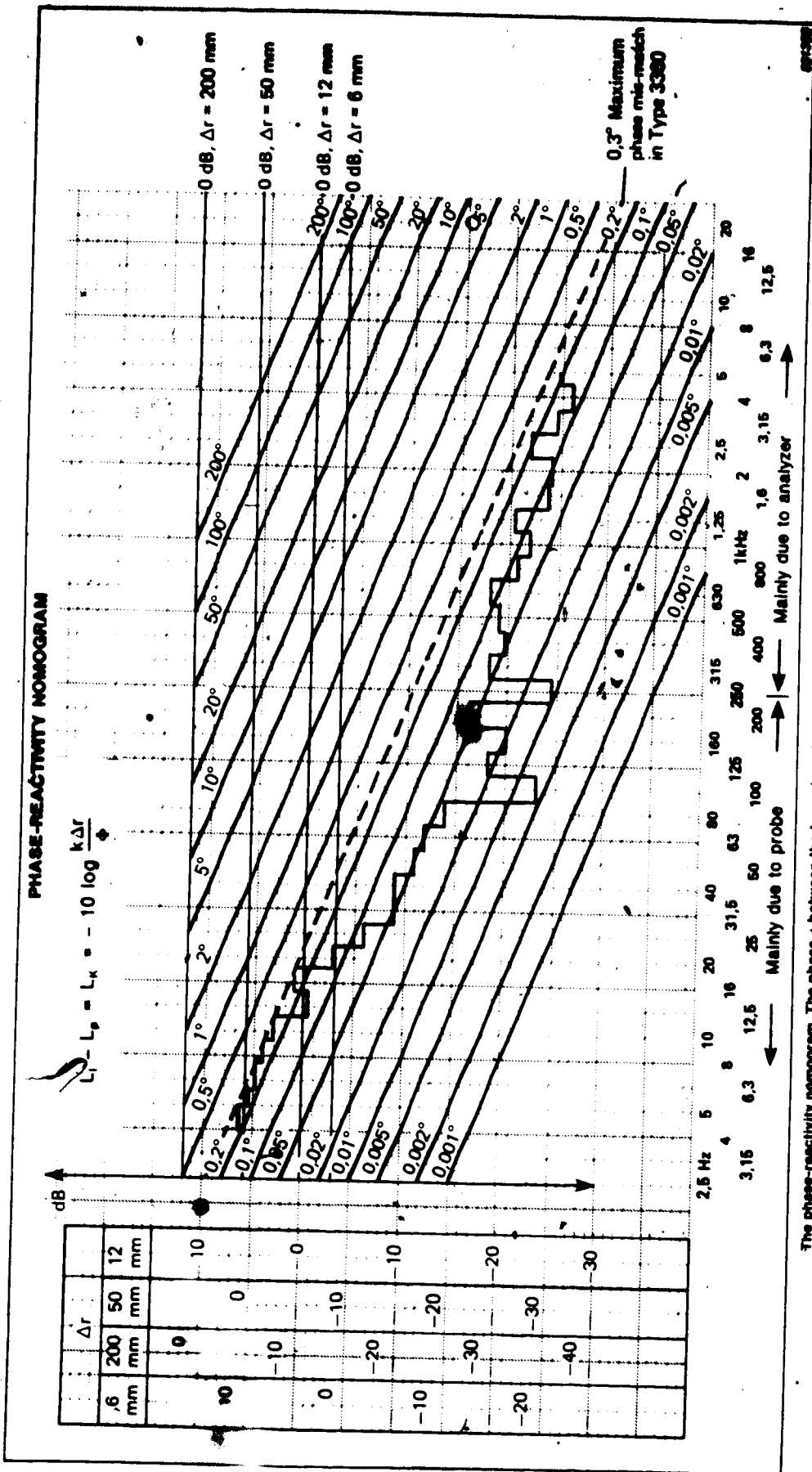
where  $L_{K,0}$  is the residual intensity obtained by the simulation and

$$L_{K,0} = L_{I,R} - L_{P,R} \quad (3.3.13a)$$

where  $L_{I,R}$  and  $L_{P,R}$  are the sound intensity and SPL obtained in the simulated zero field phase situation. Consequently, a measure of the residual reactivity index will indicate the magnitude of  $\phi$ . Substituting (3.3.10) & (3.3.12) into (3.3.5) yields the phase mismatch error expression,

$$L_{\epsilon, \text{phase}} = -10 \log [1 \mp 10^{(L_{K,0} - L_K)/10}] \quad (3.3.13b)$$

The idea is that for a certain phase mismatch  $\phi$  ( $L_{K,0}$ ), only a certain limit of field phase  $\phi$  can be accurately determined without too much uncertainty.  $\phi$  decreases as the sound field becomes more diffuse, hence the reactivity index is necessary to check  $\phi$ . (3.3.13b) is graphically illustrated by the intensity index nomogram, as shown in fig. 3.12. The phase mismatch of the system should be predetermined and the reactivity index should be measured for each measurement situation. The error in sound intensity due to phase mismatch at any frequency can then be determined from the



The phase-reactivity nomogram. The phase  $\phi$  between the two microphone positions is shown as a function of frequency, spacer  $\Delta r$  and reactivity of the sound field. The approximation error which occurs at high frequency is not taken into account by this nomogram. Note that for a free-field  $L_1 - L_p = 0$  and for a reactive field  $L_1 - L_p < 0$  dB.

To determine the influence that a phase mis-match of  $\phi_s$  in the analyzer and of  $\phi_m$  in the probe will have on the measured intensity in a field of known reactivity and using a particular spacer:

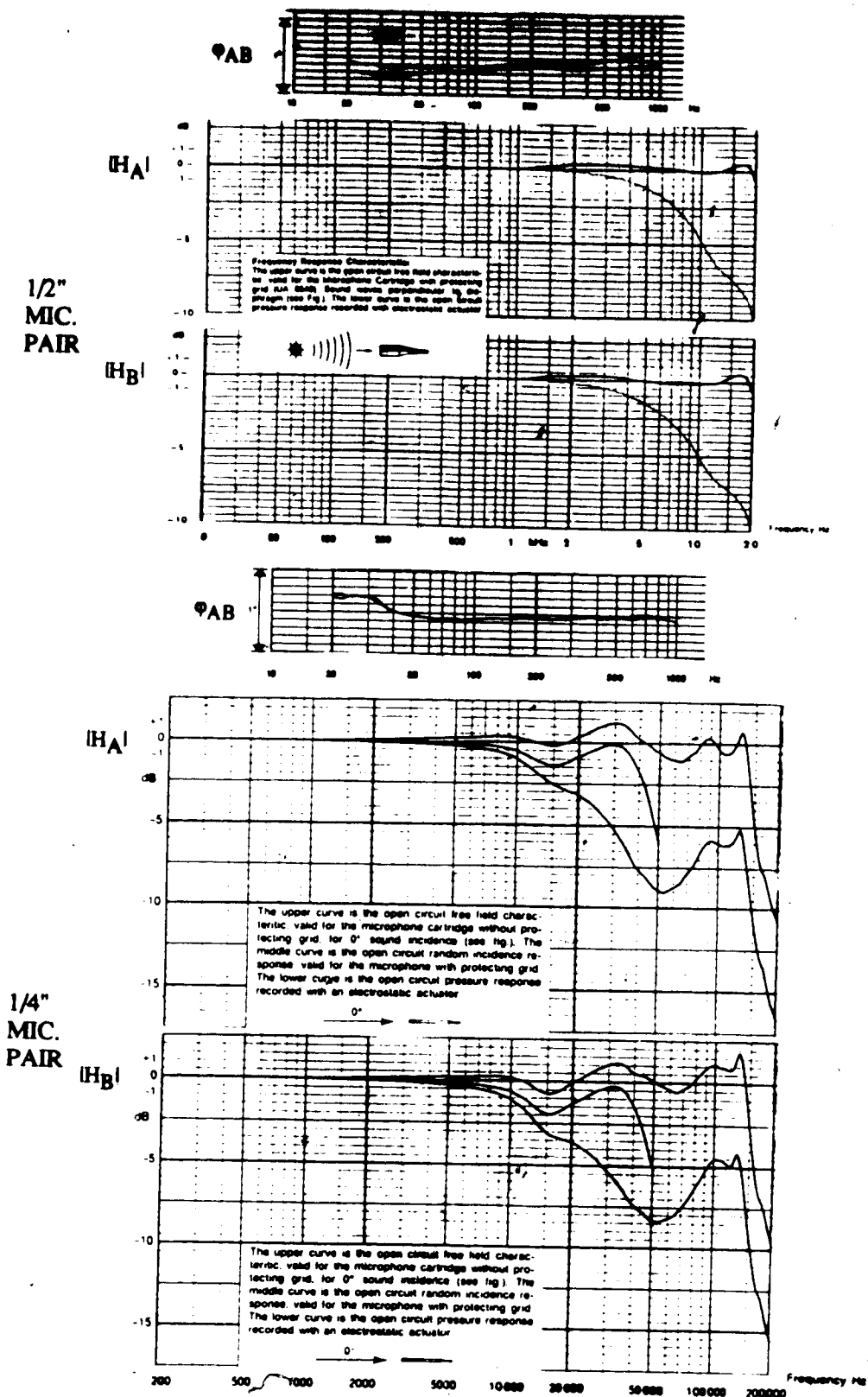
- Select the ordinate scale for the spacer employed.
- Find the horizontal line corresponding to the measured reactivity.
- At the point where the horizontal reactivity line crosses the vertical line corresponding to the frequency of interest, read off the phase of the sound field  $\phi_1$  by interpolation between the sloping phase lines.
- Calculate  $\phi_1 - \phi_s - \phi_m$  and  $\phi_1 + \phi_s + \phi_m$ . These values are the limits of error in the measured phase at this frequency and from the ordinate axis the limits of error in dB can be found for the measured intensity.

FIG. 3.12 THE PHASE-REACTIVITY NOMOGRAM (ADAPTED FROM GADE, WULFF AND GINN\*)

a low frequency limitation. Four components of the MEANU system may introduce phase mismatch, the microphones, preamps, power supply and the FFT analyser. Similar to the B & K 3360 Sound Intensity System, phase mismatch is frequency dependent. Typically above 250 Hz, it is primarily due to the analyser whereas below 250 Hz, it is primarily determined by the microphones.

The phase mismatch chart and the amplitude response charts for the two phase-matched microphones is shown in fig. 3.13. The worst phase mismatch is less than 0.2° at any frequency tested. This is expected because the microphones are phase-matched. Noise from the microphones and preamps can effectively cause an unsteady phase mismatch  $\phi$ . Similarly the effect is more significant at lower frequencies. In general, the use of high quality preamps and condenser microphones with little noise poses no threat to cause unsteady phase mismatch.

To determine the phase mismatch of the FFT analyser, white noise was amplified and fed simultaneously to the two channels of the analyser. The phase and magnitude of the transfer function between the two channels were obtained. If the two channels are perfectly identical, the phase function should be 0° throughout and the amplitude function should be 1 throughout. The transfer functions were obtained for two frequency ranges and two sets of averages. The results are shown in table 3.2. As indicated by the results of both frequency range settings, averaging removes statistical or random error, stabilizing both the phase and magnitude



**FIG. 3.13 PHASE MISMATCH AND AMPLITUDE RESPONSE CHARTS FOR THE B & K PHASE-MATCHED MICROPHONE PAIRS**



**TABLE 3.2 PHASE AND MAGNITUDE OF THE TRANSFER FUNCTION OF  
WHITE NOISE FED SIMULTANEOUSLY TO NICOLET DUAL  
CHANNEL FET ANALYSER**

FREQ. (Hz)	FREQUENCY RANGE = 20 kHz				FREQUENCY RANGE = 10kHz				
	# AVG. = 1		# AVG. = 64		FREQ. (Hz)	# AVG. = 1		# AVG. = 64	
	$\phi^\circ$	H	$\phi^\circ$	H		$\phi^\circ$	H	$\phi^\circ$	H
50	-0.3	.981	-0.1	.984	25	0.7	1.02	0.0	.987
2k	-0.4	1.00	-0.0	.993	1k	0.0	.986	0.0	.990
4k	-0.3	.988	-0.4	.992	2k	-0.4	.989	-0.3	.992
6k	-0.9	.990	-0.6	.990	3k	-0.6	.996	-0.6	.990
8k	-0.9	.985	-0.8	.990	4k	-4.6	.990	-0.8	.989
10k	0.0	1.00	-1.0	.990	5k	-0.9	1.00	-1.0	.990
12k	-0.7	.992	-1.2	.992	6k	-0.8	.990	-1.4	.990
14k	-1.1	.996	-1.6	.995	7k	-2.6	.992	-2.0	.992
16k	-2.2	.999	-2.1	.997	8k	-3.8	.997	-2.6	.993
18k	-3.3	.996	-3.1	.997	9k	-2.9	.981	-3.4	.986
20k	-4.5	1.01	-4.9	1.00	10k	-4.6	.980	-4.7	.985

of the transfer function. Particularly for the phase function, a gradually increasing pattern from 0° to about -5.0° was obtained for both frequency range settings. This means that there is no direct frequency dependence for phase mismatch in the analyser. However, it is dependent on the relative position in the frequency range. This means that phase mismatch is the same for 5 kHz in the 10 kHz range, and 10 kHz in the 20kHz range.

According to the B & K specifications, the power supply produces negligible phase mismatch and gain error. A similar set up, as shown in fig. 3.14, was used to check this. The results show that the power supply generally introduces no additional phase mismatch or magnitude difference, but a decrease in phase mismatch of 0.2 and the magnitude of 0.1 have occasionally occurred. The decrease in phase mismatch is due to phase cancellation.

To correct for phase mismatch, there is a similar channel switching approach used for both types of analyser. For the case of the FFT system, as pointed out first by Chung<sup>18</sup> and later by Pascal and Carles<sup>19</sup>, a channel switching technique can be applied in the measurement of  $\text{Im}(G_{AB})$ . (see fig. 3.15) This technique requires two measurements of the cross spectrum with the second made with the channels interchanged. The two measured spectra  $\overline{G_{AB}^1}$  and  $\overline{G_{AB}^2}$  can be expressed in terms of the true value by

$$\overline{G_{AB}^1} = G_{AB} (H_A H_B^*) \quad (3.3.14)$$

$$\overline{G_{AB}^2} = G_{AB} (H_B H_A^*) \quad (3.3.15)$$

Multiplying (3.3.14) & (3.3.15) and rearranging, the true cross

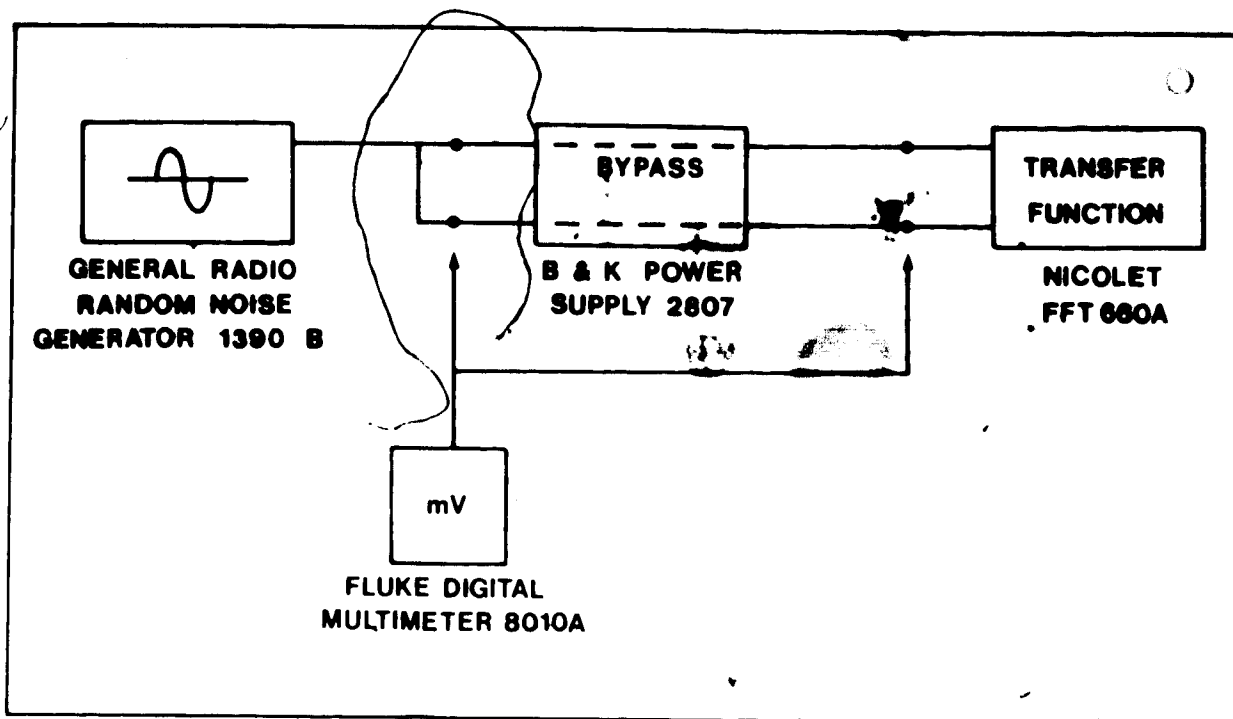


**FIG. 3.14 PHASE MISMATCH AND AMPLITUDE RESPONSE TEST SETUP FOR THE POWER SUPPLY**

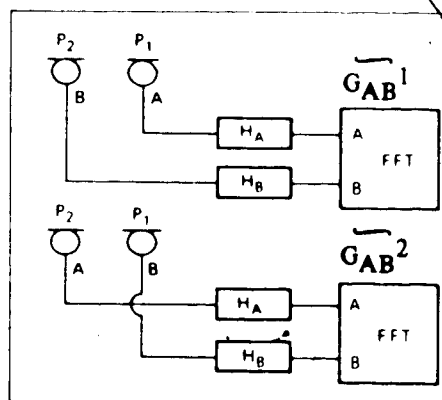


**FIG. 3.15 INTERCHANGING MICROPHONES PROCEDURE (ADAPTED FROM GADE<sup>14</sup>)**

spectrum can be expressed as

$$\begin{aligned} G_{AB} &= [\overline{G_{AB}^1} \overline{G_{AB}^2}]^{1/2} / [(H_A H_A^*) (H_B H_B^*)]^{1/2} \\ &= [\overline{G_{AB}^1} \overline{G_{AB}^2}]^{1/2} / |H_A| |H_B| \end{aligned}$$

Now only the instrument gain factors  $|H_A|$  and  $|H_B|$  remain because the switching procedure has effectively performed phase cancellation. Sound intensity can then be expressed by

$$I = \text{Im}\{[\overline{G_{AB}^1} \overline{G_{AB}^2}]^{1/2}\} / (\rho \omega \Delta r |H_A| |H_B|) \quad (3.3.16)$$

Notice that (3.3.16) is identical to (3.3.6) if  $|H_A| = |H_B| = 1$ .

For the direct method, Digital Filtering, the error due to phase mismatch can be directly represented by  $\hat{I}/I = \sin(k\Delta r + \phi)/k\Delta r$  (3.3.3). Interchanging microphones and taking the average of the two measurements reduces the error substantially since

$$\begin{aligned} \hat{I} &= (\hat{I}_1 + \hat{I}_2) / 2 \\ &= I/2 \{[\sin(k\Delta r - \phi) + \sin(k\Delta r + \phi)] / k\Delta r\} \quad (\text{from (3.3.3)}) \\ &= I \{\sin(k\Delta r)/k\Delta r\} \cos \phi \end{aligned}$$

The error is less than 0.1 dB for  $\phi = 12^\circ$ .

Theoretically, it seems to be relatively simple to correct for phase mismatch by switching microphone channels. However, in practice this is not so because in switching the two channels, as shown later in the calibration section, it is very difficult to place the probe back to the exact original position whether by hand or with the help of a probe stand. The error due to the change of position may create an error larger than the one eliminated. It was decided that the phase mismatch error would be monitored but not

eliminated. With the information of phase mismatch  $\phi$  of all the components of the FFT analyser system, the reactivity index  $L_K$  ( $L_1 - L_p$ ) would be measured and the phase mismatch error would be determined from the Intensity Index Nomogram. Alternatively, a maximum  $L_K$  can be predetermined for the known amount of phase mismatch in order to satisfy an acceptable amount of error as a result. This is the approach used by Halliwell and Warnock<sup>7</sup> as well.

Finally, it should be mentioned that the magnitude response (gain) of the two channels, which deviated from unity is generally but not completely corrected by calibration. As shown from table 3.2, for example, the magnitude response is frequency dependent. Since calibration is done by a pistonphone or calibrator, which operates at a particular frequency, other frequency points will be completely corrected only if they have exactly the same magnitude response. While this is not true, they are usually quite close as indicated by table 3.2. After all, a difference of 5% in intensity energy will only introduce a 0.2 dB. difference in sound intensity. This is the reason that the magnitude frequency response does not pose a major threat to the accuracy of sound intensity measurement.

### 3.3.3 Interference Effects of Microphones

One inevitable source of phase deviation is the finite size of the closely spaced microphones. As Pavic<sup>20</sup> pointed out, this effect causes larger phase deviations at higher frequencies. At the same time, the phase deviations become less important at higher frequencies where

the phase being measured is larger. The earlier work of Ruge<sup>21</sup> indicated the interference effect limited the use of 1/2" microphone up to 1.8 kHz. Fahy<sup>22</sup> tested the 1/4" B. & K 4135 microphones between 100 and 4000 Hz. The phase and amplitude response of these microphones placed side by side were monitored as one was moved towards the other. The results showed negligible amplitude change and no greater interference than  $\pm 1.5^\circ$  right down to the minimum physical possible separation. Typically, the microphone distance for a commonly used face to face microphone probe ranges are 5 and 10.5 mm for 1/4" microphones and 11 and 50 mm for the 1/2" microphones. The interference effect is generally considered to be small and commonly ignored within the normal frequency range of the microphone-spacer combination<sup>23</sup>.

### 3.3.4 Phase Mismatch of Recorders

Where space is limited, sound intensity measurement can be made with a dual channel tape recorder and the signals can be analyzed later. However, many imperfections of the tape recorder could introduce phase errors. For example, the deviations in the phase characteristics of the record and reproduce amplifiers and filters, the unequal geometry around the record head gap, time shift due to unequal distances from the record head to the reproduce head (azimuth adjustment) and irregularities in the tape transport. A procedure of matching by azimuth adjustment, with a reference pink noise spectrum obtained from signals directly fed to the analyser and

one obtained from the same reference signals fed through the tape recorder, can be used to correct this error.<sup>24</sup>

### 3.3.5 Random Error

It has been shown that the statistical or variance error of a digital spectrum analysis can be described by the Be T product as follows

$$\sigma/m = 1 / \sqrt{Be T} \quad (3.1.10)$$

This analysis is applicable for SPL measurement, which is basically the logarithm of an auto spectrum of a pressure signal. For sound intensity measurements, which involve two measurements simultaneously by two microphones instead of one, the statistical error expression is more complex. It can be shown<sup>15,25,26</sup> that the random error can be expressed by

$$\epsilon[I] \text{ in } \% = (1/\sqrt{Be T}) (1/\sqrt{n}) \sqrt{(1/\gamma_{AB}^2) + [\cot^2 \phi_{AB}(1 - \gamma_{AB}^2)/2 \gamma_{AB}^2]} \quad (3.3.32)$$

where  $n = \#$  of spectrum averages

$\gamma_{AB}$  = the coherence between the acoustic pressures at the two measurement points

$\phi_{AB}$  = phase angle in sound field

The inverse dependence on  $\sqrt{n}$  is a result of substituting  $nT$  as  $T_{tot}$ , where  $T_{tot}$  is the total sampling time. On the other hand, the dependence on  $\gamma_{AB}$  and  $\phi_{AB}$  can be generally explained qualitatively. As secondary sources or diffusivity increases, the signals

uncorrelated to the main propagating intensity appear as part of the correlated signals. In the case of the FFT system, for example,  $G_{AB}$  will be changed and an error is introduced. As the coherence function  $\gamma_{AB}$  is a mathematical description of how correlated the signals are, increases in  $\gamma_{AB}$  (up to maximum of 1) result in decreases of the random error, as shown in (3.3.32). Coherence is usually lower at low frequencies and random error is therefore higher. Hence a smaller phase corresponding to a lower frequency would cause a higher random error, as  $\cot \phi_{AB}$  becomes higher.

It can be shown<sup>15</sup> that measuring the reactivity index  $E_K$  is equivalent to measuring  $\gamma_{AB}$  and  $\phi_{AB}$ . Furthermore, a simplified equation using this index yields:

$$\epsilon[I] = (1/\sqrt{B_e T}) (1/\sqrt{n}) 0.42 (K + 1) \quad \text{for } K > 1 \quad (3.3.33)$$

By definition,  $K > 1$  means that  $L_I - L_P$  is negative. This is usually true since sound intensity is equal to the SPL in free field situations and the sound intensity is zero in the truly diffuse case. For the instrumentation in the current study using the Nicolet FFT analyser,  $B_e T$  is always 1. Therefore, in the case of a free progressive wave,  $K=1$ , and if  $n=64$ , the error which  $\epsilon[I] = 10.5\%$  corresponds to 0.43 dB. This equation can be applied to the measurements to estimate the random error during testing.

### 3.3.6 Near Field Limitations



43

When the intensity probe is placed too close to a point source, or a network of point sources, the assumption of a plane wave does not hold true. In this case, methods exist to calculate this error as a function of the microphone spacing,  $\Delta r$ , and the distance between the microphones and the source or sources,  $r$ . Also, tables<sup>14</sup> can be used to obtain the minimum distance between microphones and sources for the proximity error of less than 1 dB. Fig 3.16 shows the proximity error as a function of the distance ratio  $r/\Delta r$ .

### 3.3.7 Reverse Intensity

Intensity mapping is a useful tool for machine noise diagnosis. The measurement surface is divided into grids. The normal intensity data of these grid points can be interpolated to provide an intensity contour map. In measuring the intensity of these grid points, negative intensity may be encountered and should be interpreted with care. Negative intensity means that the air does work upon the surface.

It is quite possible to find sources and sinks beside each other on the same machine<sup>27</sup>. However, negative energy flow can be a very local phenomenon caused by evanescent waves. For very close measurement, such as a fraction of a wavelength from a vibrating surface, not all the waves would be propagating waves, some are evanescent waves. Energy leaving from a part of the vibrating surface may turn around and flow back into another region which is within a wavelength of the source of vibration<sup>28,29</sup>.

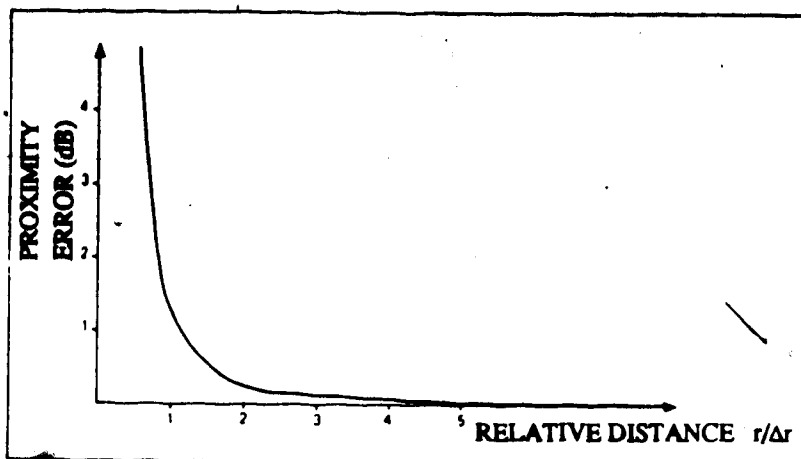


**FIG. 3.16 PROXIMITY APPROXIMATION ERROR FOR A MONOPOLE SOURCE (ADAPTED FROM GADE<sup>14</sup>)**

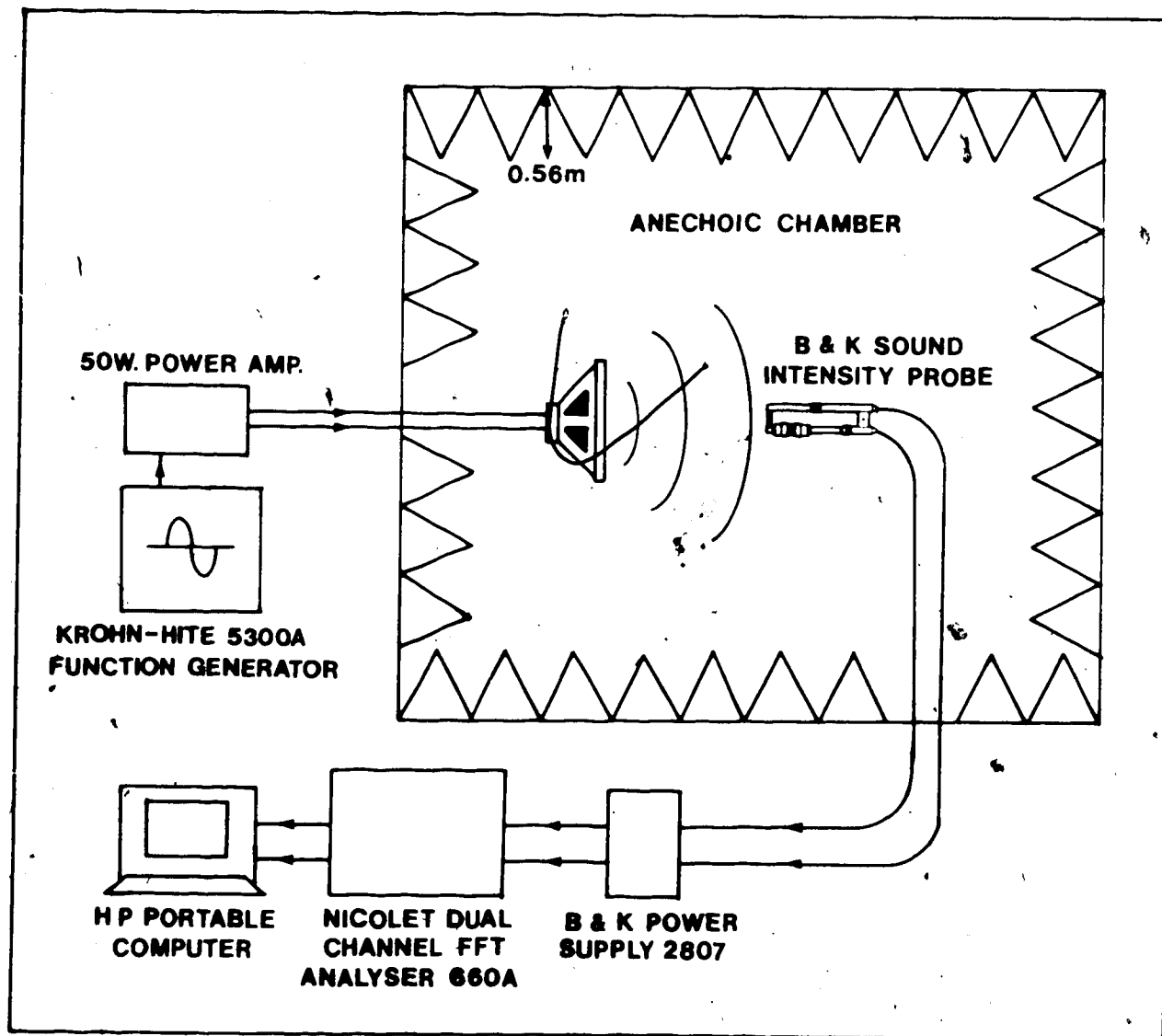


**FIG. 3.17 CALIBRATION SETUP IN THE ANECHOIC CHAMBER**

In sound intensity mapping, the spectral resolution must be smaller than the wavelength of sound, but to avoid the influence of the evanescent waves, below the coincidence frequency, the spatial resolution must also be larger than the wavelength of the source. Furthermore, in the case of sound power measurement, one could perform a sweeping measurement instead of point measurement to avoid being misled by the local effect of evanescent waves<sup>30</sup>.

### 3.3.8 Sound Intensity in the Presence of Flow

The derivation of sound intensity assumes no flow in the medium. Errors will result when there is mean flow or turbulence in the medium. In some cases such as ambient measurement with very low wind, a conventional wind screen can be added to the intensity probe. However, this approach is not suitable for low speed air flow even with Mach number less than 0.1 (e.g. building ventilation systems) and certainly introduces large errors in situations with high speed and highly turbulent flows. (e.g. gas turbine exhausts)

Either mean flow or turbulence will introduce pressure and particle velocities which are not acoustically induced. These unwanted signals have to be mathematically or physically separated from the overall signals. Munro and Ingard<sup>31</sup> have developed an analytical formulation for acoustic intensity with arbitrary, viscous and heat conducting flow and some insights have been gained by experiments performed over 0 - 0.15 Mach number range by Comparin, Rapp and Singh<sup>32</sup>. Chung and Blaser<sup>33</sup> have developed a

two microphone transfer function technique to solve the problem for a uniform, one dimensional flow field in a duct. Good experimental results were obtained with Mach number up to 0.1. Fahy, Lahei and Joseph<sup>34</sup> designed a screened probe enclosing the microphones in an acoustically transparent, streamlined windscreen. Both theories and experiments in an open circuit wind tunnel show that a screen of low flow resistance is quite adequate to produce virtually quiescent conditions in a region of low streamwise pressure gradient. The published results, from 200-5k Hz while the plane wave cut-off frequency of the tunnel was 1143 Hz, were promising. The system was recommended for measurements in low speed heating and ventilation systems.

### 3.4 Calibration

The system is calibrated in the anechoic chamber for discrete frequencies in a set up shown in fig. 3.17. By definition, sound intensity and SPL are identical in free propagating plane wave conditions. These two values are obtained and compared to determine the error of the system. Typically, a smaller speaker was used for frequencies above 1 kHz. Assuming the speaker as a point source, with the distance from the speaker of about 1 m, the relative distance  $r/\Delta r$  was always kept larger than 5 so that the proximity error was negligible. With the larger speaker used for lower frequencies, the intensity probe was moved closer to the speaker because of lower speaker efficiency. The relative distance was kept

minimum of 4 so that the proximity error would be minimal.

Initially, each set of microphones was tested for the two spacers in the frequency range recommended by B & K for their 3360 sound intensity system for a maximum error of 1 dB. While the B & K system was claimed to have a maximum phase mismatch of 0.3°, the MEANU system has shown a higher phase mismatch because of the Nicolet FFT analyser. Therefore, it was decided that the acceptable error in the calibration would be extended to 1.5 dB. The results are shown in table 3.3. The only unacceptable frequencies were the 250 Hz and 125 Hz points for the 1/4" microphone set. This is not too surprising since 125 Hz is the lower limit for the B & K system, which had less phase mismatch. The channel switching technique was tried, as described in section 3.3.3. For simplicity, the magnitude of the two transfer functions  $|H_A|$  and  $|H_B|$  were both assumed to be 1, such that (3.3.16) is equivalent to taking the arithmetic mean of the two sound intensity values in dB. This approximation was used since  $|H|$  was found to be very close to unity with a maximum deviation of 2%. The product of the two transfer functions may contribute a maximum difference of 4% in energy level or 0.17 dB. Therefore, for simplicity, the transfer function correction was not made at the beginning.

Since phase mismatch is more severe at lower frequencies, 125 Hz, 250 Hz and 500 Hz were tested for the 1/2" microphones with the channel switching technique. The average SPL and sound intensity levels were compared and negligible difference obtained

**TABLE 3.3 DISCRETE FREQUENCY CALIBRATION RESULTS IN THE ANECHOIC CHAMBER**

1/4" MICROPHONES				1/2" MICROPHONES			
$\Delta r$ (mm)	SIGNAL FREQ(Hz)	ERROR (dB)	FREQ RANGE(Hz)	$\Delta r$ (mm)	SIGNAL FREQ(Hz)	ERROR (dB)	FREQ RANGE(Hz)
10.5	5k	-1.6	10k	11	5k	-0.8	10k
	3.625k	-0.9	10k		3.75k	-1.5	10k
	2.5k	-0.6	10k		2.5k	0.3	5k
	1k	-0.9	5k		500	0.8	5k
	500	-1.1	2k		250	0.2	5k
	250	-1.8	2k		125	-1.5	2k
	125	-5.5	2k				
5	8.75k*	-1.0	20k	51	1.25k	-1.5	2k
	4.55k	0.8	20k		1k	-0.9	2k
	2.5k	-0.3	5k		500	0.7	2k
	1k	-0.4	5k		250	-1.0	2k
	500	-1.2	2k		125	-0.7	2k
	250	-1.4	2k		50	0.6	500
					37.5	0.1	500
			31.5	0.4	500		

\* the limit for the B & K 3360 system, which includes the intensity probe is 10 kHz

when compared to the results obtained without switching. Consequently, the transfer function correction was not made since that would not make a significant difference. It seems that the channel switching procedure has limited practicality when a sound intensity probe is used. As the two channels are switched, it is very difficult to reposition the probe to identically the same position. Both the SPL and the sound intensity values had to be averaged because the microphones can easily be at a different points in space. Therefore, the switching technique is not recommended for probe operations. On the other hand, it should theoretically be useful for the transfer function technique used for ducts.<sup>1,33</sup> In that application, the two side by side microphone positions are permanently defined in the duct.

There are two deficiencies in the discrete frequency calibration. First, only a few selected points were tested. Information for all frequency points would require very extensive testing. Second, the anechoic chamber is truly anechoic down to about 160 Hz. The length of the wedges is about 0.56m, which is about 1/4 wavelength of 160 Hz. Therefore, the calibration results in the anechoic chambers are not reliable below 160 Hz.

To correct these problems, the calibration was repeated using white noise instead of discrete frequency signals. The constant bandwidth results from the FFT analyser were converted to third octaves by a simple computer code. Once a frequency range is chosen in the FFT analyser, it automatically collects data 2.56 times as fast

as the upper frequency limit in that range to avoid aliasing and then outputs the first 400 spectral points out of the 512 points available. (it always collects  $1024 = 2^{10}$  data points) Therefore, each spectral point will have a bandwidth of the frequency range divided by 400. In the computing scheme, the equivalent energy of all the spectral points within the third octave were added and multiplied by the ratio of the true bandwidth of the third octave to the total bandwidth of the spectral points. An example is given in fig. 3.18 for the third octave with nominal frequency of 200 Hz. This approximation is adequate for white noise or pink noise application when the power distribution is relatively evenly distributed, and for bandwidth ratios close to 1. (This is often the case.)

The tests were done in both the anechoic chamber and outdoors for frequencies below 160 Hz to ensure anechoic conditions. In the outdoor situation, the microphones were at least 2 m away from the ground or any reflective surface. Since the intensity probe was kept close to the speaker (about 0.5 m), the ground effect could be ignored. Any reflected signal would be significantly weaker because of the increased distance from the source and usually a relatively large angle between the direction of propagation and the probe orientation.

During testing in the anechoic chamber, a B & K SPL meter was used to check the SPL results from the analyser system. The microphone of the SPL meter was placed next to the microphone center point of the sound intensity probe. The results indicate the



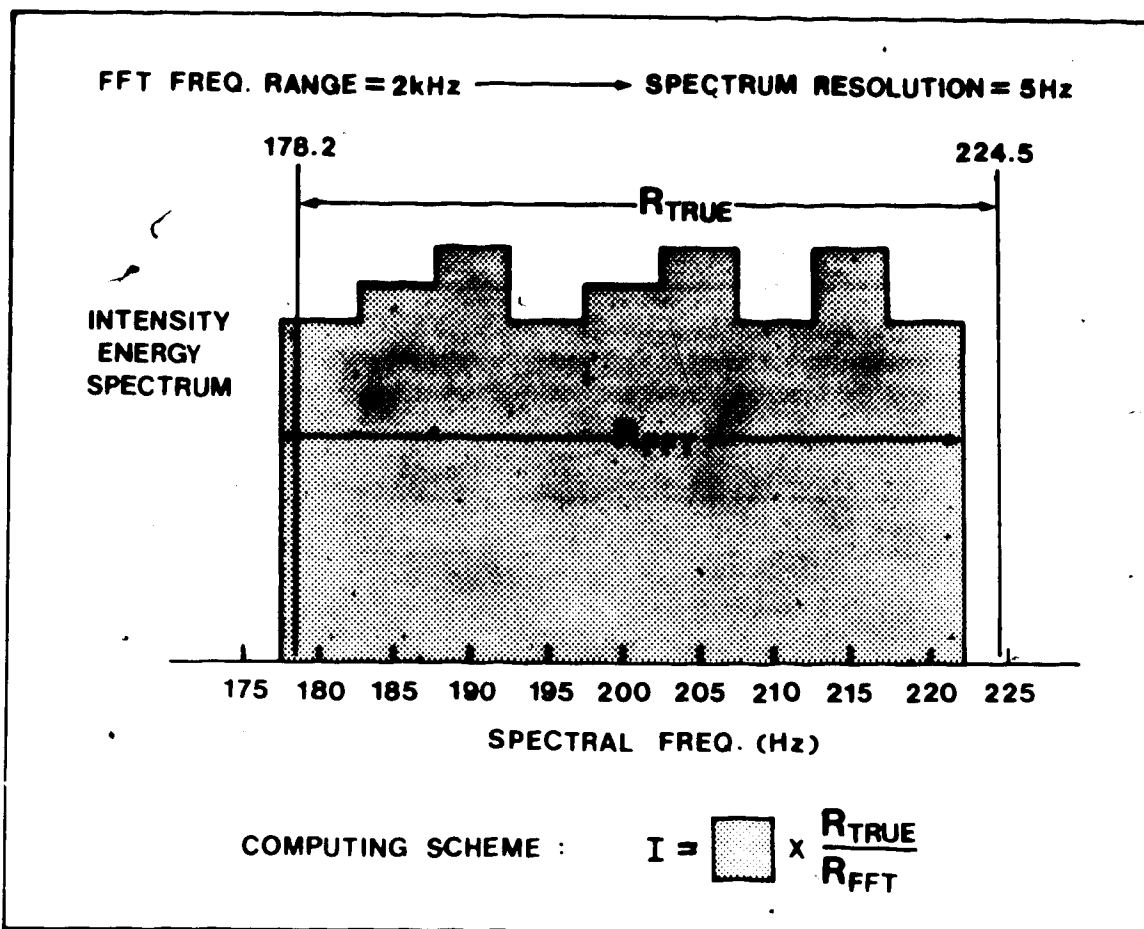


FIG. 3.18 COMPUTING SCHEME FOR THIRD OCTAVE SIMULATIONS FROM FFT SPECTRA

strange phenomenon that the third octave results from the analyser system are always about 3 dB higher than the SPL meter results. An investigation indicates that the error is caused by a fundamental limitation of the FFT analyser. As explained in section 3.1, the FFT algorithm assumes that the data sample is periodic and repeats itself after the sample period. In practice, this will never happen. Considering the case when the data is collected from a pure sine wave at a discrete frequency. Unless the sampling period captures a perfect integer number of cycles, the "wrap around" of data will always introduce an abrupt change instead of a smooth continuation. This will effectively cause the spectral quantity to spread into the neighboring frequency bands. Actually, when the discrete frequency calibration signal was fed to the analyser, a highly repeatable pattern was observed: 50% of the power is correctly captured by the correct frequency band, and the other 50% is evenly distributed by the two immediately adjacent bands in the FFT analyser. If the 50% power is mistaken as the total power (94 dB at 1 kHz for the B & K 4230 calibrator), an overshoot factor of 2 (or equivalently 3 dB) is introduced. This is the reason that there is a consistent difference of 3 dB between the analyser and the SPL meter results. For all practical purposes, the calibration signal is simply considered as 91 dB, 3 dB lower than the quoted value, since that is the amount of energy the analyser is capable of capturing at the specified frequency. This correction may not be necessary when only the change of two intensity measurements is considered, such as the two

microphone technique for transmission loss of silencers<sup>35</sup>. However, this correction is necessary if the absolute intensity is needed, such as sound power measurements and the ITL test when only the transmitted intensity is measured directly.

With the correction made, the typical sets of results for the 1/2" microphones with the 51 mm spacer and a frequency range of 2 kHz are listed in table 3.4. The results for the anechoic chamber and outdoors are similar in terms of error and pattern when the frequency range is varied. Therefore, the discussion which follows is based on the outdoor results.

This test was carried out eight times. Basically, the low frequency limit is 63 Hz; below which the error is often excessive. The error at 63 Hz is more than the 1.5 dB limit two out of eight times. It also exceeds that limit at 160 Hz five out of eight times. The reason for the error in 160 Hz is unknown, and it was decided that the 1/2" microphones would be used down to 63 Hz with reservations on the 160 Hz band with the 51mm spacer.

A lower frequency range was used to see if a higher resolution and consequently a higher bandwidth ratio would improve the results. Actually, the 63 Hz values had a larger discrepancy with the frequency range set at 1 kHz while the problem at 160 Hz remained. When the frequency range was lowered to 500 Hz and 200 Hz, the results were unacceptable overall. Even though the resolution increased, phase mismatch of the analyser increased. This is because the spectral points are in the upper part of the frequency range,

**TABLE 4 TYPICAL SIMULATED THIRD OCTAVE CALIBRATION RESULTS FOR 1/2" MICROPHONES IN THE ANECHOIC CHAMBER AND OUTDOOR**

		ANECHOIC CHAMBER		QUIET OUTDOOR		
		FREQ.(Hz)	INTENSITY(dB)	SPL(dB)	INTENSITY(dB)	SPL(dB)
Δr    51 mm	FREQ. RANGE    2kHz	31.5	38.8	40.5	59.0	68.0
		39.7	37.2	41.9	61.3 apparant	63.6
		50.0	51.0 apparant	45.4	68.6 limit	66.1
		63.0	57.2 limit	49.0	69.4	68.0*
		79.4	51.2	51.2	71.8	71.1
		100.0	55.2	54.4	71.5	72.1
		126.0	55.5 anechoic	55.5	72.2	73.4
		158.7	58.5 limit	58.7	74.2	75.0**
		200.0	60.3	61.0	77.1	77.1
	252.0	69.5	68.9	75.6	74.7	
	317.5	76.0	76.3	76.4	76.3	
	400.0	77.1	77.4	79.7	79.8	
	504.0	77.3	78.1	80.5	80.9	
	635.0	80.5	81.0	80.3	80.1	
	800.0	83.9	84.5	80.2	80.1	
	1008.0	86.7 apparant	87.1	78.3 apparant	78.7	
	1270.0	87.4 limit	88.5	76.6 limit	77.5	
	1600.1	80.1	81.9	82.5	84.1	
Δr    11 mm	FREQ. RANGE    10kHz	31.5	53.7	45.8	64.3	60.1
		39.7	43.3	46.5	60.8	63.2
		50.0	56.3	47.1	61.0	65.6
		63.0	58.0	48.3	59.4 apparant	67.9
		79.4	57.7	49.9	68.4 limit	70.3
		100.0	55.2	51.2	70.9	71.6
		126.0	55.2 anechoic	53.4	72.3	73.0
		158.7	60.8 limit	55.9	75.4	74.6
		200.0	63.5 apparant	59.0	77.1	76.3
	252.0	67.3 limit	66.7	75.7	75.7	
	317.5	75.2	73.7	76.0	76.6	
	400.0	76.9	75.7	80.0	79.2	
	504.0	76.5	76.4	80.9	80.2	
	635.0	79.2	79.6	80.4	80.1	
	800.0	83.3	82.7	80.4	79.5	
	1008.0	85.5	85.1	79.3	77.8	
	1270.0	86.9	85.6	77.7	76.6	
	1600.1	81.1	79.8	83.8	83.5	
2016.0	82.7	81.1	85.1	84.1		
2540.0	83.4	84.2	79.0	77.9		
3200.0	80.6	80.5	75.1	74.5		
4032.0	82.2	82.3	72.5	72.5		
5080.0	80.1 apparant	81.1	62.5 apparant	62.7		
6400.4	74.0 limit	75.1	57.1 limit	57.5		
8064.0	76.1	78.6	54.1	56.2		

\* failed 2 out of 8 times      \*\* failed 5 out of 8 times

where the phase mismatch is severe. Therefore, the optimum range for the 1/2" microphones with the 51mm spacer is 2 kHz.

A typical set of results for the 1/2" microphone with the 11 mm spacer is also listed in table 3.4. Since the spectral points were available, calibration was done including the 6.3 kHz band even though the B & K system is recommended for use only up to the 5 kHz band in that situation. The results for a frequency range setting of 10 kHz show that the system was good from 125 Hz to 6.3 kHz five out of six times. Again, the lower frequency limit does not improve by lowering the frequency range to increase the resolution. Actually, the 400 Hz result is unacceptable when a 500 Hz range is used since phase mismatch increases. Therefore, it is concluded that the 1/2" microphones with a 11mm spacer can be used from the 125 Hz to 6.3 kHz bands with the FFT analyser set at a 10 kHz frequency range. Since the 51mm spacing has difficulties with the 160 Hz band, the 51 mm spacing will be used from 63 Hz to 125 Hz bands whereas the 11 mm spacing will be used from 160 Hz to 6.3 kHz bands.

The 1/4" microphones were not tested in the simulated third octave mode for two reasons. First, the frequency range of interest, 63 Hz to 6.3 kHz, where results of other researchers' are available for comparison, is already covered by the 1/2" microphones. Secondly, outdoor calibration is not necessary for the 1/4" microphones since its theoretical lower frequency limit is 250 Hz, above which the anechoic chamber is indeed anechoic.

## Chapter 4 Sound Transmission Loss Using Sound Intensity (ITL)

### 4.1.1 Point by Point Technique Test Procedure

As explained in the introduction, it is practically impossible to measure the incident intensity directly in the reverberation room. As a result, the new ITL test suggests that only the transmitted intensity be measured directly while the incident intensity is approximated by measuring SPL, and assuming a diffuse sound field in the source field. To ensure a more diffuse field over a wider frequency range, the larger room was used as the source room. The test procedure was basically the same as the CTL test up to the point of measuring the source SPL spectrum, with the exception that the pink source spectrum was modified slightly.

It is not clearly specified in the ASTM E-90 standard whether white or pink noise should be used for the source room. As mentioned by Warnock<sup>7</sup>, the definitions given in ASTM C634 for sound transmission coefficient and sound transmission loss also make no mention of the bandwidth of the signal being considered. It is reasonable to assume that the definitions apply at a single frequency and that single frequency values should be integrated over the required bandwidth to give the final value, such that

$$\tau(f) = I_t(f) / I_i(f)$$

and 
$$\int_{f_1}^{f_2} \tau(f) df = \int_{f_1}^{f_2} (I_t(f) / I_i(f)) df$$

where  $f_1$  and  $f_2$  are the frequency limits for the bandwidth being

considered. In reality, the integrated intensities  $\int I_i(f) df$  and  $\int I_r(f) df$  are measured over the bandwidth and the ratio of the two is calculated for  $\int_{f_1}^{f_2} \tau(f) df$ . Strictly speaking this is only correct if  $I_i(f)$  is constant over the bandwidth considered, i.e. white noise. Otherwise, a bias error is introduced. However, a pink noise spectrum is commonly used for TL tests for several reasons.

First, the receiver spectrum from a white source spectrum usually falls out of the dynamic range of most frequency analysers. A white noise spectrum on a third octave filter will have a -1 dB per third octave slope. There will be a -21 dB difference over the frequency range of 63 Hz - 6.3 kHz. If the mass law is applied to the TL behavior of the wall, which is equivalent to -2 dB per third octave and -42 dB in total. Coupling these two factors together, one obtains a source spectrum with a 63 dB difference over that frequency range. This requires the measurement analyser to have at least a dynamic range of 63 dB, which is often beyond the limit of many frequency analysers.

On the other hand, a pink noise spectrum has a zero slope on a third octave analyser. Therefore, the dynamic range of the analyser has to cover only the difference due to the mass law. At MEANU, a third octave frequency analyser (IVIE model IE-30A) with an accurate 35 dB dynamic range is used. The pink noise source spectrum is actually slightly adjusted at MEANU. A pink spectrum with an average of about +0.4 dB/third octave slope on the IVIE

frequency analyser is used such that the receiver spectrum will fall within the accurate 35 dB dynamic range of the frequency analyser.

Second, the difference between a white noise and pink noise at the two extremes of the third octave bandwidth is only 1 dB. In practice, the convolution of the source spectrum with the speakers and room response would make it difficult to distinguish that difference. Therefore, the difference between using a white and a pink noise source is negligible.

Ideally, one would hope to measure a flat, i.e. pink, receiver intensity spectrum such that the signals are equally strong from one band to the other. However, this would mean that the source pink noise spectrum would have a very steep additional slope of +6 dB/octave to compensate for the mass law. This would result in two problems. First, the bias error due to the use of a non-white source spectrum would be excessive, and second, this non-white source spectrum would be too demanding for most sound systems. A compromise solution of a pink noise spectrum with an approximately additional +0.8 dB/third octave slope was tried for the ITL tests to improve the flatness of the receiver spectrum and limit the bias error. The TL results have no significant difference compared to using the pink noise spectrum with a +0.4 dB/third octave slope. Consequently, the +0.4 dB/third octave pink noise spectrum was used for further testing.

Once the source spectrum was obtained, each channel of the intensity analyser system was pressure calibrated individually by the B & K 4230 calibrator. The transmitted intensity spectrum was



measured with the diffusers in the source room on, such that the diffusivity of the source sound field was maintained. Two spacers were used for the 1/2" microphones, 51 mm for 63 - 125 Hz bands and 11 mm for 160 - 6300 Hz bands, based on the calibration results. The midpoint of the probe was kept at 5 cm from the wall surface, the same as used by Warnock<sup>7</sup>. The specimen surface was divided into 25 grid points, and the intensity probe was placed at about the center of the grid, perpendicular to the surface. 25 grids were chosen as Warnock's results showed a negligible decrease in precision from 100 to 25 grids. For each grid point measurement, both the sound intensity and SPL were obtained such that the difference would approximate the reactivity index. This was limited to -10 dB to ensure that the error due to phase mismatch was less than 1.5 dB. The reactivity index limit used by Warnock was 8 dB since the B & K intensity system type 3360 (including analyser type 2134) was specified for less than 1 dB error.

#### 4.1.2 Sweeping Technique Test Procedure

It has been reported<sup>6,7,36</sup> that sweeping the sound intensity probe over the measurement surface is equivalent to making measurements at fixed grid positions. While Warnock claimed that the point by point technique had a higher repeatability, Cops and Minten<sup>6</sup> concluded the opposite. The sweeping technique is interesting; not only to verify these claims, but to see if it can reduce measurement time as well. Each intensity measurement with the MEANU system took about 5 minutes, which added up to about 24

hours with 25 grid points and 2 spacers. This would extend the total ITL test time to over 5 hours, which is long compared to about 1 1/2 hours for the CTL test. With the sweeping technique, one could sweep the probe over all five horizontal grids at a steady speed in the time duration of a stationary grid point measurement. (about 15 seconds for 64 averages) As a result, the ITL test could be completed in less than 2 hours, which is comparable with the CTL test.

The probe was clamped to a stand with rollers which was pulled on a track across the surface of the wall specimen. (see fig. 4.1) The center of the microphones was kept at a larger distance of 10 cm, instead of 5 cm, from the wall surface in order not to hit the angle iron frame when the probe was traversing across the specimen.

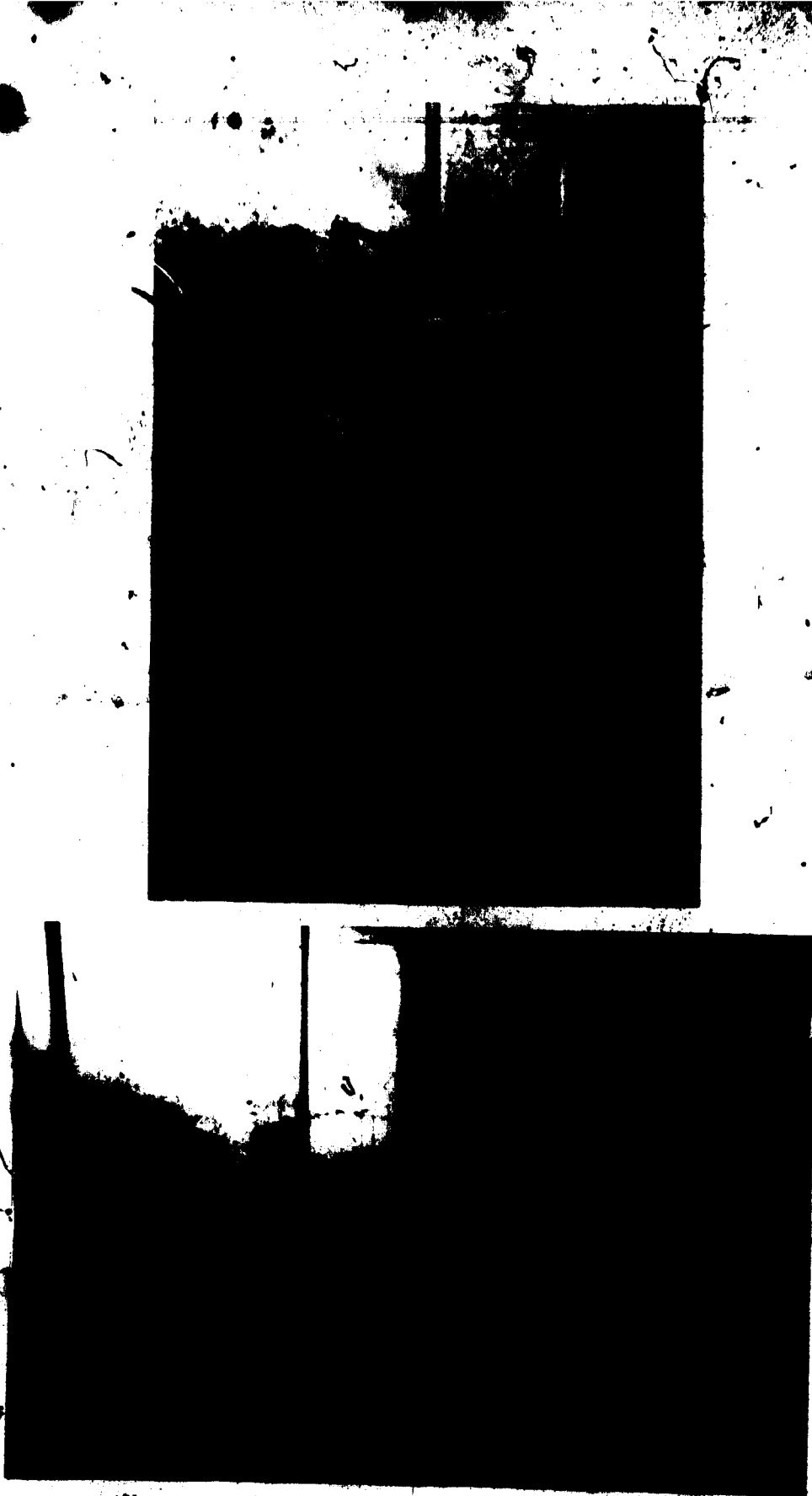


**FIG. 4.1. SWEEPING THE SOUND INTENSITY PROBE ACROSS THE WALL SPECIMEN**

## Chapter 5 Proposed Outdoor ITL Test to Improve Low Frequency Reliability

### 5.1 Concept Development

In principle, one would hope to be able to measure sound transmission loss accurately down to the hearing limit of 20 Hz, since low frequency noise problems are often encountered. The CTL test is reliable only down to the diffusivity limit of the reverberation rooms. The mathematical approximation of sound intensity by SPL is unreliable when the assumption of diffusivity fails at low frequencies, typically below 150 Hz. The ITL method solves half of the problem, with the remaining problem that the incident intensity is still an approximation obtained from the SPL. Logically, there are two ways to solve the problem. First, the diffusivity could be improved in the source room such that the approximation becomes reliable. Second, the incident intensity could also be measured directly as well such that no approximation is necessary.

The first idea is basically limited by the room volume, which governs the diffusivity limit. Current versions of ASTM standards dealing with reverberation room measurements require that the minimum room volume be greater than  $4 \lambda^3$ , where  $\lambda$  is the wavelength of sound at the center of the lowest third octave band to be measured. This criterion is based on the requirement of at least 20 eigenmodes in the lowest measurement band. This implies that the larger room ( $313 \text{ m}^3$ ) is allowed for third octave measurement down to 80 Hz and the smaller ( $230 \text{ m}^3$ ) is acceptable down to 100 Hz. Indeed, the room qualification test based on ANSI S1.31 (section

3.2) shows that both rooms have acceptable standard deviations down to the 100 Hz band. (1.0 dB and 0.9 dB for the larger and smaller room respectively, compared to the 1.5 dB limit) The rooms were not tested below 100 Hz because the limits were not specified in the standard. It is possible that the 80 Hz band measurement will not have a standard deviation higher than 1.5 dB providing that there is no sharp decrease in diffusivity. However, there is really no basis to believe that the 63 Hz or lower bands will be as precise. A larger standard deviation would definitely indicate a lower diffusivity, and the approximation of a diffuse field is then unreliable.

Rotating diffusers are used at MEANU to improve diffusivity. The size and weight of the 2.4m by 1.2m diffusers was limited to keep the induced noise from the diffuser mechanism to a minimum. Unfortunately, the light weight and relatively small size compared to low frequency wavelengths are not effective in significantly improving low frequency diffusivity.

In general, the minimum room volume criterion suggests that the larger room could be used down to 80 Hz and the smaller down to 100 Hz. Nevertheless, one should also understand that an acceptable standard deviation does not mean that the sound field is highly diffuse. The limits are set only as a general guide for the existing facilities. It appears that the approach of increasing diffusivity was fundamentally limited by the room volume and the approach of measuring  $I_1$  directly should be investigated.

Some B & K literature<sup>37</sup> suggests that  $I_1$  can be measured with

the wall specimen removed such that there is no reflected wave at the measurement point, as shown in fig 5.1. This method is valid provided that first, the energy density inside the chamber  $E_{int}$  is greater than outside,  $E_{ext}$ , and second,  $E_{int,1} = E_{int,2}$ . The first condition may be satisfied by making the receiver room semi-anechoic by adding absorption materials. However, the second condition can only be satisfied if the wall specimen is acoustically very transparent in all frequency bands and therefore its presence does not affect the source room field. This is difficult unless the specimen is only a small fraction of the total surface in the source room and would therefore require a large room.

As Chung<sup>1</sup> has developed a transfer function technique to distinguish separate incident intensity and the reflected intensity in a plane wave duct, the possibility of measuring TL in a duct was investigated. (see fig. 5.2) The approach is limited by duct acoustics. In order to have only plane wave propagation down the duct with no cross modes, the rule of thumb is that the lateral dimension should be half the wavelength of the cut off frequency, below which plane wave conditions are obtained. This means that a plane wave duct up to 50 Hz should have a lateral dimension of 3.4m square and one up to 150 Hz should be 1.1m square. One would like to have the latter for a wider frequency range where the conventional technique is unreliable, but the specimen size has to be decreased. Originally, the specimen size was chosen to represent a typical wall structure in buildings. A smaller specimen such as 1/4 the size of the original would not have the same transmission

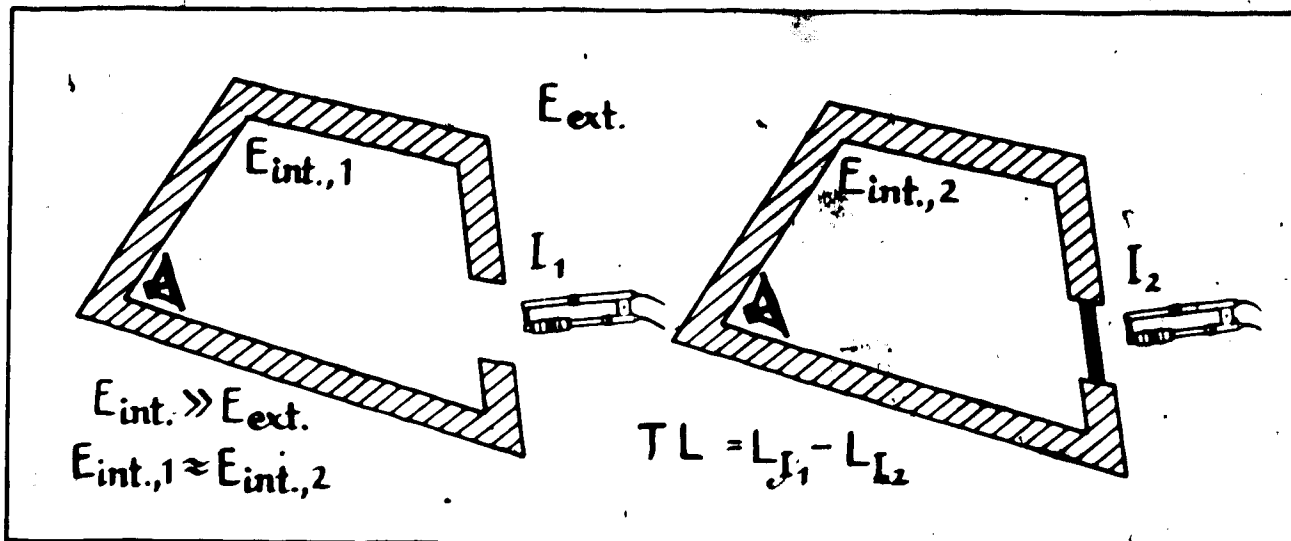


**FIG. 5.1 MEASUREMENT OF INCIDENT INTENSITY DIRECTLY WITHOUT THE WALL PANEL PROPOSED BY B & K LITERATURE (ADAPTED FROM LECTURE GUIDE<sup>37</sup>)**

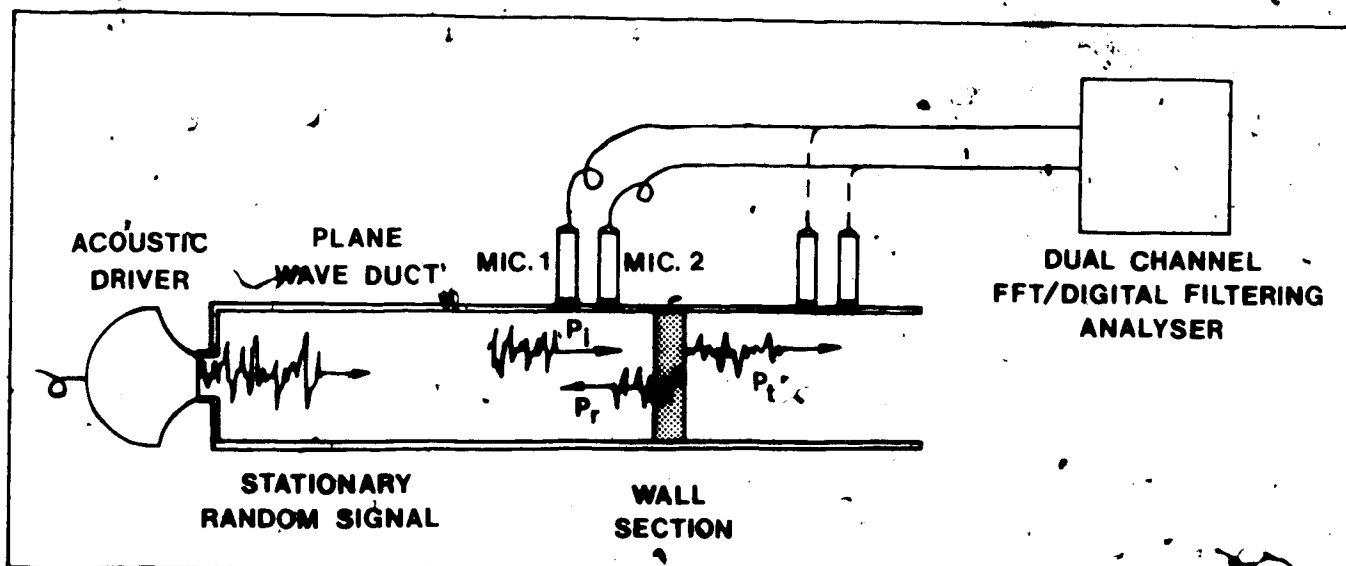


**FIG. 5.2 SOUND TRANSMISSION LOSS TESTING BY THE TRANSFER FUNCTION TECHNIQUE**

characteristics. This is particularly true at low frequencies where the transmission characteristics are stiffness dependent. One may suggest scaling down the wall characteristics such that a smaller specimen and a higher frequency sound be used. In practice, however, it is next to impossible to scale down acoustically a structure as complicated as a wall.

As well as size, absorption characteristics and stiffness have to be scaled down by the same factor as that of the frequency. One has to find a different absorption material which has a similar absorption curve but stretched out by a factor of 2 in the frequency domain. (see fig. 5.3) This may not exist at all. This scaling also has to be applied to stiffness (for low frequency transmission characteristics) and weight (for the mass law) such that a structure half the size will have the same sound transmission curve, but again stretched out by a factor of 2 in the frequency domain. As a result, the application of the transfer function technique to separate the incident intensity from the reflected is limited by the problems associated with duct acoustics and scaling.

As shown above, scaling is impractical and the wall dimensions have to be maintained to ensure realistic results. One way to measure incident intensity directly is to measure the intensity in an anechoic environment at a distance away from the wall surface where the reflected wave is relatively weak compared to the incident. (see fig. 5.4) If the distance travelled by the reflected wave back to the measurement point is four times that travelled by the incident, the reflected wave is only  $1/16$  as strong based on the



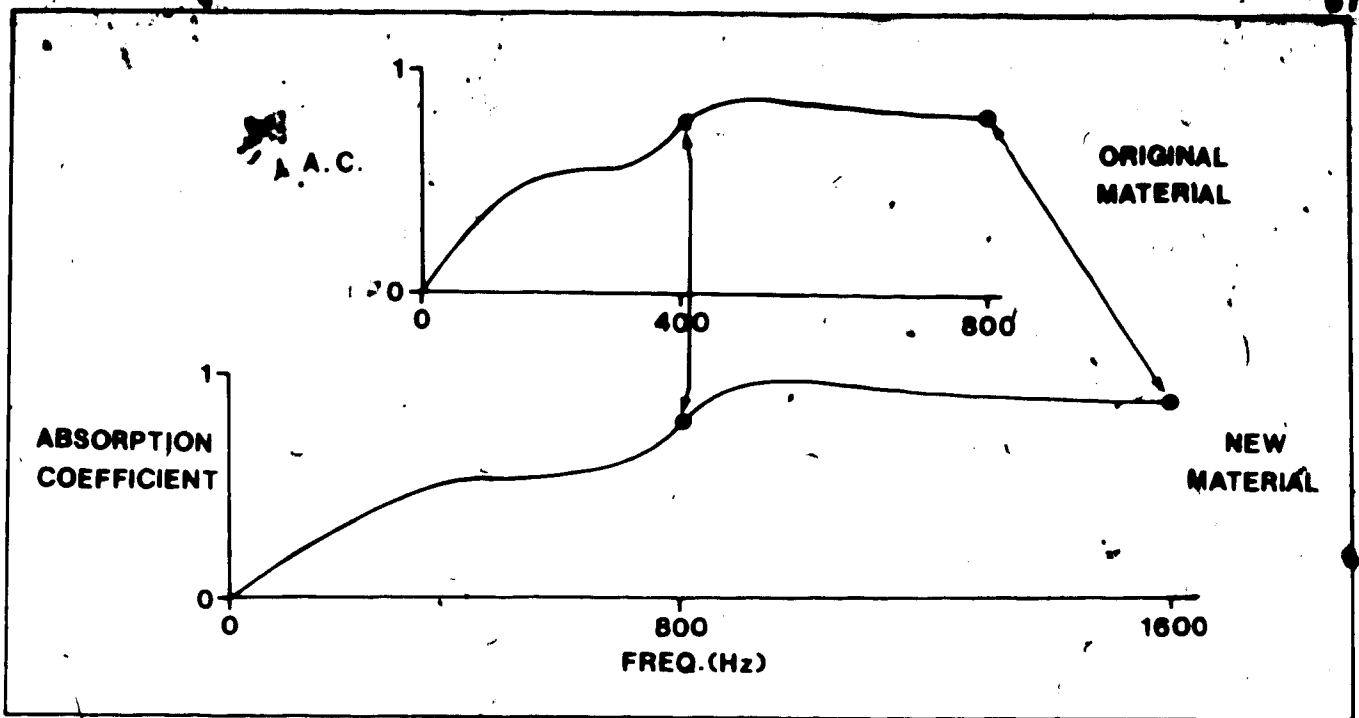


**FIG. 5.3 THE REQUIRED ABSORPTION CHARACTERISTICS FOR A SCALING FACTOR OF 2**

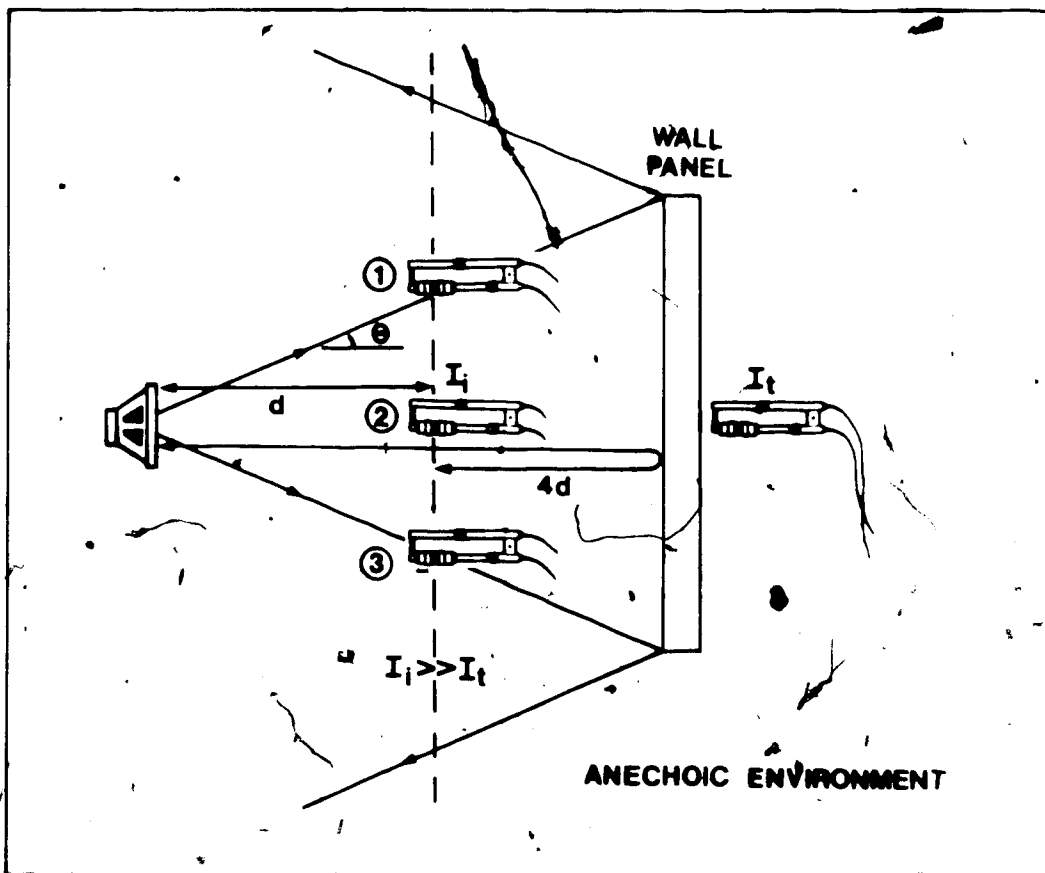


**FIG. 5.4 MEASUREMENT OF INCIDENT SOUND INTENSITY AWAY FROM THE WALL SURFACE IN AN ANECHOIC ENVIRONMENT**

inverse square law. Assuming further that half the energy gets reflected, the reflected wave is only  $1/32$  or 3 % as strong. This is equivalent to 0.13 dB difference. The true incident intensity next to the wall surface can then be extrapolated by the inverse square law using simple geometry. Also, the distance between the speaker and the wall surface should be at least equal to the larger lateral dimension of the wall. By keeping  $\theta$  to  $14^\circ$ , this limits the variation in normal intensity to 0.13 dB. This process is possible only in an anechoic environment, where the only energy flow incident onto the wall surface is from the speaker. On the other side of the wall, the transmitted intensity can be measured directly like the ITL test.

The process described requires that a larger anechoic chamber with a large wall opening is needed. One possibility is to convert the existing reverberation chamber into anechoic. A preliminary calculation shows that wedges 1.7 m deep are needed for the entire room such that it becomes anechoic down to 50 Hz. This is difficult and expensive.

The existing anechoic chamber cannot be used either because it is only anechoic down to about 150 Hz and the window opening is only 1.1m by 1.1m. Logically, a quiet outdoor situation would be the ideal anechoic chamber for this application. It is anechoic virtually at all frequencies and it would allow the integrity of the actual wall to be maintained. In order to minimize ground effects, the wall could be raised above the ground or alternatively a ditch or depression dug.

In the outdoor situation, another way to measure incident intensity is to simply measure directly next to the receiver side of

the wall without the presence of the wall. Then the wall can be put in place for the measurement of the transmitted intensity. This approach is similar to the idea proposed in the B & K literature (fig. 5.1) except that this is now done in the outdoor anechoic situation.

### 5.2 Preliminary Test

The idea of measuring incident intensity directly at a distance from the wall surface or next to the wall without the presence of the wall in an anechoic environment can be tested in the anechoic chamber at frequencies above the anechoic limit of 150 Hz. Also, the incident intensity can be measured before the specimen is installed. These two concepts will be further addressed as the semi-direct and direct ITL method respectively. The wall opening is only 1.1m by 1.1m. A smaller specimen may introduce a different TL pattern. Hopefully, if the test is done in the mass controlled region, ie higher frequencies, the change in stiffness due to the decrease in wall size, will not impose any significant difference in the results. The TL results from these two alternative methods to measure the incident sound intensity can then be compared.

A smaller steel specimen wall was constructed for the anechoic chamber. The mounting characteristics of the specimen onto the angle iron were followed as close as possible to the original. During testing, it was discovered that the 20 Watt 6" wide range speaker used for calibration (referred to as the smaller speaker earlier) could only provide a very weak signal (1/16 signal level or 0.06V) registered at the lowest input range setting in the FFT analyser.

(0.1 V maximum) Consequently, a high power horn was used as the source speaker such that the transmitted intensity was reasonably strong enough for the FFT analyser to measure. The white noise signal was fed to a three-way crossover (1.6 and 7 kHz) and the midrange signals were passed to the horn speaker, which was placed normal to the center of the specimen wall at a distance of 2m from the speaker driver to the wall surface.

The transmitted intensity at one arbitrarily chosen wall surface position, lower middle, was compared with the background noise. (see table 5.1). Since the sound intensity level of the 1 kHz band is significantly above the background level by 37 dB, further analysis would be between 1 and 6.3 kHz. A closer examination of table 5.1 indicates that the reactivity index reaches the 10 dB limit at 5 and 6.3 kHz. This could be caused by the leakage of sound through the gaps between the steel frame and the angles as well as the angles and the steel specimen, contaminating the sound field. Caulking and duct tape were added around the gaps (see fig. 5.6) and the transmitted intensity was measured again, as shown in table 5.1. The reactivity index is down to a maximum of 7 dB, which is acceptable.

The center of the microphones of the intensity probe was then mounted 0.8m from the speaker driver such that the reflected wave had to travel 3.2m to reach the microphones. This ensured that the reflected wave is a maximum of 1/16 as strong as the incident wave. (0.26 dB) The incident intensity is also measured next to the receiver side of the wall before it is installed. Then the transmitted intensity is measured with the wall in place. Measurement of incident and

**TABLE 5.1 PRELIMINARY CHECK ON BACKGROUND LEVEL AND REACTIVITY INDEX FOR THE DIRECT ITL TEST SETUP**

FREQ.(Hz)	BACKGROUND INTENSITY(dB)	UNTAPED FRAME			TAPED FRAME		
		TRANSMITTED INTENSITY(dB)	SPL(dB)	L <sub>K</sub> (dB)	TRANSMITTED INTENSITY(dB)	SPL(dB)	L <sub>K</sub> (dB)
125	50.0	48.8	52.8	-4.0	44.1	49.4	-5.3
160	56.5	57.4	57.2	0.2	57.8	50.6	7.2
200	56.9	56.2	57.2	-0.1	59.2	51.1	8.1
250	44.3	40.0	49.2	-9.2	46.9	48.2	-1.3
315	54.3	45.4	50.0	-4.6	44.2	49.9	-5.7
400	48.4	44.2	52.3	-8.1	53.2	51.5	-1.7
500	46.9	55.6	57.7	-2.1	54.8	57.2	-2.4
630	42.4	57.2	58.8	-1.6	55.5	57.0	-1.5
800	34.8	58.1	62.3	-4.2	54.6	58.6	-4.0
1000	20.7	57.2	66.5	-9.3	56.7	59.2	-2.5
1250	21.9	61.8	66.6	-4.8	61.9	63.8	-1.9
1600	10.1	60.5	63.8	-3.3	59.2	61.7	-2.5
2000	24.8	59.7	65.3	-5.6	59.4	61.8	-2.4
2500	21.9	62.0	68.8	-6.8	60.9	63.7	-2.8
3150	17.8	57.4	66.2	-8.8	57.1	63.3	-6.2
4000	5.9	56.9	65.6	-8.7	57.6	62.5	-4.9
5000	13.9	59.4	72.5	-13.1	52.9	60.1	-7.8
6300	12.7	60.6	70.6	-10.0	51.4	58.7	-7.3
8000	.5	48.0	59.3	-11.3	44.9	52.8	-7.9

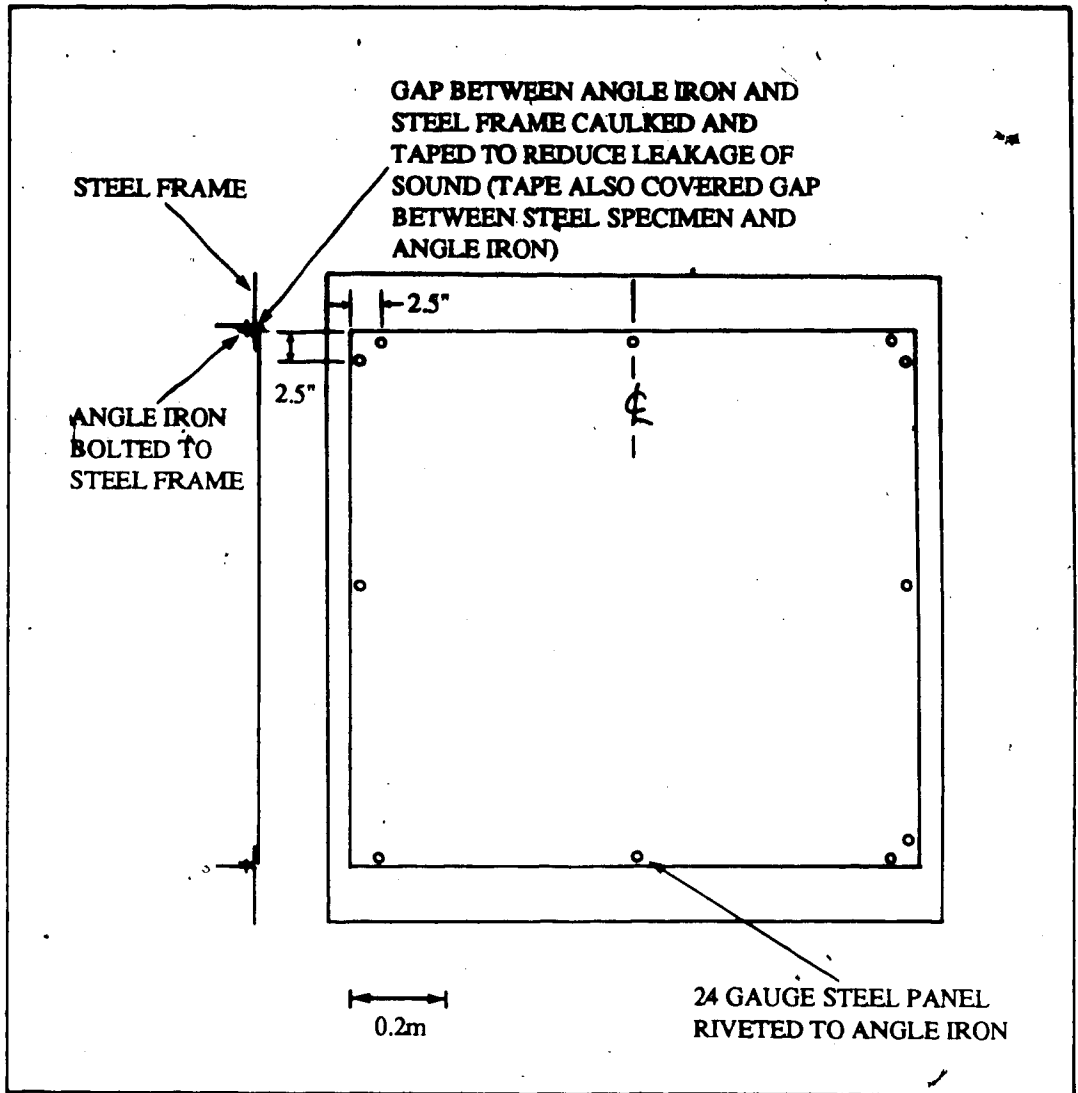


**FIG. 5.6 CAULKING AND TAPING LOCATIONS OF THE SMALL STEEL SPECIMEN**

transmitted intensity is made at nine positions of the measurement surface, and the  $L_{eq}$  values are used for the calculation of the sound transmission loss.

## Chapter 6 RESULTS AND DISCUSSIONS

### 6.1 Comparison between CTL results

The use of the reference ASTM wall allowed the comparison of TL results with those of previous investigators for both the CTL and the ITL data. These CTL tests are as much a check of the MEANU facility as an evaluation of the sound intensity technique. The surface density of the galvanized metal and assembled panels are listed in table 6.1. It should be noted that the surface density of the sheet metal of MEANU's is about 7% lower than the other two. The forward CTL results are compared to Warnock's<sup>42</sup> and Sherry's<sup>38</sup> in fig. 6.2. As Warnock reported several sets of results, there was some difficulty in deciding which set should be used for comparison. This is because there is a 1.2 m deep tunnel, which allows for easy installation of the test walls between the two test rooms at the National Research Council (NRC). Testing was carried out with the wall placed at four locations in the tunnel. (see fig. 6.1a) It has been reported<sup>7,42</sup> that the tunnel effect is particularly obvious at low frequencies, ie. below 160 Hz, and at higher frequencies, such as above 2500 Hz, though not as severe. On the other hand, an ITL test has been done at two positions. (see fig. 6.1b) One of them is to have the specimen at the edge of the tunnel towards the larger test room. In the reverse configuration used by the ITL test, there will not be any tunnel effect on the source side since there is no tunnel. On the receiver side, sound intensity is measured so close to the wall surface that the measurement should be free from any tunnel effect. Therefore, position 2 in fig. 6.1b is chosen for comparison to the



**TABLE 6.1 WALL SPECIMEN SURFACE DENSITIES**

	MEANU	WARNOCK	SHERRY
SHEET METAL SURFACE DENSITY (kg/m <sup>2</sup> )	5.02	5.48	5.53
ASSEMBLED PANEL SURFACE DENSITY (kg/m <sup>2</sup> )	8.69	8.82	N/A

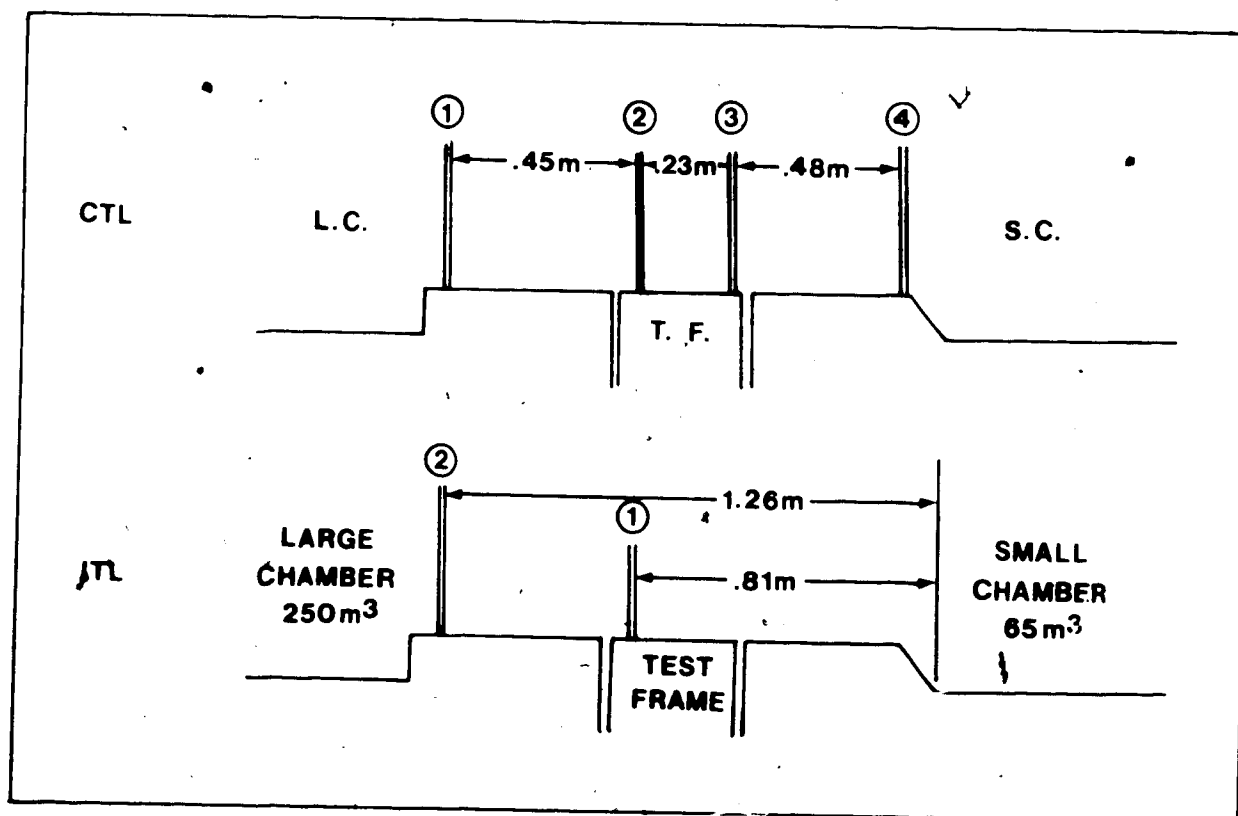


**FIG. 6.1 TEST WALL POSITIONS FOR CTL AND ITL TESTS AT NRC**

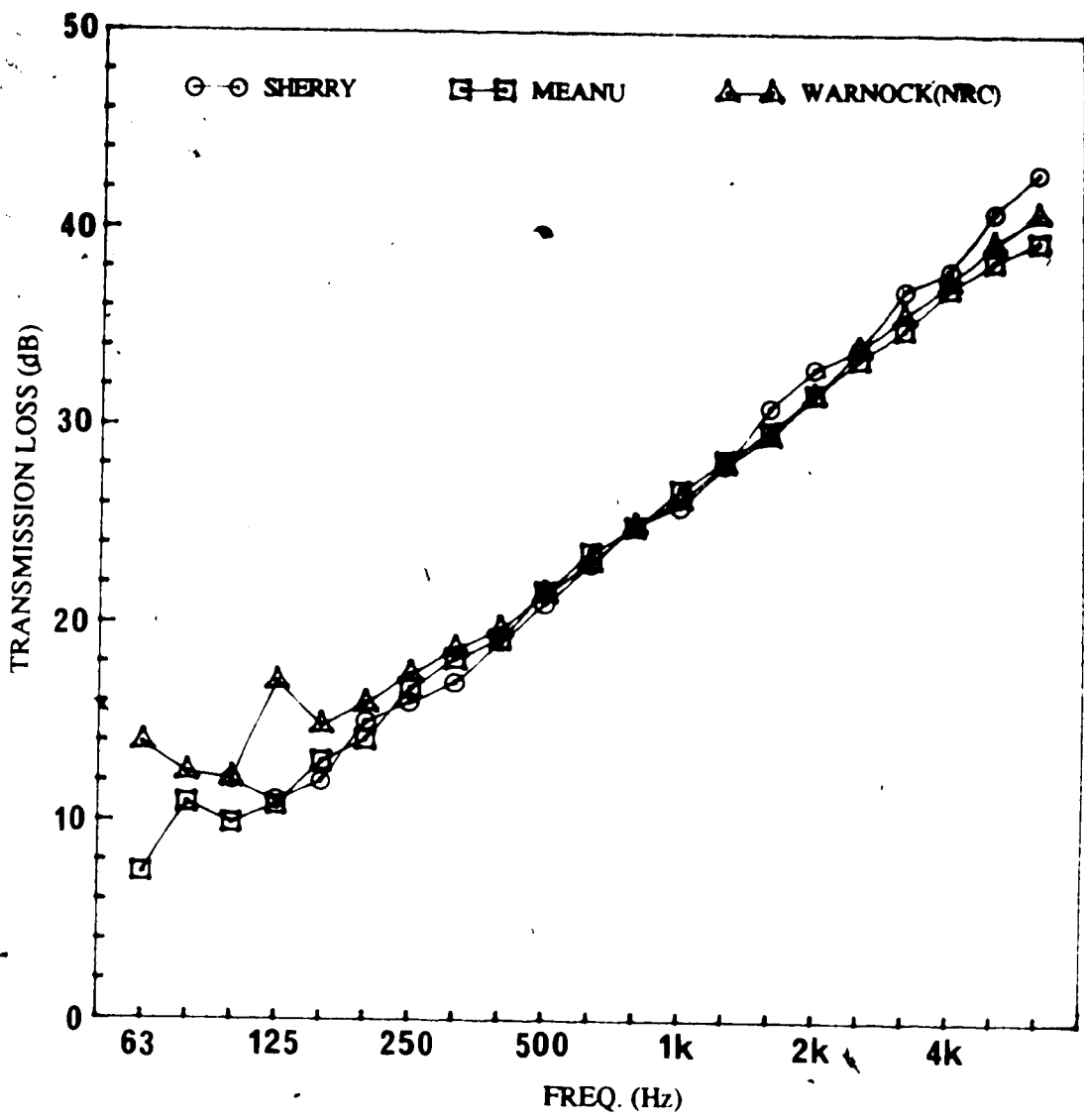


FIG. 6.2 COMPARISON OF FORWARD CTL RESULTS

current tests. The CTL results are also chosen with the wall located at the edge of the tunnel towards the source room. (position 4 for forward CTL and position 1 for reversed CTL)

In fig. 6.2, the agreement between MEANU's and Warnock's results is better than 1 dB from 250 to 5000 Hz and generally better than 0.5 dB from 500 to 4000 Hz. The results differ significantly from 200 Hz and below, particularly at 125 and 63 Hz. According to the minimum room volume requirement, as described in section 5.1, the MEANU results should be more reliable at these frequencies because of its larger room volume. (229 m<sup>3</sup> compared to 65 m<sup>3</sup>) In addition, there is a much reduced tunnel for the test wall installation at MEANU. As seen in the figure, the agreement between Sherry's and MEANU's results is better in the low frequency region. (Sherry reported TL results to as low as 100 Hz) There are some differences between all three sets of results in the higher frequency region, up to 3.5 dB at 6300 Hz. Many factors may contribute to this. First, the mass density of the wall specimen at MEANU differ by 7% with the others. Second, there is possibly a tunnel effect in Warnock's results. Third, Sherry's results are reported in integer form, which could produce jaggedness in comparison.

Fig. 6.3 shows the reversed CTL results of MEANU's and Warnock's and the differences compared to the forward configuration. Sherry does not report reversed CTL results. As shown from the figure, the overall agreement has improved, compared to the forward results. The results differ by less than 1 dB from those above 160 Hz. A better agreement to a lower frequency limit is likely

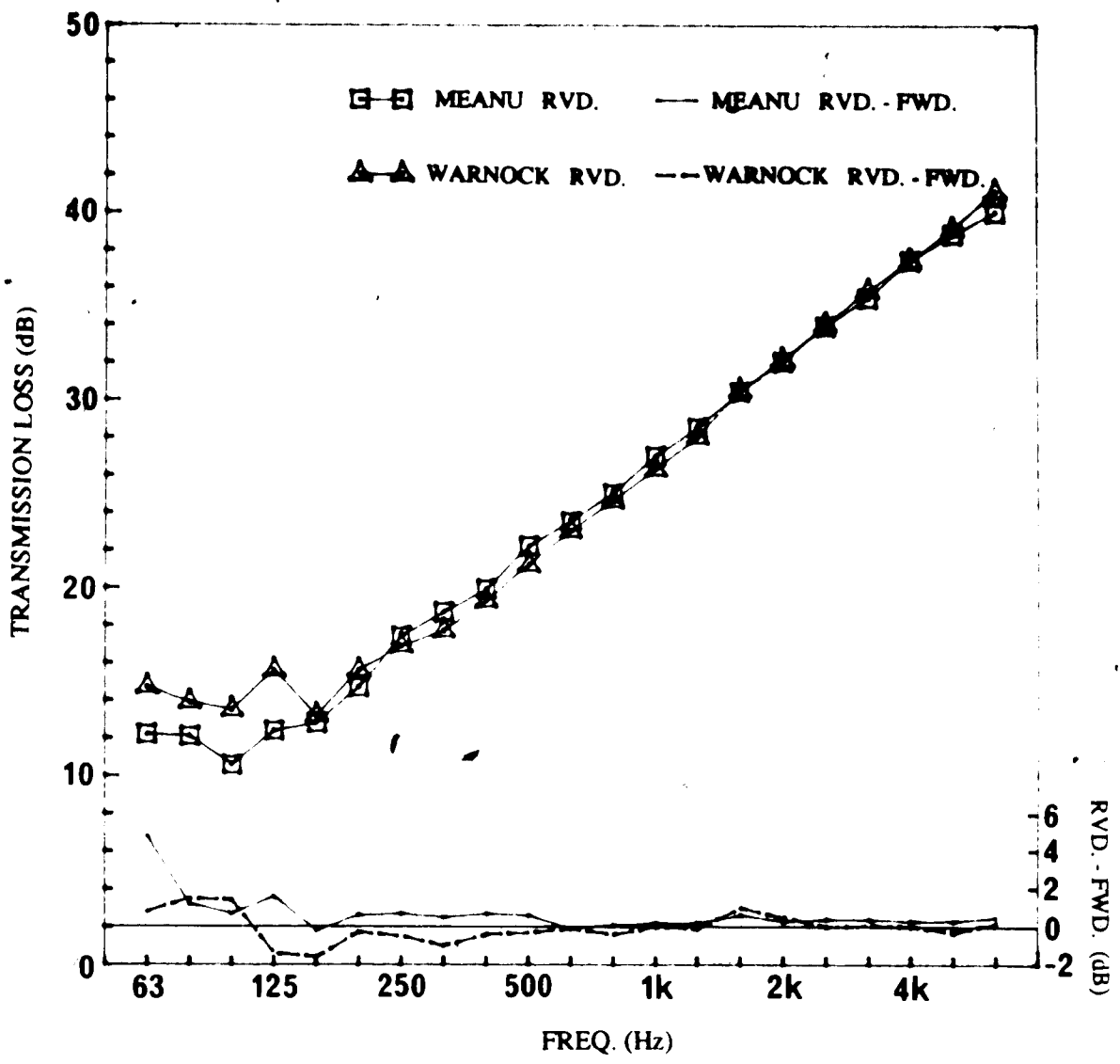


FIG. 6.3 COMPARISON OF REVERSED CTL RESULTS

a result of the larger source room volume in both cases (313 m<sup>3</sup> and 250 m<sup>3</sup> respectively for MEANU and NRC) which increases low frequency diffusivity. A higher diffusivity in the source room also means a higher diffusivity in the receiver room. Therefore, the SPL measurement in both rooms will be more reliable. The maximum deviation is only 3.2 dB at 125 Hz, compared to 6.2 dB at that frequency for the forward configuration. As shown by the two lower curves, the difference between forward and reversed configuration for both facilities are generally good, except below 160 Hz. Above 315 Hz, they differ by less than 0.7 dB.

Following the procedure stated in the E-90 standard, the TL values were converted to integer values for standard transmission class (STC) calculations. The STC values evaluated from 125 Hz to 4 kHz is 26 for both the forward and reverse CTL tests done by MEANU and Warnock, while it is 25 for Sherry's forward test. Considering standard deviations of all the results, the current tests are well within acceptable limits of the previous investigations and the STC class are essentially the same.

## 6.2 Comparison between CTL and ITL results

Since the ITL method requires the receiver room to be non-reverberant, fiber glass absorption panels are added to the walls and placed vertically on the floor up to limit reverberation of sound waves. Two sets of reverberation times were obtained from two amounts of absorption material used in the smaller room. They are tabulated with Warnock's data<sup>7</sup> in table 6.2. The A1 and A2

**TABLE 6.2 60-dB REVERBERATION TIMES FOR MEANU AND NRC**

ABSORPTION CONDITION	MEANU			NRC		
	A1	A2	A0	A1	A2	A3
FREQUENCY(Hz)	RECEIVER ROOM REVERBERATION TIMES (s)					
63	2.23	1.40	3.5	2.2	1.6	1.1
80	1.87	1.30	1.9	1.2	1.0	0.8
100	1.38	1.21	1.7	0.9	0.6	0.5
125	1.27	1.06	1.8	1.0	0.6	0.5
160	1.27	1.08	2.1	0.8	0.5	0.5
200	1.13	0.89	1.8	0.8	0.4	0.5
250	0.98	0.72	1.8	0.6	0.4	0.3
315	0.93	0.68	2.1	0.6	0.3	0.3
400	0.85	0.61	2.1	0.6	0.3	0.2
500	0.78	0.57	2.3	0.5	0.3	0.2
630	0.71	0.56	2.5	0.6	0.3	0.2
800	0.72	0.55	2.4	0.5	0.3	0.2
1000	0.70	0.53	2.5	0.6	0.3	0.2
1250	0.68	0.53	2.5	0.6	0.3	0.2
1600	0.67	0.51	2.3	0.6	0.3	0.2
2000	0.66	0.50	2.1	0.6	0.3	0.2
2500	0.63	0.49	1.4	0.6	0.3	0.2
3150	0.59	0.47	1.7	0.6	0.3	0.3
4000	0.55	0.44	1.5	0.6	0.3	0.3
5000	0.51	0.41	1.2	0.5	0.3	0.2
6300	0.46	0.38	1.0	0.5	0.3	0.2

conditions were tried, with the point by point technique to decide how much absorption material was needed for the ITL test. However, during the analysis of the ITL results with A1 absorption condition, an instrumentation problem was discovered.

Based on the anechoic third octave calibration results (section 3.4), the 1/2" microphones were used for the 63-125 Hz bands with the 50 mm spacer, and 160-6300 Hz bands with the 12 mm spacer. The phase mismatch due to the analyser and the rest of the system were added, as shown in fig. 6.4a. The limit of intensity reactivity index for each frequency band was determined from the corresponding phase mismatch to limit the error to be less than 1.5 dB. With this scheme, a high portion of 13 out of 25 sets of intensity measurements (52%) suffer from excessive reactivity index, mainly caused by the low frequency region of the 12 mm spacer. Even though the other 48% of the data were considered to be reliable, it was too low a portion of the data being used to adequately represent the whole specimen.

The choice of the smaller spacer down to a low frequency limit of 160 Hz has limited the dynamic range of the analyser system, as shown by the limits of the reactivity index. The decision on which spacer to use for which frequency range was made based on the calibration results in anechoic conditions. These results indicated a problem with the 50 mm spacer at 160 Hz, where the 1.5 dB limit was exceeded 5 out of 8 times. However, ITL tests were not in an anechoic situation, but rather in a semi-reverberant one. The higher dynamic range as a result of using a larger spacer at low frequency

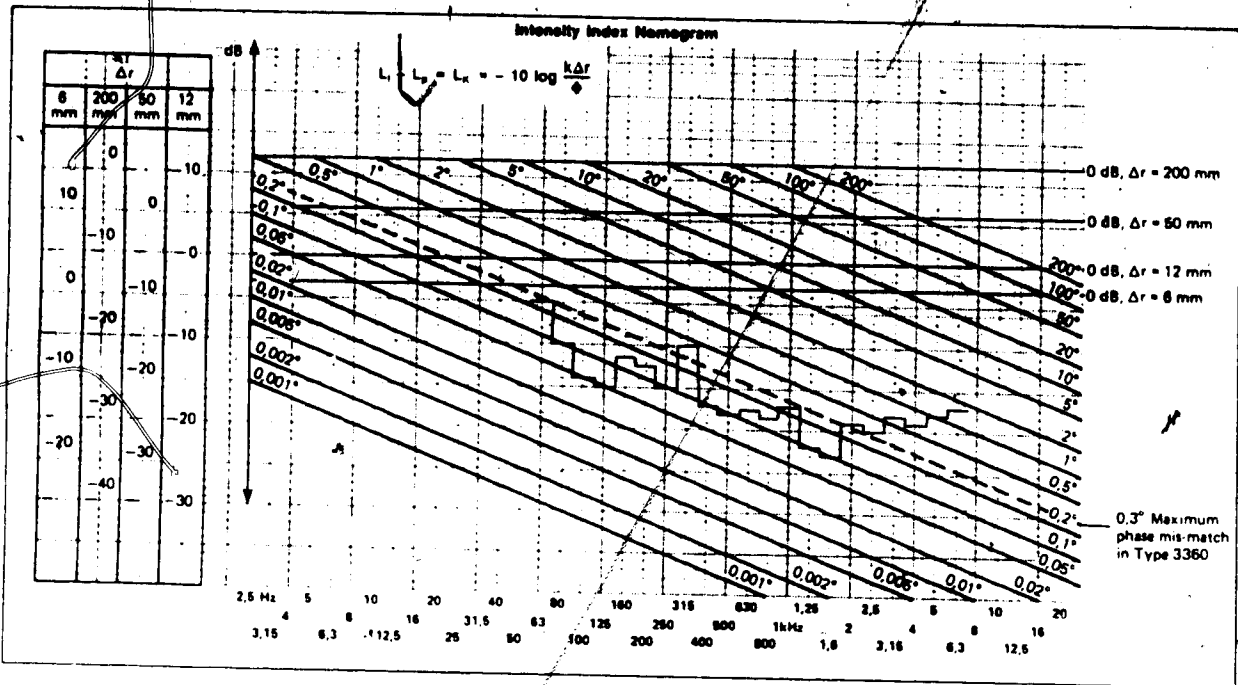


**FIG. 6.4a TOTAL SYSTEM PHASE MISMATCH AND LIMITS OF REACTIVITY INDEX FOR 11 mm SPACER USED FROM 125 Hz AND ABOVE**

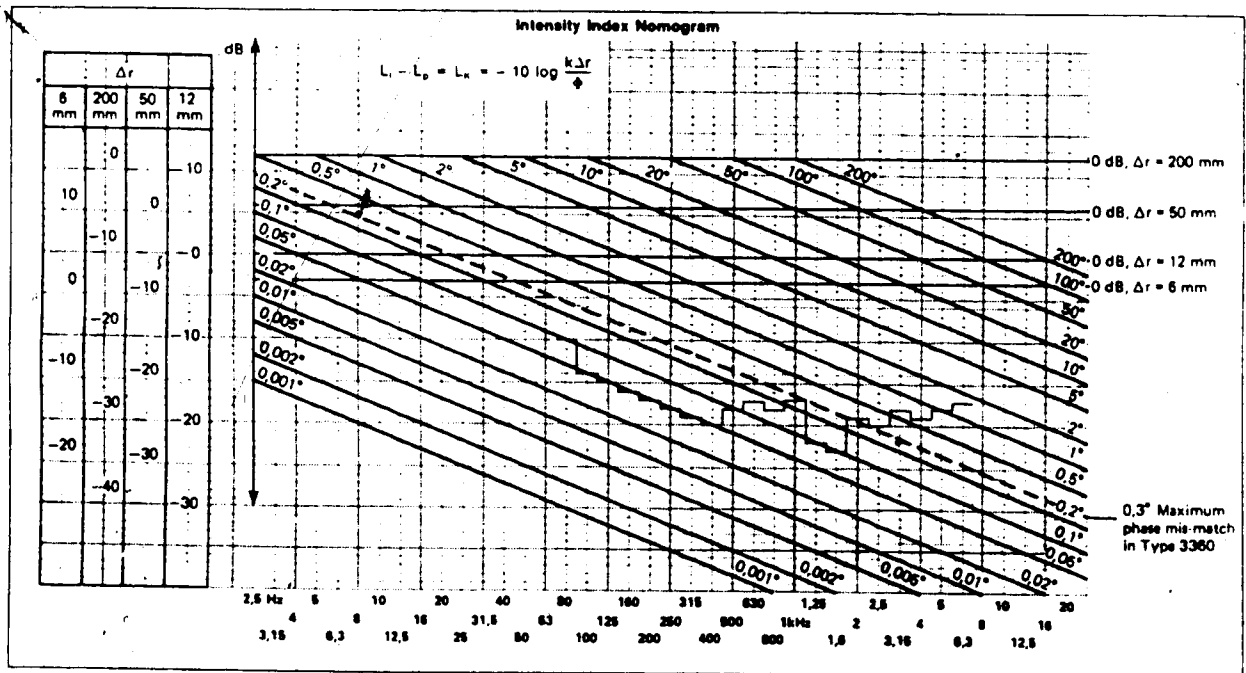


**FIG. 6.4b TOTAL SYSTEM PHASE MISMATCH AND LIMITS OF REACTIVITY INDEX FOR 11 mm SPACER USED FROM 630 Hz AND ABOVE**



should be used to advantage. Also, the absolute value of the phase mismatch error will be less since a larger spacer represents a larger field phase. It was decided that the frequency range choice based on anechoic conditions was inappropriate in the semi-reverberant chamber and the 50 mm spacer should be used in the 63-500 Hz range instead. Caution must be taken at 160 Hz, where a problem was encountered in the calibration results.

The new system phase mismatch and reactivity index limits are shown in fig. 6.4b. With this new scheme, a lower rejection rate of 32% was obtained for the test carried out in the A1 absorption condition, and 25% for the A2. Not only does the rejection rate decrease, the actual transmission loss values in the 160-500 Hz range are higher, ranging from 0.5 to 2 dB, when the larger spacer is used. These values are closer to the reversed CTL results, possibly indicating that the phase mismatch error is reduced significantly by using the larger spacer. The difference could also be caused partially by a higher resolution of the FFT spectral points. A 2 kHz frequency range was used when the larger spacer is used, instead of 10 kHz for the 11 mm spacer. In a fixed 400 line spectrum, the resolution has increased by a factor of 5. A higher resolution will result in a more accurate third octave simulation, as described in section 3.4.

The ITL results under the two absorption conditions, with the standard deviations of the transmitted intensity measurement, are shown in fig. 6.5. The agreement is very good with less than 0.5 dB difference, except for a couple of regions. The low frequencies 80 and 100 Hz have a difference of 1 and 0.7 dB respectively, whereas a 0.8

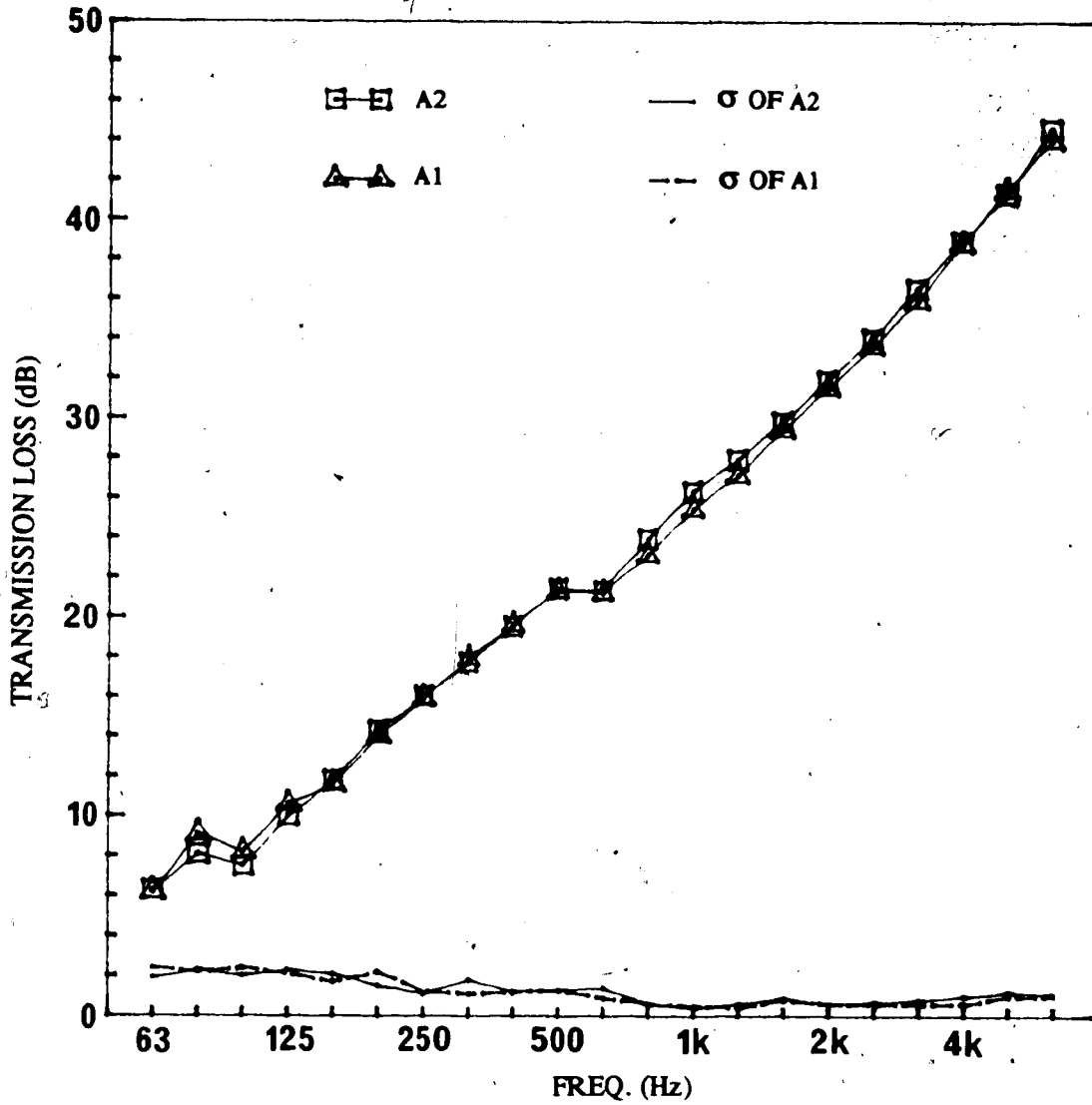


**FIG. 6.5 ITL RESULTS WITH ABSORPTION CONDITION A1 AND A2 AT MEAN U**

dB difference is obtained from 800 to 1250 Hz. The low frequency difference is possibly caused by the randomness of the source spectrum as a result of the lack of diffusivity. The 0.8 dB difference is acceptable considering the limitations of the instrumentation (up to 1.5 dB error) and the excellent agreement for the rest of the frequency bands. This agreement in the results of A1 and A2 conditions is not surprising since negligible difference was also obtained by Warnock among the three absorption conditions used for his 3 mm hardboard specimen<sup>7</sup>. Subsequent ITL tests on his ASTM specimen were carried out in the A2 condition. The close agreement of the standard deviations also indicate the negligible differences between the two absorptive conditions.

It should be noted that the TL values at 630 Hz are about 1.5 dB below the straight mass-law pattern. Since 630 Hz is the lower frequency limit for the 12 mm spacer, the difference could be caused by the relatively higher phase mismatch error, described earlier. In fact, the available data from the 50 mm spacer shows the difference is lowered to about 0.5 dB if 630 Hz was tested with the larger spacer.

The CTL and ITL results are compared in fig. 6.6. Generally, the agreement between the CTL and ITL results is good except at 630 Hz. The difference is less than 1 dB from 160 to 2500 Hz, except 250 and 630 Hz. The STC is 26 and 25 respectively for the CTL and ITL test. The ITL results are plotted with the 68% confidence limits ( $\pm 1 \sigma$ ). These ITL standard deviations were actually calculated in a semi-direct fashion. As one recalls, the ITL test consists of measuring

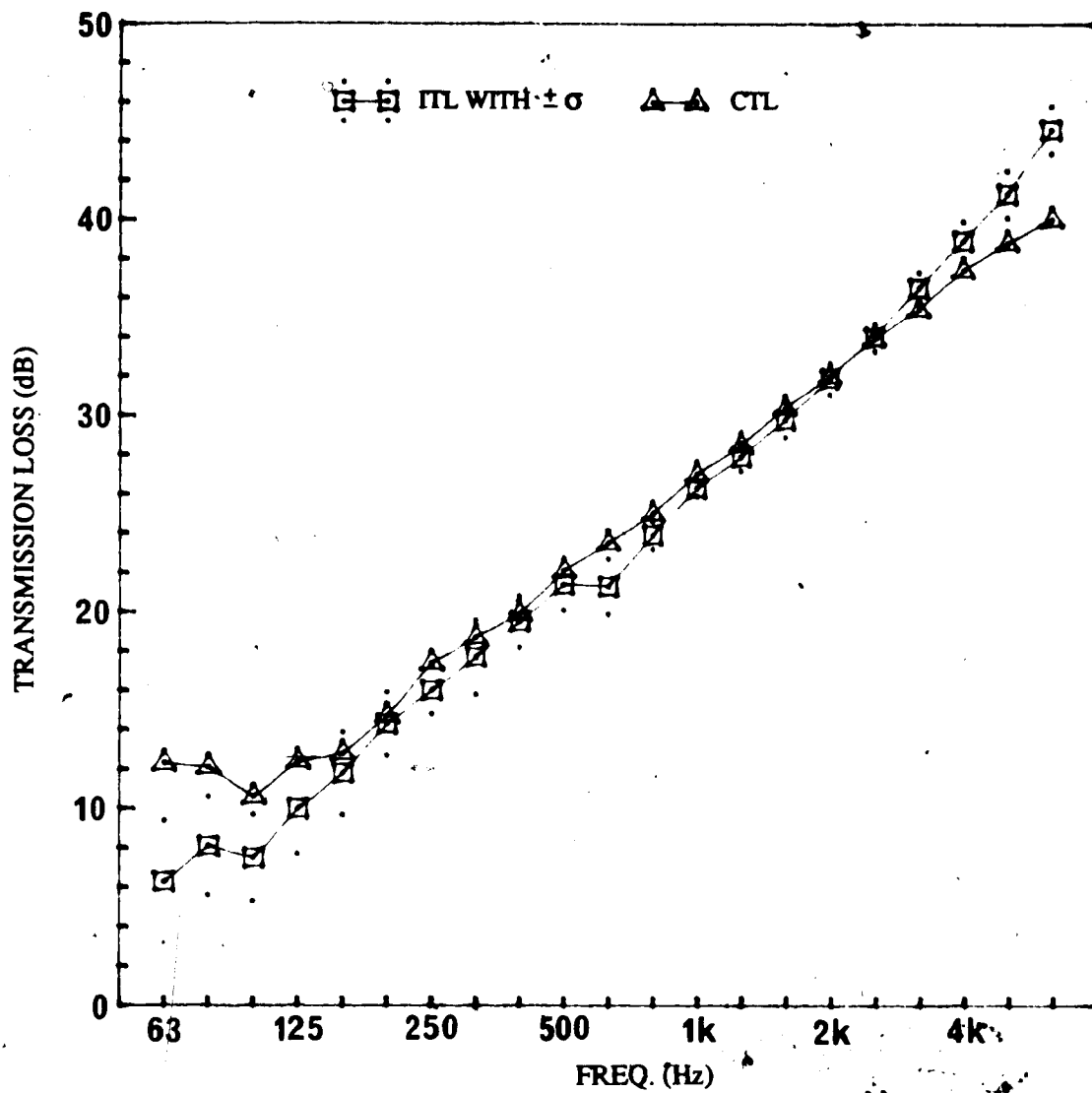


FIG. 6.6 COMPARISON OF CTL TO ITL RESULTS FROM MEANU

the far field SPL in the source room and the transmitted intensity in the receiver room. The use of the point measurement technique in measuring sound intensity allows a direct evaluation of the precision of the transmitted intensity. In approximating the incident intensity from SPL in the source room, the use of the rotating boom consists of only one measurement in the 10 rotation duration. Therefore, the standard deviation of SPL or the approximated incident intensity does not exist. To obtain some idea of the standard deviation of the source SPL, the standard deviation of the SPL's in the complete survey of the large room as the source room (fig. 2.3) were used as an upper estimate of the actual value. Those are the upper limits since the boom traverse actually consists of no more than three statistically independent points down to 100 Hz, as shown in fig. 2.2, compared to 12 in the complete survey.

The standard deviations of the source SPL from the complete survey and the transmitted intensity are then used to estimate those of the ITL test, as shown in table 6.3. Also shown in the table are the corresponding standard deviations from Warnock's ITL test. It is encouraging to see that these data are very close to each other; they differ mostly by less than 0.5 dB, which is well within the experimental limitation of the intensity systems. (1.5 dB for MEANU and 1.0 dB for NRC) It should be noted that the excessive standard deviation at 63 and 80 Hz for the transmitted intensity measurement at NRC are caused by the negative intensity encountered when the probe was placed too close to the specimen surface, as explained in section 3.3.7. These negative intensity values do not change the TL

**TABLE 6.3 STANDARD DEVIATIONS FOR ITL TEST RESULTS**

FREQ.(Hz)	SOURCE ROOM SPL $\sigma$ (dB)		RECEIVER ROOM $L_1$ $\sigma$ (dB)		ITL TEST $\sigma$ (dB)	
	MEANU	NRC	MEANU	NRC	MEANU	NRC
63	2.4*	2.5	1.9	51.0	3.1	51.1
80	0.9*	1.9	2.3	25.5	2.5	25.6
100	0.9	1.7	2.0	1.9	2.2	2.5
125	0.6	0.7	2.2	2.0	2.3	2.1
160	1.1	0.9	1.8	1.9	2.1	2.1
200	0.8	0.7	1.4	1.5	1.6	1.7
250	0.5	0.6	1.1	0.9	1.2	1.1
315	0.5	0.7	1.8	1.0	1.9	1.2
400	0.4	0.5	1.2	1.5	1.3	1.6
500	0.3	0.5	1.3	0.9	1.3	1.0
630	0.4	0.5	1.3	0.9	1.4	1.0
800	0.3	0.5	0.6	0.8	0.7	0.9
1000	0.1	0.6	0.4	0.5	0.4	0.8
1250	0.3	0.6	0.6	0.8	0.7	1.0
1600	0.2	0.5	0.9	0.6	0.9	0.8
2000	0.2	0.5	0.8	0.5	0.8	0.7
2500	0.2	0.4	0.7	0.6	0.7	0.7
3150	0.2	0.4	0.8	0.8	0.8	0.9
4000	0.3	0.4	1.0	0.9	1.0	1.0
5000	0.2	0.5	1.2	0.5	1.2	0.7
6300	0.4	0.4	1.1	0.3	1.2	0.5

\* obtained below the frequency limit defined by the distance between microphone positions

values for Warnock's results significantly since  $L_{eq}$  is used to calculate the average transmitted intensity. As shown in fig. 6.6, most MEANU ITL results are close enough to the CTL curve to include the CTL results into the 68% confidence band, except from 63 to 100 Hz, 630 Hz, and from 5000 to 6300 Hz. Should the 95% confidence limits be plotted, which is common for transmission loss testing, all the points of the CTL curve will fall within the the  $2\sigma$  band, except 6300 Hz.

The comparison of results is more clear when the data are plotted with respect to a reference contour with a TL of 0 dB at 63 Hz and an ideal mass-law slope of 6 dB/oct, as shown in fig. 6.7. Generally, the ITL technique gives lower transmission loss values at low frequencies and higher values at high frequencies than does the CTL technique. This general result has been commonly reported by other researchers<sup>6,7,39,42</sup>. If the results followed mass-law perfectly, the curves in fig. 6.7 should have a zero slope. Actually, the CTL results indicate an approximately 5 dB/oct slope whereas the ITL results show about a 5.5 dB/oct, instead of 6 dB/oct.

The referenced CTL and ITL curves from both MEANU and NRC are plotted in fig. 6.8. It is the difference between the CTL and ITL curves for each facility that is important to be compared, rather than the absolute values of the curves. This is because the facilities have different characteristics, such as tunnel effects and room volumes, which may cause fundamentally different results. In general, the deviation is consistently less for the MEANU results both in the low and high frequencies. From 63 to 125 Hz, the average deviation is 3.9

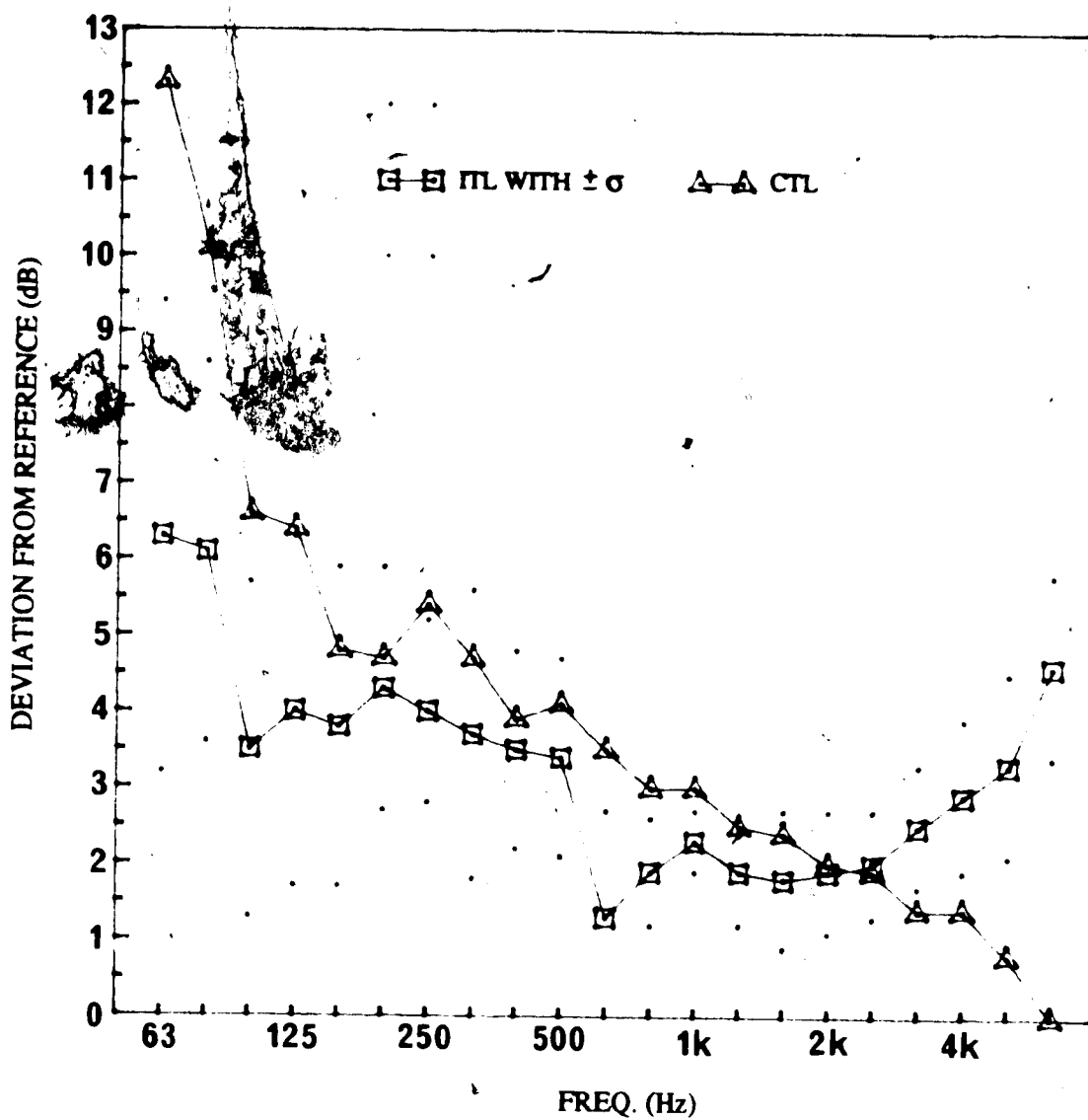


**FIG. 6.7 COMPARISON OF CTL TO ITL RESULTS WITH RESPECT TO THE REFERENCE CURVE**



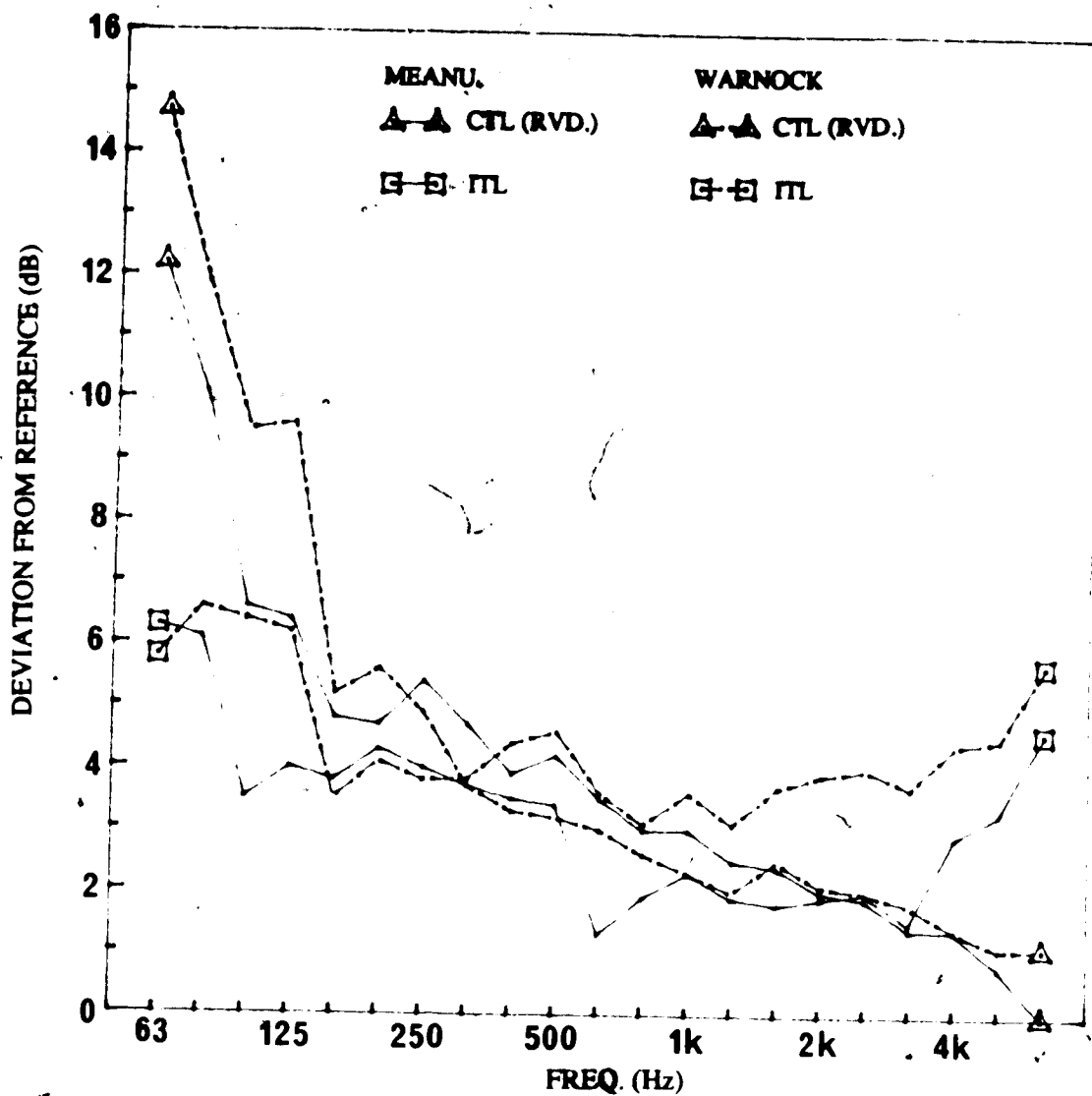


**FIG. 6.8 COMPARISON OF CTL TO ITL RESULTS FROM MEANU AND NRC**

dB for MEANU, compared to 5.2 dB for Warnock. For the bands from 1000 to 5000 Hz, it is 0.8 dB compared to 2.0 dB. The central frequency region (125 to 1000 Hz) basically has approximately the same average deviation without a consistent pattern. The distinctively large deviation of 2.2 dB at 630 Hz for the MEANU results could be a result of using the 11 mm spacer, causing a relatively larger phase mismatch error and a coarser frequency resolution, as explained earlier. It is also interesting to note that for the MEANU tests the ITL results are significantly higher than the CTL results for frequencies above 4 kHz. This effect occurs in Warnock's results starting at a lower frequency of 2 kHz.

Present measurement standards in reverberation room require users to avoid the room surfaces and corners, and use only the far field to estimate the energy in the room. However, as Waterhouse<sup>40</sup> pointed out, in a reverberation room there is an increase of energy density at the surfaces, at the junction of surfaces and in the corners because of the interference between the incident and reflected waves. Therefore, the estimates of total room energy determined from sampling in the central portions of the room will be too low. The Waterhouse correction is equivalent to adding a term

$$10 \log_{10} (1 + S \lambda / 8V) \quad (6.1)$$

to the mean SPL obtained in the far field, where  $\lambda$  is the wavelength of the nominal frequency of the band,  $S$  is the total surface area of the room including the specimen area and  $V$  is the volume of the room. Since the CTL technique requires SPL measurement in two rooms instead of only one in the case of ITL, the Waterhouse effect is

different for the two techniques. The corrections were made in the SPL values to see how the Waterhouse effect may contribute to some of the differences between the results of the two techniques. The corrected CTL and ITL referenced curves for MEANU, together with the original ones, are shown in fig. 6.9. The CTL values are very much the same because the volume of the two rooms at MEANU are relatively close, 313 and 230 m<sup>3</sup>. The increase of energy using eqn. (6.1) in each room virtually cancels one another. In the ITL results, however, correction is used for only one room and significant changes, particularly at lower frequencies, can be expected. Below 500 Hz, the differences are lowered by about 50%. The corrected ITL curve also shows a closer slope to the one of the CTL curve, particularly from 200 to 3150 Hz, except at 630 Hz.

Similarly, the corrected CTL and ITL referenced curves of Warnock's are plotted against MEANU's for comparison, as shown in fig. 6.10. At high frequencies, this is virtually the same as in fig. 6.8 because the Waterhouse correction is very small for small wavelength  $\lambda$ . However, from 63 to 125 Hz, the average deviation changes from 3.9 to 2.2 dB for MEANU, compared to 5.2 to 2.8 dB for Warnock. It is fair to say that there is no significant difference between these deviations (2.2 and 2.8 dB) at low frequencies after the Waterhouse effect is accounted for. From 1 kHz to 5 kHz, the difference between the MEANU results is still significantly less than Warnock's. This may be contributed by a stronger tunnel effect between the test rooms at NRC<sup>7</sup>.

It would be interesting to see if the ITL test gives the same STC

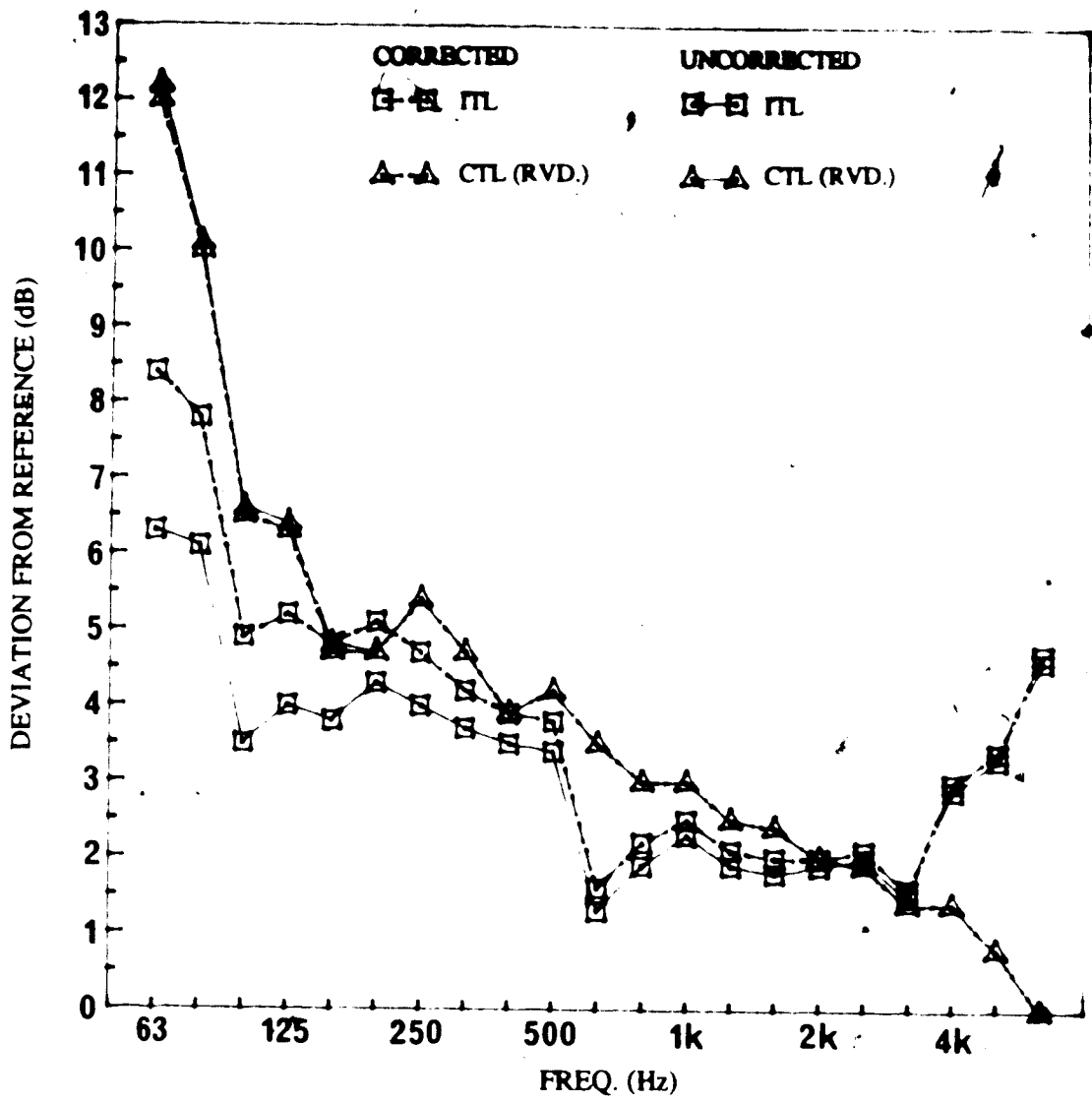


**FIG. 6.9 COMPARISON OF REFERENCED-ITL TO CTL RESULTS FROM MEANU BEFORE AND AFTER WATERHOUSE CORRECTION**

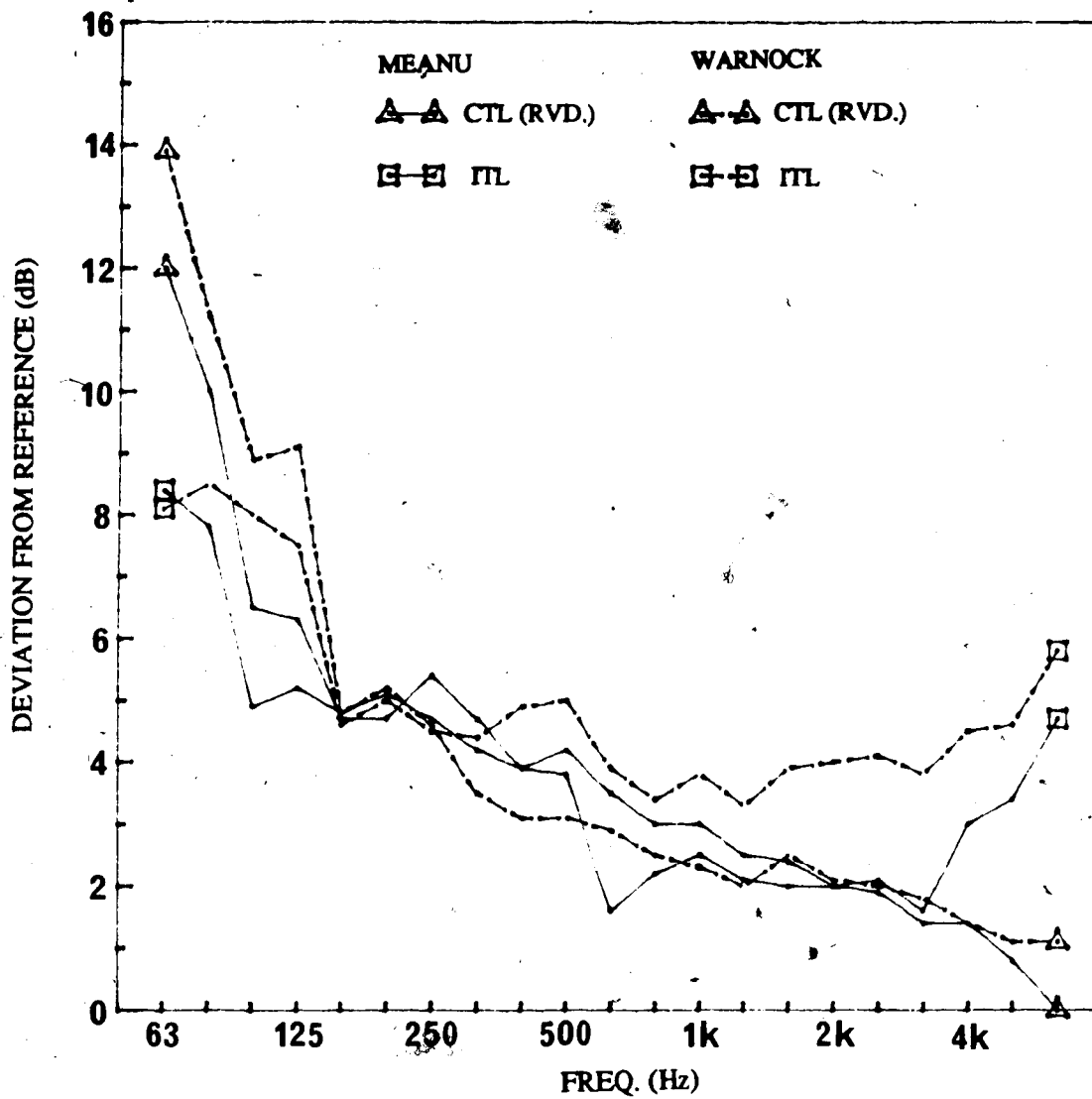


**FIG. 6.10 COMPARISON OF WATERHOUSE CORRECTED CTL TO ITL RESULTS FROM MEANU AND NRC**

value as the CTL test. The rounded TL values from the ITL test also give a STC value of 25, which is the same as obtained from the ITL results with one decimal point. When this is compared to a STC of 26 from the CTL test, the difference is negligible considering that a difference of 1 in STC also exists between Sherry's CTL test compared to MEANU's and Warnock's CTL tests. In addition, the Waterhouse corrected TL values for the ITL test does not change the STC value because the correction in the high frequencies is negligible and the change of TL values at lower frequencies down to 125 Hz is considerable but not excessive.

### 6.3 Comparison between sweeping ITL to point by point ITL results

Each ITL test using the sweeping technique consists of five sweeps, with each at a different elevation on the receiver side of the wall specimen. The  $L_{eq}$  value for these five sweeps is calculated to represent the transmitted intensity. The original set of results of the sweeping ITL test compares very favourably to the point by point results. Therefore, the test was repeated four more times to further confirm the agreement. Figure 6.11 shows the arithmetic mean and standard deviation of the five TL curves of the sweeping technique plotted against the point by point curve, which is considered to be the correct reference. It shows that the TL curve from the sweeping technique is highly repeatable with a standard deviation of less than 0.5 dB in all frequency bands. Most of the average TL values of the sweeping technique are slightly higher (by about 0.3 dB overall), but

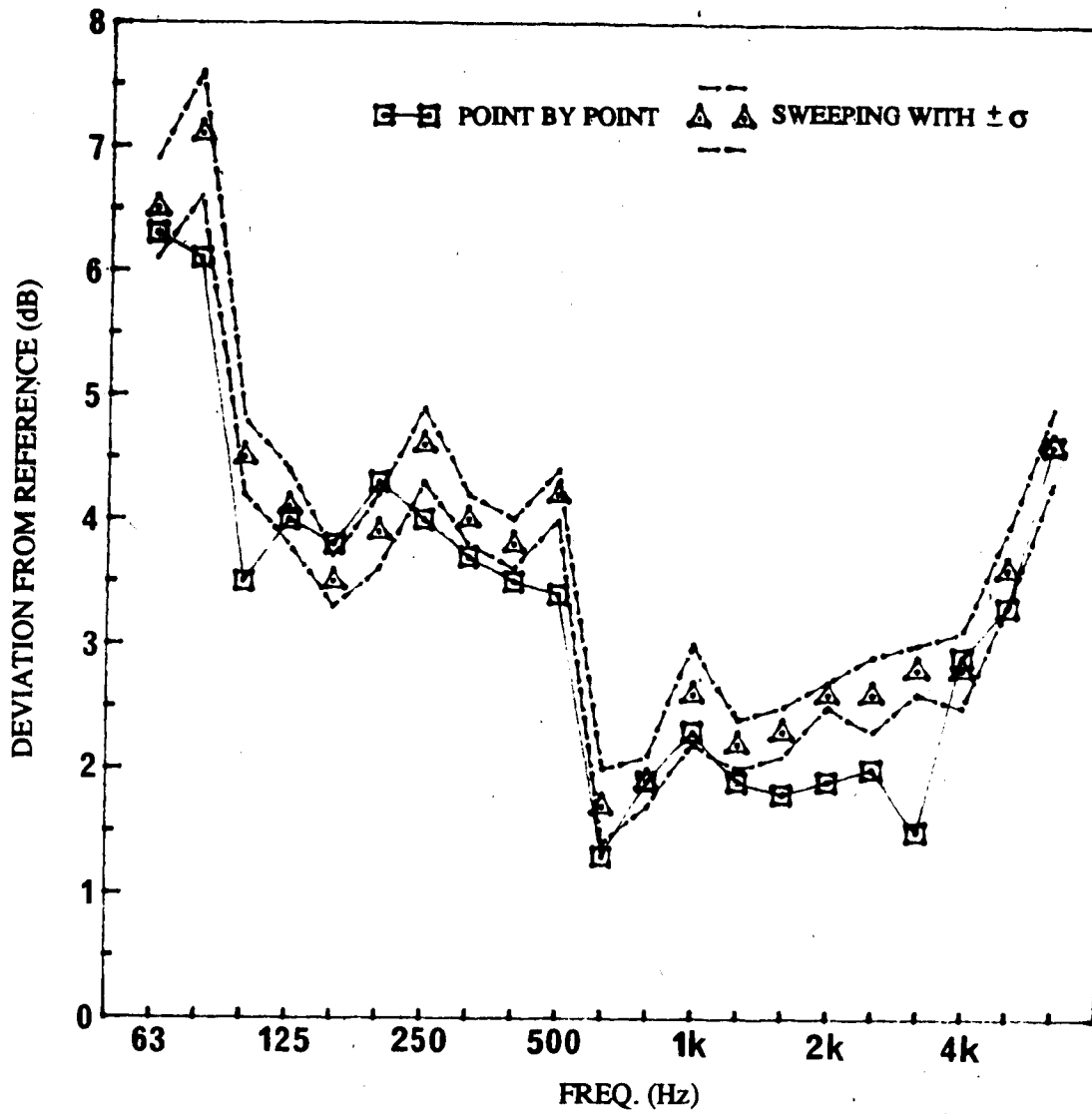


**FIG. 6.11 COMPARISON OF TL VALUES FROM THE SWEEPING TECHNIQUE TO THE POINT BY POINT TECHNIQUE**

this is not a significant difference. Furthermore, the TL limits of the 68% confidence band ( $\pm 0.1 \sigma$ ) for the sweeping technique differ by no more than 0.5 dB from the point by point technique, except at 100, 2000 and 3150 Hz. Therefore, the sweeping technique provided equivalent results to the point by point technique in a significantly shorter test period.

It has been reported by Cops and Minten<sup>6</sup> that the sweeping technique provides more precise results, while the opposite is shown by Warnock<sup>7</sup>. Each sweeping ITL test at MEANU consists of five sweeps on the receiver side of the specimen. This is equivalent to 5 intensity measurements, compared to 25 in the point by point technique. The standard deviation of these five measurements provides some idea of the precision of the ITL technique, while the SPL measurement in the source room by a rotating microphone boom allows no precision calculations. Theoretically, it is sufficient to compare the standard deviation of one set of sweeping ITL results (5 measurements) to that of the point by point ITL results (25 measurements). But since there are five sets of sweeping test results available, there are five standard deviation curves that can be used for comparison. Instead of choosing one randomly, the arithmetic average and standard deviation of the five standard deviation curves were calculated and used for comparison with the single standard deviation curve of the 25 point ITL test results. As shown in fig. 6.12, the sweeping technique is consistently more precise, particularly at lower frequencies. In fact, the mean standard deviation of the sweeping technique is only 0.3 dB overall, compared to 1.3 dB for the



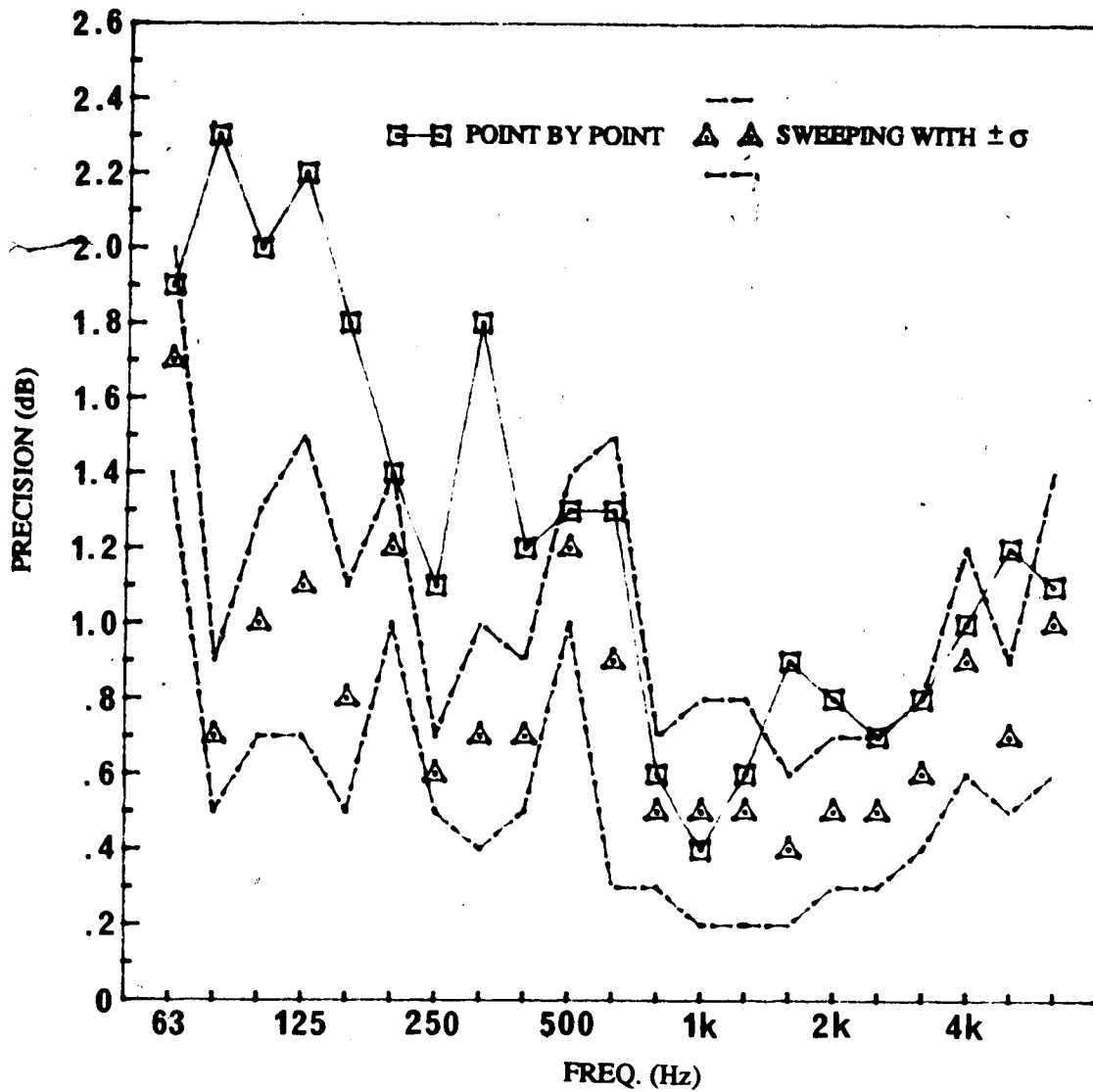


**FIG. 6.12 COMPARISON OF THE PRECISION OF THE SWEEPING TECHNIQUE TO THE POINT BY POINT TECHNIQUE**

point by point technique. The precision of the point by point technique is also shown to be better by about 1 dB in the work of Cop and Minten. This result is not surprising since sweeping is a better space average technique in principle because it really physically samples over a larger area. Consequently, it smears out any local influence, such as a lack of diffusivity or evanescent waves possibly encountered by a point measurement. In fact, the 25 combined sweeping measurements of the 5 sets of sweeping tests only had 2 that were rejected because of too high a reactivity index, compared to 5 of those in the 25 point measurements in the point by point test. Effectively, the rejection rate was lowered from 20% to 8%.

#### 6.4 Preliminary Direct and Semi-direct ITL Tests

The TL results from the preliminary direct and semi-direct ITL tests are shown with the ITL and CTL results in fig. 6.13. The vertical scale is kept the same as fig. 6.6 for a fair comparison. The difference of the results between the preliminary tests and the ITL test is large, with up to 9.9 dB at 1 kHz for the semi-direct approach. Also, the preliminary test results do not follow the linear mass law as the CTL and ITL results do.

The following theoretical curves<sup>41</sup> for the infinite panel below the critical frequency are used to provide some hints to the large differences:

$$\text{Mass Law at Angle : } TL_{\theta} = 10 \log [1 + \{(\omega \rho_s / \rho c) \cos \theta\}^2] \text{ dB} \quad (6.2)$$

$$\text{Normal-incidence Mass Law : } TL_0 = 10 \log [1 + (\omega \rho_s / \rho c)^2] \text{ dB} \quad (6.3)$$

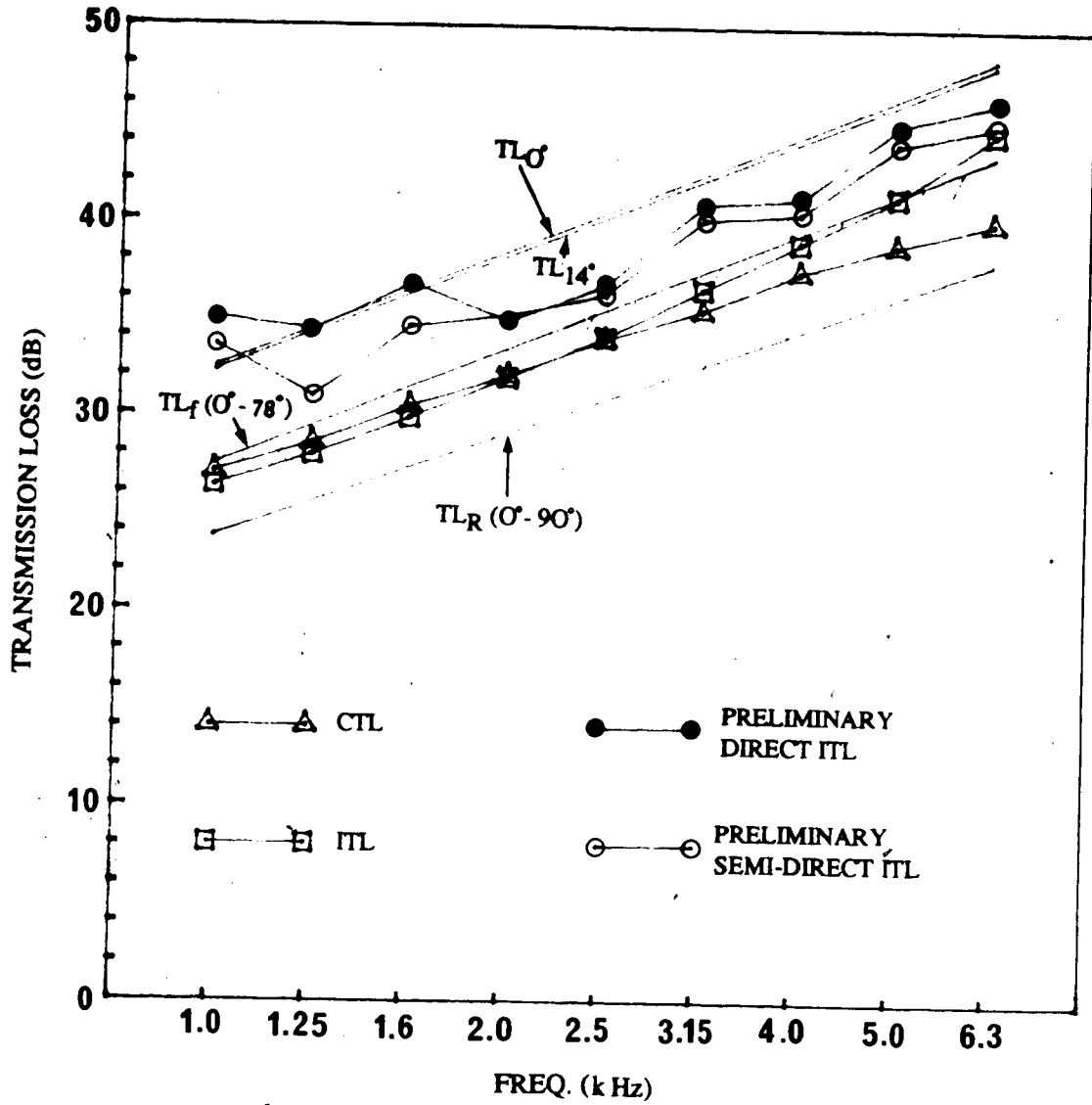


**FIG. 6.13 COMPARISON OF PRELIMINARY DIRECT AND SEMI-DIRECT ITL RESULTS TO CTL AND ITL RESULTS**

$$\text{Random-incidence Mass Law : } TL_R = TL_0 - 10 \log (0.23 TL_0) \text{ dB} \quad (6.4)$$

$$\text{for } TL_0 > 15 \text{ dB}$$

$$\text{Field-incidence Mass Law : } TL_F = TL_0 - 5 \text{ dB} \quad (6.5)$$

$$\text{for } TL_0 > 15 \text{ dB}$$

where  $\rho_s$  = surface density of specimen, kg/m<sup>2</sup>

$\rho$  = air density, kg/m<sup>3</sup>

$c$  = speed of sound, m/s

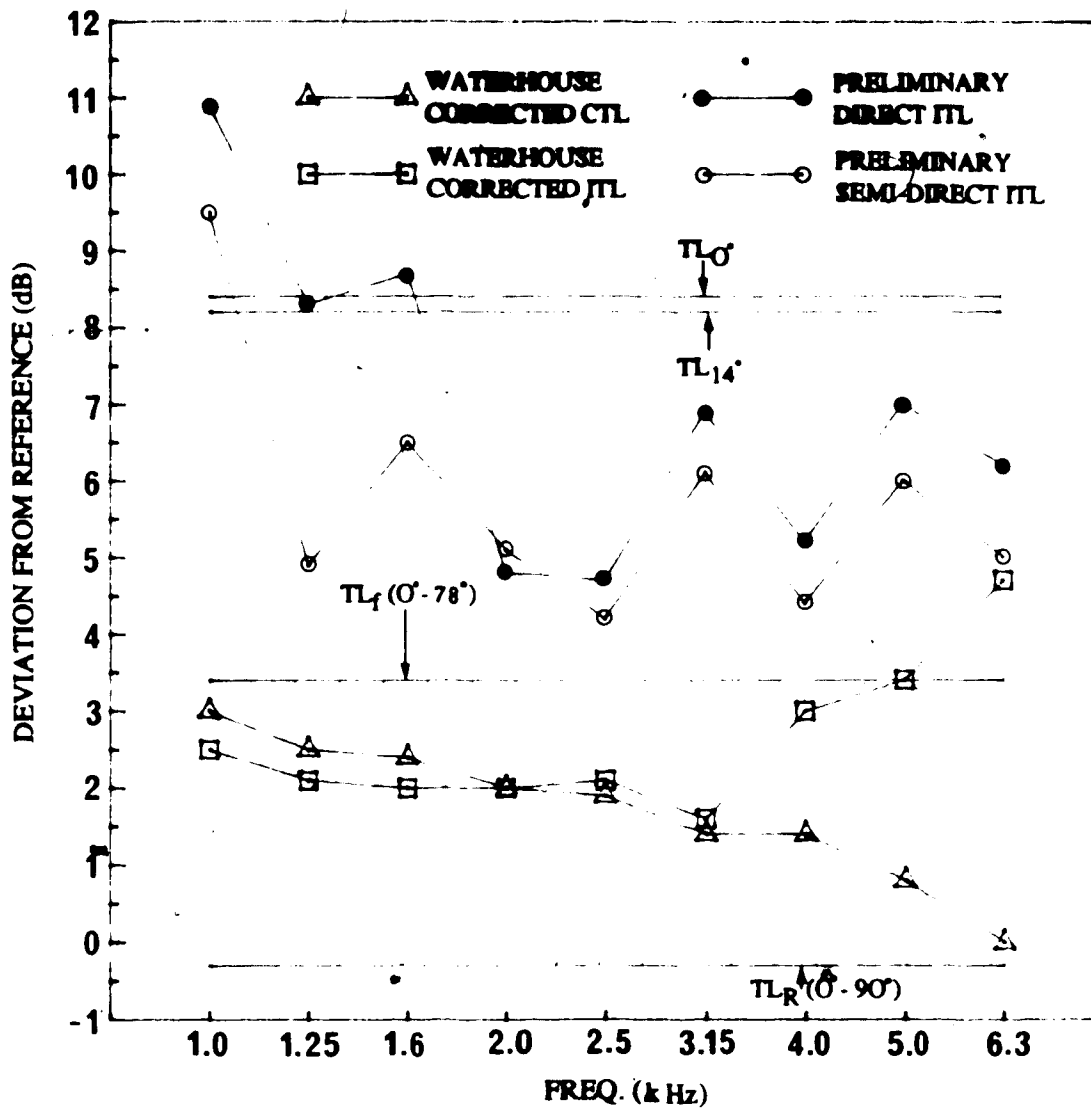
The TL curves from the CTL and ITL tests show that the critical frequency is above 6.3 kHz. Therefore, the above theoretical curves can be used for comparison, assuming an infinite panel.

As shown in fig. 6.13, the CTL and ITL results fall between the theoretical field-incidence and random-incidence curves, except one ITL point at 6.3 kHz by about 1 dB. This is expected since the angle of incidence should be between 0° and 86°, as a result of a small tunnel connecting the reverberation rooms at MEANU. Also, the large size (2.4m by 1.2m) of the individual panel may not be too far from the infinite panel model. The TL curve for the normal and 14° incidence are drawn as a reference for the preliminary tests, where the angle of incidence ranges from 0° to 14° based on geometry. The preliminary test results are within this band of theoretical curves. In fact, most points are below that by 2 to 4 dB, and the TL curves are quite jagged instead of linear. The reason for this disagreement may be that the size of the panel becomes more significant as the absolute dimension decreases to 1.1m by 1.1m. As the specimen gets smaller, the boundary conditions (mounting)

become more significant and the deviation from the model of an infinite panel will increase.

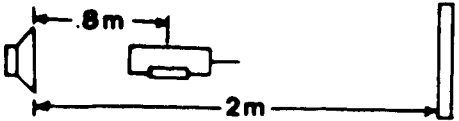
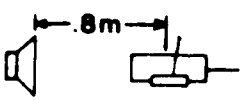
The same results in fig. 6.13 are plotted with respect to the reference contour with the addition of the Waterhouse corrected curves in fig. 6.14. It is clear that since the Waterhouse correction is very small for the ITL and CTL tests at high frequencies, with a maximum of 0.2 dB at 1 kHz for the ITL test, the comparison between the preliminary tests and the CTL and ITL tests does not improve significantly by Waterhouse correction.

The TL values of the preliminary direct ITL test seem to be systematically higher than the semi-direct ITL test. It is possible that the semi-direct method may include reflected intensity reducing the net value being measured. Consequently the TL values will be lower. To check the magnitude of the reflected intensity, the incident intensity was measured at a position 0.8m from the horn driver, which is 2m away from the specimen surface, with and without the wall installed. The difference in the measurements would indicate the magnitude of the reflected intensity. The results are listed in table 6.4. The reactivity index is generally small, mostly less than 1 dB. The small positive values could be caused by random errors or the fluctuation of the input signal from the white noise generator in the duration of the test. This small reactivity index values indicate the accuracy of the measured intensity. They also imply that the magnitude of the reflected intensity is small because reflected intensity should decrease the measured net intensity and increase SPL, resulting in a larger reactivity index.

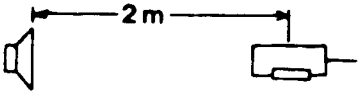
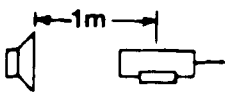


**FIG. 6.14 COMPARISON OF REFERENCED PRELIMINARY DIRECT AND SEMI-DIRECT ITL RESULTS TO REFERENCED CTL AND JTL RESULTS**

**TABLE 6.4 ACCURACY OF MEASURING INCIDENT INTENSITY IN THE PRESENCE OF REFLECTED INTENSITY**

CASE 1		CASE 2			
					
FREQ.(Hz)	$L_{I_1}$ (dB)	$L_p$ (dB)	$L_K$ (dB)	$L_{I_2}$ (dB)	$L_{I_2} - L_{I_1}$ (dB)
1000	92.9	93.1	-0.2	93.5	0.6
1250	97.8	97.7	0.1	98.3	0.5
1600	95.6	96.0	-0.4	96.2	0.6
2000	97.4	97.1	0.3	97.7	0.3
2500	100.9	101.7	-0.8	102.6	1.7
3150	102.1	102.7	-0.6	103.1	1.0
4000	101.4	102.4	-1.0	101.9	0.5
5000	100.6	101.6	-1.0	101.6	0.6
6300	96.1	98.0	-1.9	96.8	0.7

**TABLE 6.5 VERIFICATION OF THE INVERSE SQUARE LAW**

CASE 1		CASE 2	
			
FREQ.(Hz)	$L_{I_1}$ (dB)	$L_{I_2}$ (dB)	$L_{I_2} - L_{I_1}$ (dB)
1000	87.4	92.6	5.2
1250	90.8	96.2	5.4
1600	89.0	94.7	5.7
2000	91.9	97.3	5.4
2500	95.0	100.6	5.6
3150	92.8	99.4	6.4
4000	93.3	99.8	6.5
5000	92.4	98.9	6.5
6300	90.5	96.0	5.5

As expected, the incident intensity is higher without the specimen installed. The difference ranges from 0.3 to 1.7 dB with an average of 0.7 dB. This average is not too close to the theoretical difference of 0.26 dB based on the inverse square law, assuming all the incident energy is reflected. The deviation from the average could be a result of random errors, which is theoretically up to 0.4 dB based on 64 averages and a free progressive wave.

The inverse square law was further tested by measuring sound intensity at 1 m and 2 m from the horn driver without the wall specimen installed. The results are listed in table 6.5. Theoretically, the sound intensity measurements should all differ by 6 dB. The measured difference actually ranges from 5.2 to 6.5 dB, with an average of 5.9 dB. This is a good agreement considering a possible random error of 0.4 dB.

The results from table 6.4 and 6.5 basically indicates the incident intensity measured away from the specimen surface in the semi-direct ITL method is accurate with acceptable errors. In fact, if the difference in table 6.4 are added to the measured incident intensity in the semi-direct ITL method as a correction, a better agreement will be obtained at frequencies above 2.5 kHz. The disagreement below 2.5 kHz would still be high. Further investigation is necessary for a complete explanation.

Theoretically, there is no advantage to the measurement of incident sound intensity between the source speaker and the wall surface in the semi-direct ITL method over the direct measurement at a distance from the speaker where the wall surface would be in



the direct ITL method. However, the semi-direct approach may be useful in some field situation when space is limited. It is not conclusive whether the semi-direct or direct ITL approach works well or not because of the difference in the wall specimen. Nevertheless, the low reactivity index, small difference between the incident sound intensity measured 0.8m from the horn driver with and without the wall installed, and the verification of the inverse square law all indicate a high potential of measuring the incident sound intensity in the semi-direct manner. This should serve to be an acceptable alternative to the direct approach in some field situations.

## Chapter 7 Conclusions and Recommendations

In this work, the sound intensity technique is evaluated as an alternative to the conventional technique to measure sound transmission loss of wall panels. The potential of the intensity technique to improve low frequency reliability has also been investigated. From these the following conclusions can be drawn.

- (1) The test room facilities at MEANU are qualified within specified limitations down to 100 Hz for broadband acoustic property evaluations. In particular, the rotating microphone boom provides equivalent results compared to the conventional point measurement scheme in evaluating the reverberant sound field.
- (2) The FFT analyser is capable of capturing only 50% of the true power generated by the calibrator to the frequency band including the quoted calibration frequency. Therefore, the signal strength should be 3 dB less than the quoted value to ensure correct pressure calibration, and consequently a correct sound intensity measurement. This correction is necessary in sound power measurements or ITL tests when the absolute value of intensity, instead of the relative difference of two, is needed.
- (3) The ITL method is a reliable alternative to the CTL method in sound transmission evaluation of wall panels. In testing the ASTM proposed reference wall, the STC from the ITL test is very close to the one of the CTL. (25 compared to 26 respectively) This is an insignificant difference since the STC

values also differ by among the CTL test reported by Sherry, Warnock and MEANU. (25, 26 and 26 respectively)

- (4) At MEANU, the TL pattern of the ASTM wall from the ITL method generally shows significantly lower values at lower frequencies (approximately below 125 Hz) and higher values at higher frequencies (approximately above 1 kHz), compared to the corresponding CTL results. The Waterhouse correction is redundant for CTL tests, but necessary and recommended for ITL tests. The Waterhouse correction reduces the difference between the two methods at lower frequencies by about 50% at MEANU, although the differences remain the same at higher frequencies.
- (5) The deviation of the CTL and ITL results seem to be less for the facility at MEANU than NRC. Before the Waterhouse correction, this is true for both lower (below 160 Hz) and higher frequencies (above 1 kHz). After the correction, this is still true at the higher frequency region. The remaining difference could be contributed by the stronger tunnel effect at NRC.
- (6) The sweeping ITL technique is shown to provide equivalent TL results in a shorter test time with a higher precision for this ASTM wall. The results show that the sweeping technique smears out the local effects such as evanescent waves and reverse intensities. Also, it is a more statistically reliable space averaging technique because it actually samples over a larger area.

- (7) The preliminary testing in the anechoic chamber shows that it is possible to accurately measure the incident intensity either directly without the presence the wall, or indirectly at a distance in front of the incident surface where the reflected intensity is negligible, such as halfway between the speaker and the wall.
- (8) The ITL results by measuring directly or indirectly the incident sound intensity using a smaller specimen in the anechoic chamber does not agree well with the CTL and the original ITL results. This may be due to the decrease in size of the specimen and differences in mounting. Since testing shows that the measurement of the incident sound intensity by the two methods are promising, the new ITL concepts should be further tested with the original full size test wall in the outdoor anechoic situation. The results from the new ITL tests may even be more useful data since in actual situations, there is usually a specific incident angle for low frequency sound because of the limited space for diffusivity.

**REFERENCES**

- [1] J.Y. Chung and D. A. Blaser, "Transfer Function Method of Measuring In-duct Acoustic Properties, part I and II", *Journal of Acoustical Society of America* 68 (3); September 1980, pg. 907-921
- [2] D. M. Yeager, "A comparison of Intensity and Mean Square Pressure Methods for Determining Sound Power Using a Nine Point Microphone Array", IBM Acoustics Laboratory, Poughkeepsie, New York; 1983
- [3] S. Gade, H. Wulff and K. B. Ginn, "Sound Power Determination Using Sound Intensity Measurements", part I and II, Bruel and Kjaer Application Note # B0 0055
- [4] S. Gade, K.B. Ginn, O. Roth and M. Brock, "Sound Power Determination in Highly Reactive Environments", Bruel and Kjaer application note # B0 0074-11
- [5] M. J. Crocker, P. K. Raju and Bjorn Forssen, "Measurement of Transmission Loss of Panels by the Direct Determination of Transmitted Acoustic Intensity", *Noise Control Engineering Journal*, July - August 1981, pg. 6-11
- [6] A. Cops and M. Minten, "Comparative Study Between the Sound Intensity Method and the Conventional Two-room Method to Calculate the Sound Transmission Loss of Wall Constructions", *Noise Control Engineering Journal*, May - June 1984, pg. 104-111
- [7] R. E. Halliwell and A. C. C. Warnock, "Sound Transmission Loss: Comparison of Conventional Techniques with Sound Intensity Techniques", *Journal of Acoustical Society of America* 77 (6); June 1985, pg. 2094-2103
- [8] G. Krishnappa, "Investigation of Diamond Drilling Equipment Noise by the Sound Intensity Method", *Noise Control Engineering Journal*; May - June 1984, pg. 112-116

- [9] J. Hee, S. Gade, K. B. Ginn and P. Cornu, "Sound Intensity Measurements Inside Aircraft", Bruel and Kjaer application note # B0 0022
- [10] K. B. Ginn and M. Brock, "Noise Control Investigation Using Sound Intensity Measurements", Bruel and Kjaer application note # 1-043 0023-1A
- [11] D. E. Newland, *An Introduction to Random Vibration and FFT Analysis*, Longman, London, 1975
- [12] R. B. Randall, *Application of B & K Equipment to Frequency Analysis*, 2<sup>nd</sup> Edition, Bruel and Kjaer, 1977
- [13] R. B. Blackman, J. W. Tukey, *The Measurement of Power Spectrum*, Dover, New York, 1959
- [14] S. Gade, "Sound Intensity, I Theory, II Instrumentation and Application", Bruel and Kjaer Technical Review no. 3 & 4, 1982
- [15] S. Gade, "Validity of Intensity Measurements in Partially Diffuse Sound Field", Bruel and Kjaer Technical Review no. 4, 1985
- [16] J. Nicolas and G. Lemire, "Precision of Active Sound Intensity Measurement in a Progressive and Nonprogressive Field", *Journal of Acoustical Society of America* 78, August 1985, pg. 414-422
- [17] J. Roland, "What are the Limitations of Intensity Technique in a Hemi-diffuse Field", *Internoise Proceeding* 1982, pg. 715-718
- [18] J. Y. Chung, "Cross Spectral Method of Measuring Acoustic Intensity Without Error Caused by Instrument Phase Mismatch", *Journal of Acoustical Society of America* 64, 1978, pg. 1613-1616
- [19] J. C. Pascal and C. Carles, "Systematic Measurement Error with

- Two Microphone Sound Intensity Meters", *Journal of Sound and Vibration* (1982) 83(1), pg. 53-56
- [20] G. Pavic, "Measurement of Sound Intensity", *Journal of Sound and Vibration*, 1977, 51(4), pg. 533-545
- [21] R. Rage, "The Two-microphone Method of Measuring Acoustic Intensity", *Mechanical Engineering Honours Project Dissertation* (University of Southampton, 1975)
- [22] F. J. Fahy, "A Technique for Measuring Sound Intensity with a Sound Level Meter", *Noise Control Engineering*, Nov. - Dec. 1977, pg. 155-163
- [23] "Errors in Acoustic Intensity Measurements", *Journal of Sound and Vibration* (1981) 78(3), pg. 439-445
- [24] M. Brock, "Intensity Measurement Using a Tape Recorder", *Bruel and Kjaer application note B0 0081-11*
- [25] A. F. Seybert, "Statistical Error in Acoustic Intensity Measurements", *Journal of Sound and Vibration* (1981) 75(4), pg. 519-526
- [26] "A Note on Stastical Errors in Acoustic Intensity Measurements", *Journal of Sound and Vibration* (1983) 90(4), pg. 585-589
- [27] K. B. Ginn and S. Gade, "Sound Intensity Measurements Inside a Motor Vehicle", *Bruel and Kjaer application note B0 0019 2-043 0019-1A*
- [28] J. D. Maynard and E. G. Williams, "A New Technique for Noise Radiation Measurement", *Noise Conference 1981*, pg. 19-24
- [29] F. Friundi, "The Utilization of Intensity-meter for the Investigation of Sound Radiation of Surfaces", *Unikeller*, 1977
- [30] J. Y. Chung, "Fundamental Aspects of the Cross Spectral Method

- of Measuring Acoustic Intensity", 1<sup>st</sup> International Congress on Acoustic Intensity, Senlis, 1981
- [31] D. H. Munro and K. U. Ingard, "On Acoustic Intensity Measurements in the Presence of Flow", *Journal of Acoustical Society of America* 65(6), June 1979, pg. 1402-1406
- [32] R. J. Comparin, J. R. Rapp and R. Singh, "Measurement of Acoustic Intensity in the Presence of One-dimensional Flow", *Journal of Acoustical Society of America* 72(1), July 1982, pg. 7-12
- [33] J. Y. Chung and D. A. Blaser, "Transfer Function Method of Measuring Acoustic Intensity in a Duct System with Flow", *Journal of Acoustical Society of America* 68(6), Dec. 1980, pg. 1570-1577
- [34] F. J. Fahy, T. Lahti and P. Joseph, "Some Measurements of Sound Intensity in Air Flow", 2nd International Congress on Acoustic Intensity, Senlis, 1985, pg. 185-192
- [35] C. J. Buma and A. Craggs, "Experimental Measurements on Lined Expansion Chamber Silencers", *Proceedings of Canadian Acoustical Association Conference, Calgary 1987*, pg. 139-144
- [36] P. Rasmussen, "Sound Power Measurement by Different Operators", *Internoise 86*, vol. 2, pg. 1121-1124
- [37] Bruel and Kjaer lecture guide on sound intensity # 1310.8
- [38] C. Sherry, memo for task group D of E33.05, Domtar Research, P. O. Box 300, Senneville, Quebec H9X SL7
- [39] K. W. Walker, "Measurement of Sound Transmission Loss with a Two Microphone Sound Intensity Analyser", *Journal of Acoustical Society of America* suppliment 176, S50 (1984)
- [40] R. V. Waterhouse, "Interference Patterns in Reverberant Sound



Fields", *Journal of Acoustical Society of America* 27, 1955, pg. 247-258

- [41] L. L. Beranek, *Noise and Vibration Control*, McGraw-Hill, New York, 1971, pg. 282-283
- [42] A. C. C. Warnock, *Further Measurements on the Proposed ASTM Steel Reference Specimen*, National Research Council of Canada, Division of Building Research, Montreal Road, Ottawa, Ontario, Canada K1A 0R6